Supporting Information

# Solvent-Induced Transient Self-Assembly of Peptide Gels: Gelator-Solvent Reactions and Material Properties Correlation

*Romain Chevigny,[†] Henna Rahkola,[†] Efstratios D. Sitsanidis,[†] Elsa Korhonen,[†] Jennifer R. Hiscock,[‡] Mika Pettersson,[†] and Maija Nissinen*[†]*

† Department of Chemistry, Nanoscience Center, University of Jyväskylä, P.O. Box 35, FI-40014 JYU Finland

‡ School of Physical Sciences, University of Kent, Canterbury, Kent, CT2 7NH, UK

# Table of Contents

## 1. Synthesis and characterization

### 1.1. Synthesis of diprotected precursors 1-8

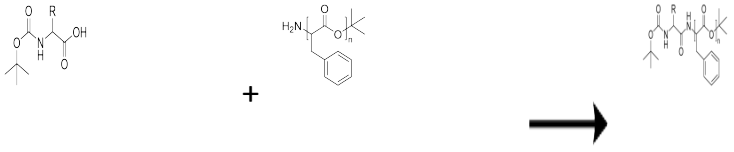

General protocol: Boc-protected amino acid (1.0 equivalent), TBTU (1.0 equivalent) and $NaHCO_3$ (1.0 equivalent) were suspended in anhydrous DMF (10 mL) under $N_2$ atmosphere. The solution

was left to stir at R.T. for 1 hour. *tert*-butyl protected amino acid (1.1 equivalent) and $NaHCO_3$ (1.1 equivalent) were suspended in anhydrous DMF (10 mL). The two solutions were mixed and allowed to stir under $N_2$ atmosphere at R.T. overnight. The solvent was then evaporated under vacuum (co-evaporation with toluene x3), and the residue was dissolved in DCM. The organic phase was extracted with water (x2), subsequently with an aqueous HCl solution (0.1 M), water (x2) and a saturated aqueous solution of $NaHCO_3$. The organic phase was then dried with $MgSO_4$ and evaporated under vacuum, yielding the desired compounds.

### 1.1.1. Boc-Phe-Phe-O*t*Bu 1

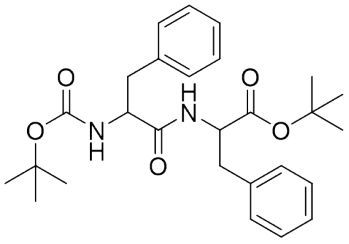

Yellow powder (70 % yield). **Melting point**: 129-133 ˚C.

**$^1$H NMR** (500 MHz, $d_6$-DMSO) δ 8.21 (d, $J$ = 7.5 Hz, 1H), 7.33 – 7.16 (m, 10H), 6.84 (d, $J$ = 8.8 Hz, 1H), 4.38 (q, $J$ = 7.3 Hz, 1H), 4.19 (td, $J$ = 9.8, 3.9 Hz, 1H), 2.96 (ddt, $J$ = 31.5, 13.8, 5.7 Hz, 4H), 2.73 – 2.66 (m, 1H), 1.32 (s, 9H), 1.28 (s, 9H).

**$^{13}$C NMR** (126 MHz, $d_6$-DMSO) δ 171.8, 170.4, 155.2, 138.2, 137.1, 129.3, 129.2, 128.2, 128.0, 126.5, 126.2, 80.7, 78.0, 55.5, 54.1, 37.4, 36.9, 28.1, 27.5.

**HR-MS**: *m/z* for $C_{27}H_{36}N_2O_5$ $[M + H]^+$ calculated 469.2700, found 469.2675.

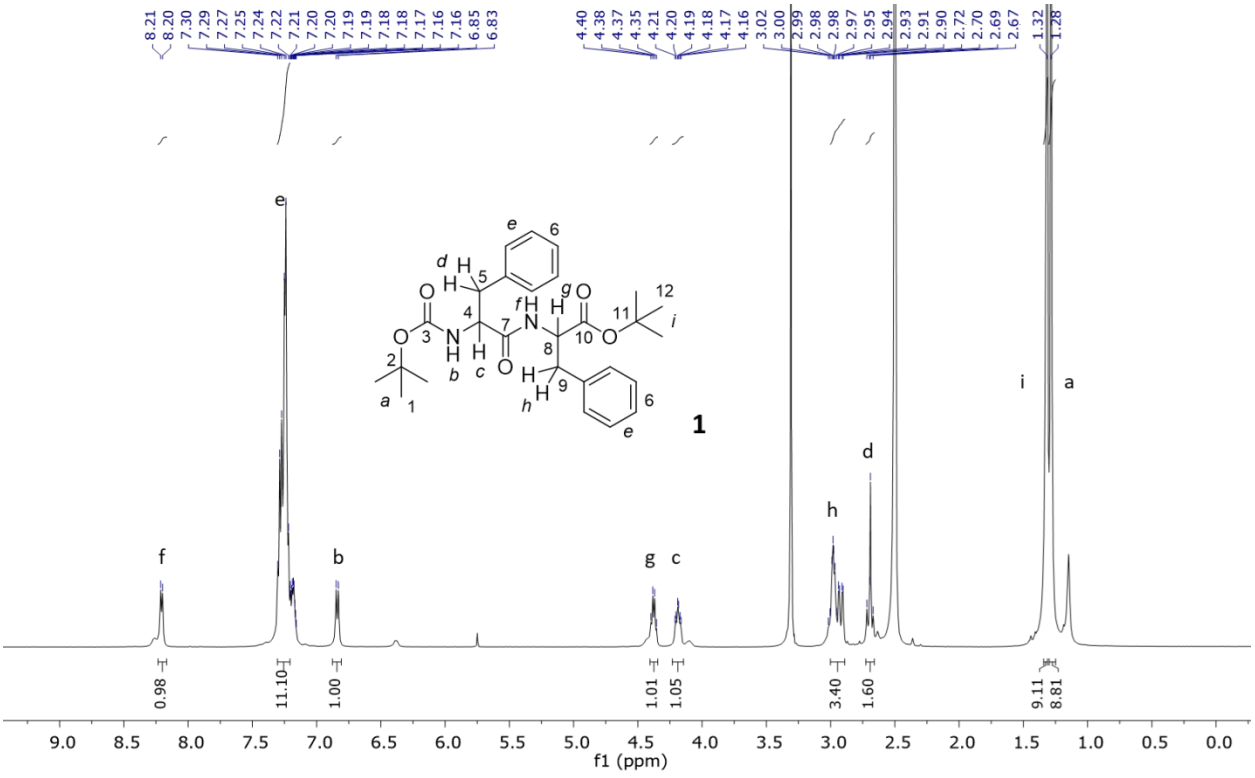


**Figure S1.** $^{1}$H NMR (500 MHz, $d_6$-DMSO) spectrum of Boc-Phe-Phe-O*t*Bu **1**.

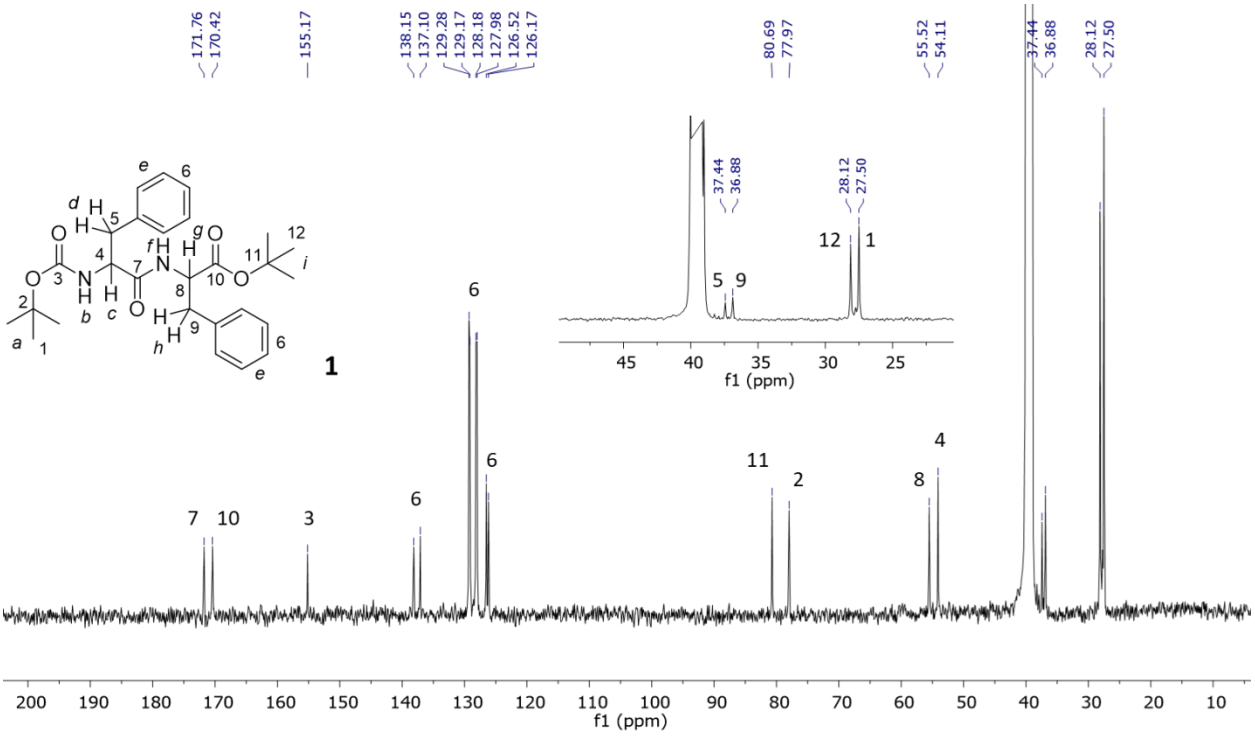

**Figure S2.** $^{13}$C NMR (126 MHz, $d_6$-DMSO) spectrum of Boc-Phe-Phe-O*t*Bu **1**.

### 1.1.2. Boc-Phe-Phe-Phe-O*t*Bu 2

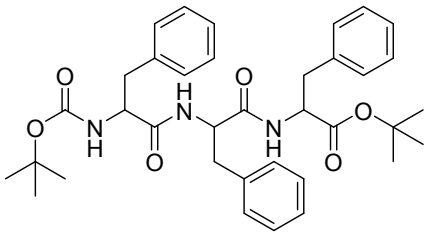

Yellow powder (74 % yield). **Melting point**: 78-83 ˚C.

**$^1$H NMR** (500 MHz, $CDCl_3$) δ 7.31 – 6.96 (m, 15H), 6.44 (d, $J$ = 7.2 Hz, 1H), 6.27 – 6.16 (m, 1H), 4.85 (s, 1H), 4.56 (dq, $J$ = 14.9, 7.4, 6.8 Hz, 2H), 4.35 – 4.25 (m, 1H), 3.06 – 2.89 (m, 6H), 1.36 (s, 9H), 1.34 (s, 9H).

**$^{13}$C NMR** (126 MHz, $CDCl_3$) δ 171.0, 169.8, 169.7, 155.3, 136.5, 136.2, 136.0, 129.5, 129.3, 128.7, 128.6, 128.4, 127.0, 127.0, 82.3, 80.3, 55.7, 54.4, 53.9, 38.1, 28.2, 27.9.

**$^1$H NMR** (500 MHz, $d_6$-DMSO) δ 8.46 (d, $J$ = 7.5 Hz, 0.7H), 8.33 (d, $J$ = 7.5 Hz, 0.3H), 8.03 (d, $J$ = 8.6 Hz, 0.3H), 7.90 (d, $J$ = 8.4 Hz, 0.7H), 7.34 – 7.12 (m, 15H), 6.84 (d, $J$ = 8.9 Hz, 0.7H), 4.62 (td, $J$ = 8.8, 4.4 Hz, 0.7H), 4.58 – 4.52 (m, 0.3H), 4.38 (q, $J$ = 7.5 Hz, 1H), 4.10 (td, $J$ = 9.7, 3.9 Hz, 0.7H), 4.02 (s, 0.3H), 3.07 – 2.94 (m, 3H), 2.85 – 2.76 (m, 2H), 2.65 – 2.57 (m, 1H), 1.31 (s, 9H), 1.27 (s, 9H). Note: presence of a rotamer (N-H peaks at 8.33 ppm and 8.03 ppm and C-H peak at 4.58 – 4.52 ppm). Peaks corresponding to the rotamer in DMSO vanishes in $CDCl_3$ (Figure S3) and higher temperature measurements (Figure S6).

**$^{13}$C NMR** (126 MHz, $d_6$-DMSO) δ 171.7, 171.4, 170.8, 155.5, 138.6, 137.9, 137.5, 129.8, 129.6, 128.7, 128.4, 127.0, 126.7, 126.6, 81.2, 78.6, 56.3, 54.7, 53.7, 38.4, 38.1, 37.4, 28.6, 28.0.

**HR-MS**: *m/z* for $C_{36}H_{45}N_3O_6$ $[M + Na]^+$ calculated 638.3100, found 638.3192.

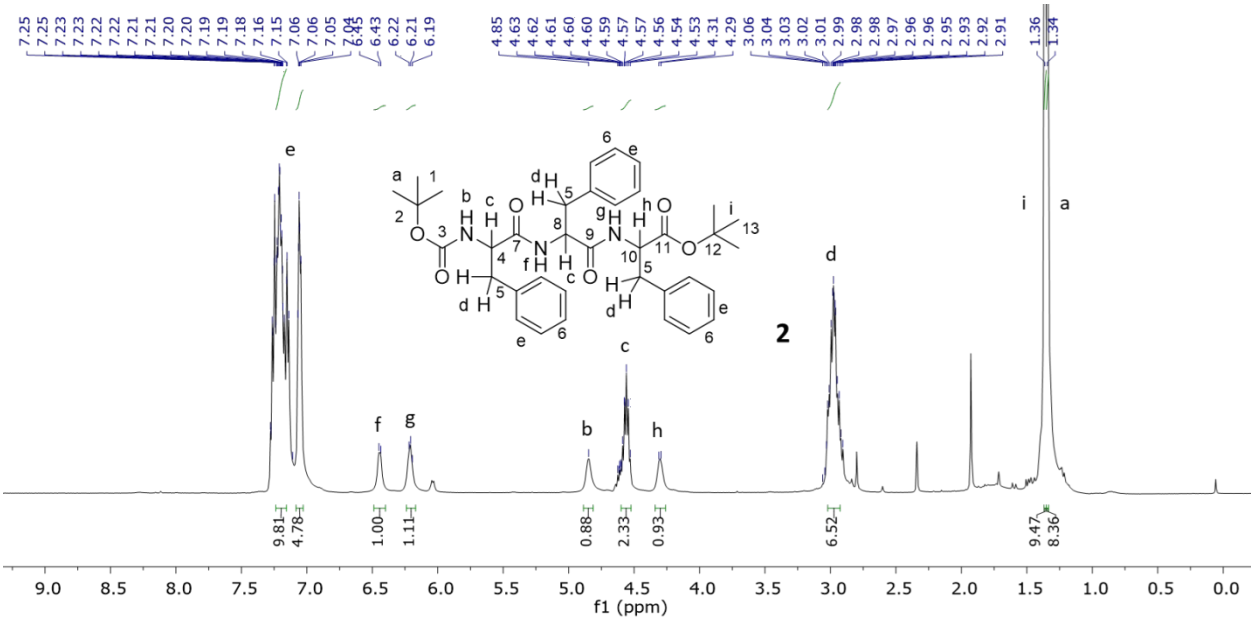


**Figure S3.** $^{1}$H NMR (500 MHz, $CDCl_3$) spectrum of Boc-Phe-Phe-Phe-O*t*Bu **2**.

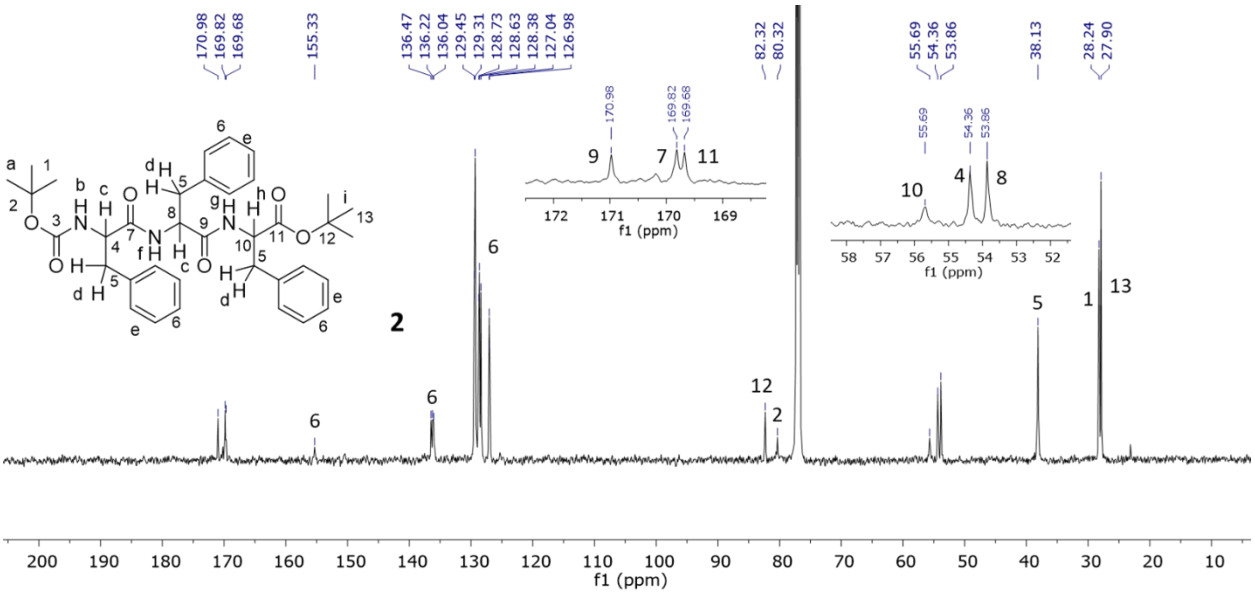


**Figure S4.** $^{13}$C NMR (126 MHz, $CDCl_3$) spectrum of Boc-Phe-Phe-Phe-O*t*Bu **2**.

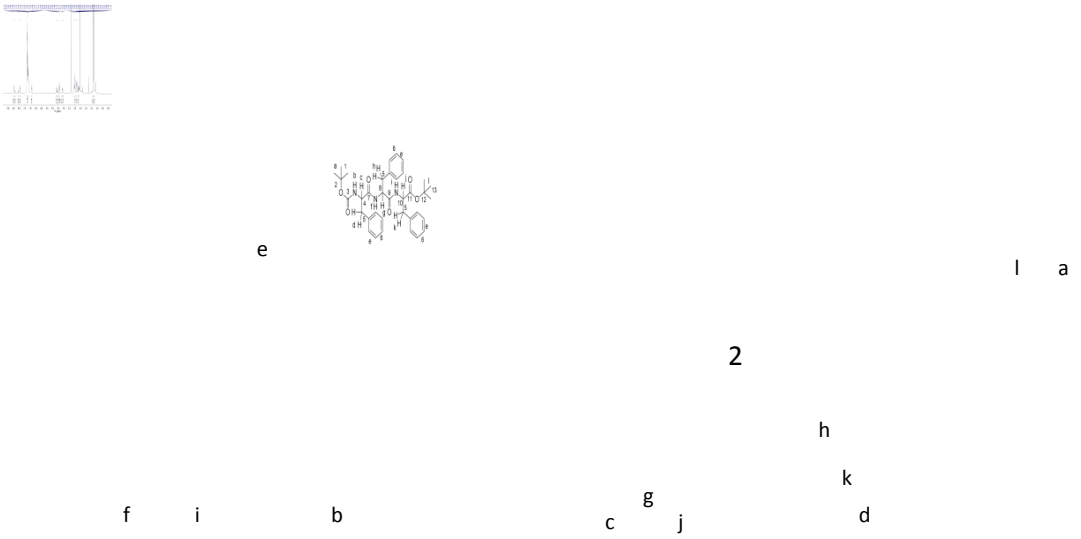


**Figure S5.** $^{1}$H NMR (500 MHz, $d_6$-DMSO) spectrum of Boc-Phe-Phe-Phe-O*t*Bu **2**. Presence of a rotamer.

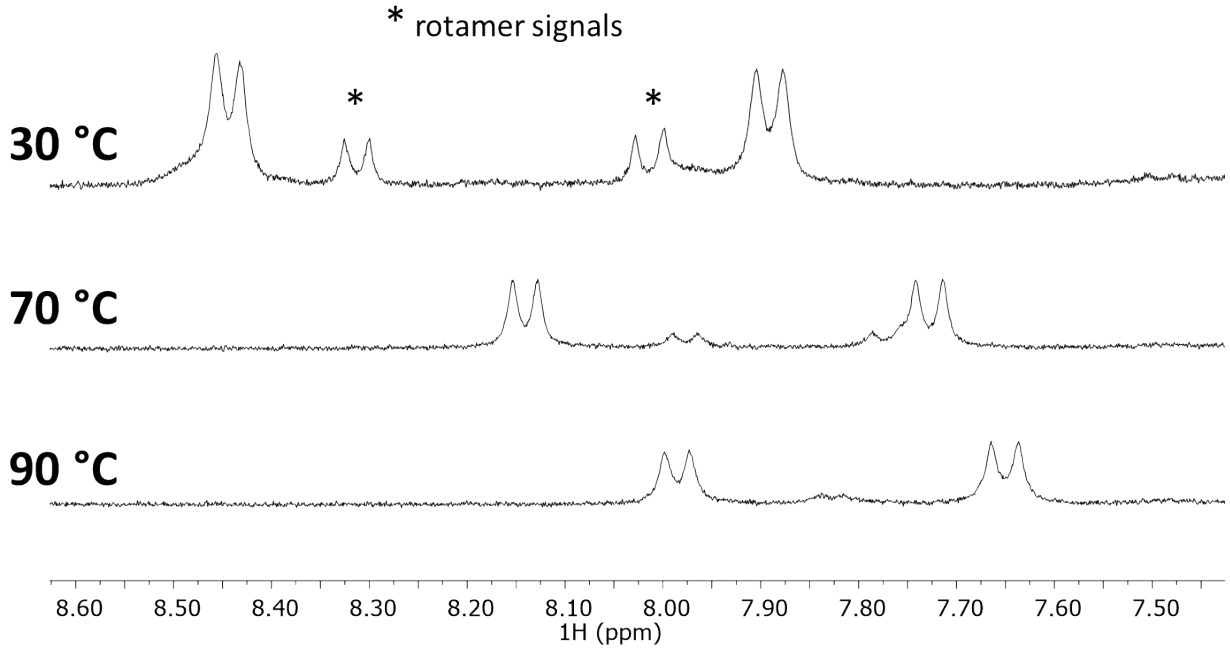

**Figure S6.** $^{1}$H NMR (500 MHz, $d_6$-DMSO) spectrum of Boc-Phe-Phe-Phe-O*t*Bu **2** magnified in the NH amide region showing the rotamer signal at R.T. (30 ˚C, top row). Temperature increase to 70 ˚C (middle row) and 90 ˚C (bottom row) showing the disappearance of the rotamer signals.

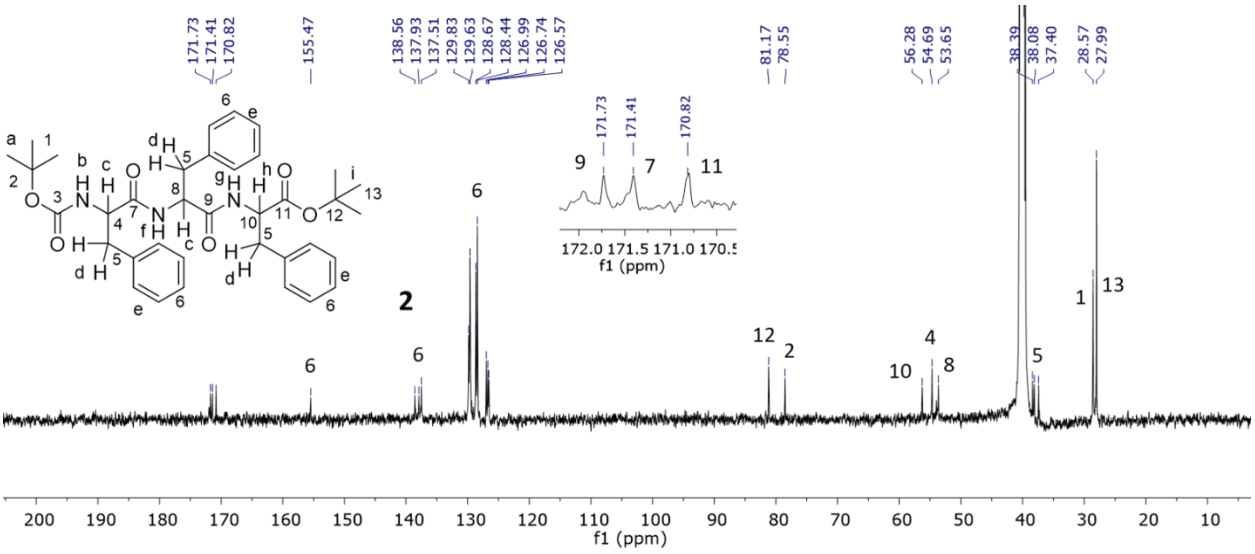


**Figure S7.** $^{13}$C NMR (126 MHz, $d_6$-DMSO) spectrum of Boc-Phe-Phe-Phe-O*t*Bu **2**.

### 1.1.3. Boc-Leu-Phe-O*t*Bu 3

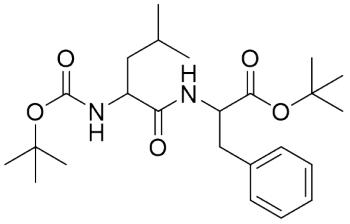

Yellow powder (63 % yield). **Melting point**: 123-126 ˚C.

**$^1$H NMR** (500 MHz, $d_6$-DMSO) δ 7.99 (d, $J$ = 7.6 Hz, 1H), 7.23 (dd, $J$ = 22.5, 7.1 Hz, 5H), 6.80 (d, $J$ = 8.7 Hz, 1H), 4.35 (q, $J$ = 7.5 Hz, 1H), 3.97 (dt, $J$ = 14.8, 7.0 Hz, 1H), 2.94 (qd, $J$ = 13.6, 6.9 Hz, 2H), 1.59 – 1.51 (m, 1H), 1.37 (s, 9H), 1.34 (m, 2H), 1.31 (s, 9H), 0.84 (dd, $J$ = 14.2, 6.6 Hz, 6H). Note: 1.34 ppm peak is hidden within 1.37 ppm and 1.31 ppm peaks.

**$^{13}$C NMR** (126 MHz, $d_6$-DMSO) δ 172.4, 170.3, 155.1, 137.1, 129.2, 128.1, 126.4, 80.6, 77.9, 53.8, 52.6, 40.8, 36.8, 28.1, 27.5, 24.1, 22.9, 21.5.

**HR-MS**: *m/z* for $C_{24}H_{38}N_2O_5$ $[M + Na]^+$ calculated 457.2600, found 457.2650.

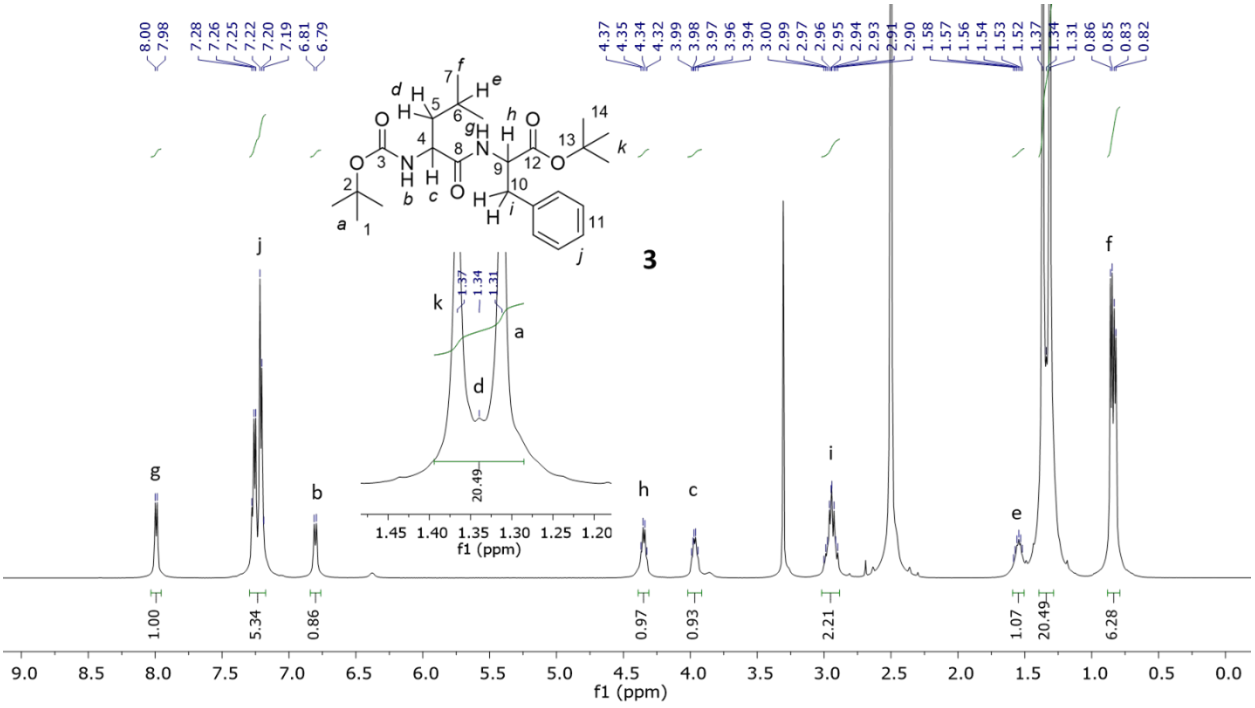


**Figure S8.** $^{1}$H NMR (500 MHz, $d_6$-DMSO) spectrum of Boc-Leu-Phe-O*t*Bu **3**.

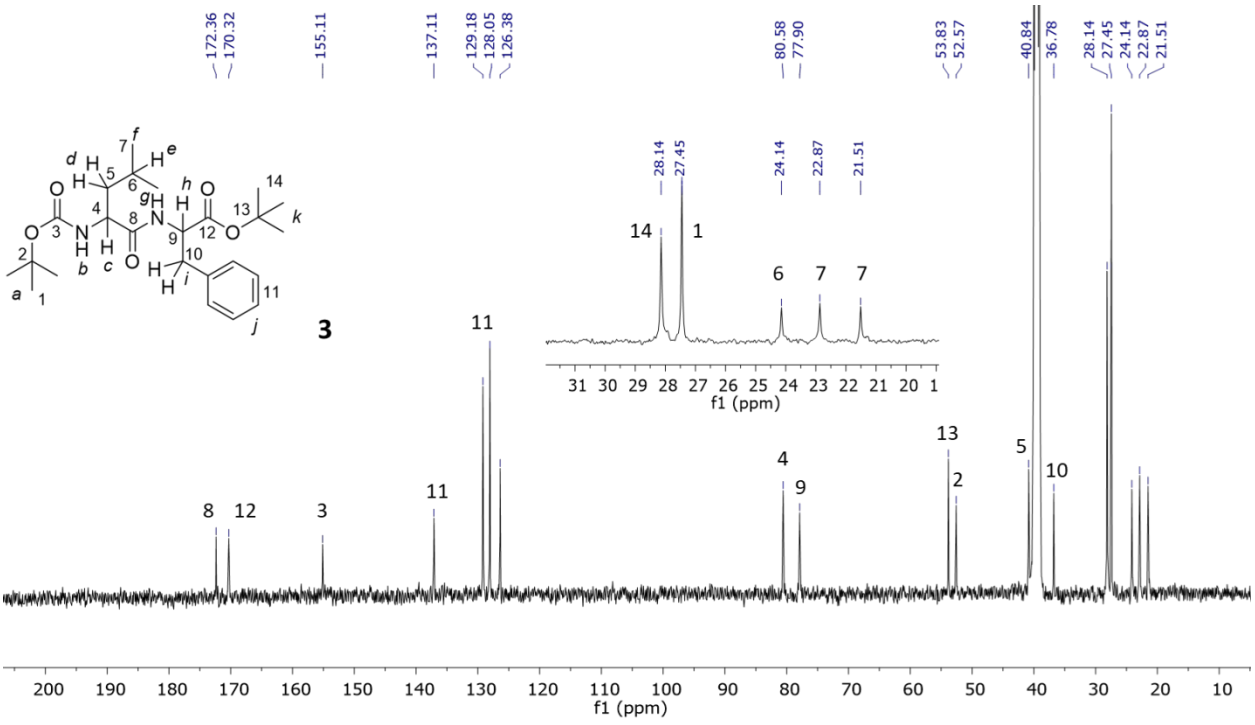


**Figure S9.** $^{13}$C NMR (126 MHz, $d_6$-DMSO) spectrum of Boc-Leu-Phe-O*t*Bu **3**.

### 1.1.4. Boc-Ile-Phe-O*t*Bu 4

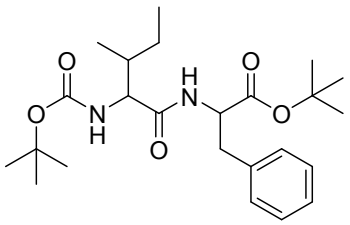

Yellow powder (54 % yield). **Melting point**: 106-110 ˚C.

**$^1$H NMR** (500 MHz, $d_6$-DMSO) δ 8.11 (d, $J$ = 7.7 Hz, 1H), 7.22 (dq, $J$ = 14.9, 7.6 Hz, 5H), 6.56 (d, $J$ = 9.3 Hz, 1H), 4.37 (d, $J$ = 7.4 Hz, 1H), 3.82 (t, $J$ = 8.4 Hz, 1H), 2.91 (qd, $J$ = 13.8, 7.4 Hz, 2H), 1.64 – 1.56 (m, 1H), 1.36 (s, 9H), 1.32 (m, 1H), 1.29 (s, 9H), 1.02 (dt, $J$ = 14.6, 7.7 Hz, 1H), 0.80 – 0.69 (m, 6H). Note: 1.32 ppm peak is hidden within 1.36 ppm and 1.29 ppm peaks.

**$^{13}$C NMR** (126 MHz, $d_6$-DMSO) δ 171.2, 170.4, 155.1, 137.1, 129.1, 128.1, 126.4, 80.5, 77.9, 58.5, 53.9, 36.9, 36.7, 28.1, 27.5, 24.2, 15.2, 10.9.

**HR-MS**: *m/z* for $C_{24}H_{38}N_2O_5$ $[M + Na]^+$ calculated 457.2600, found 457.2682.

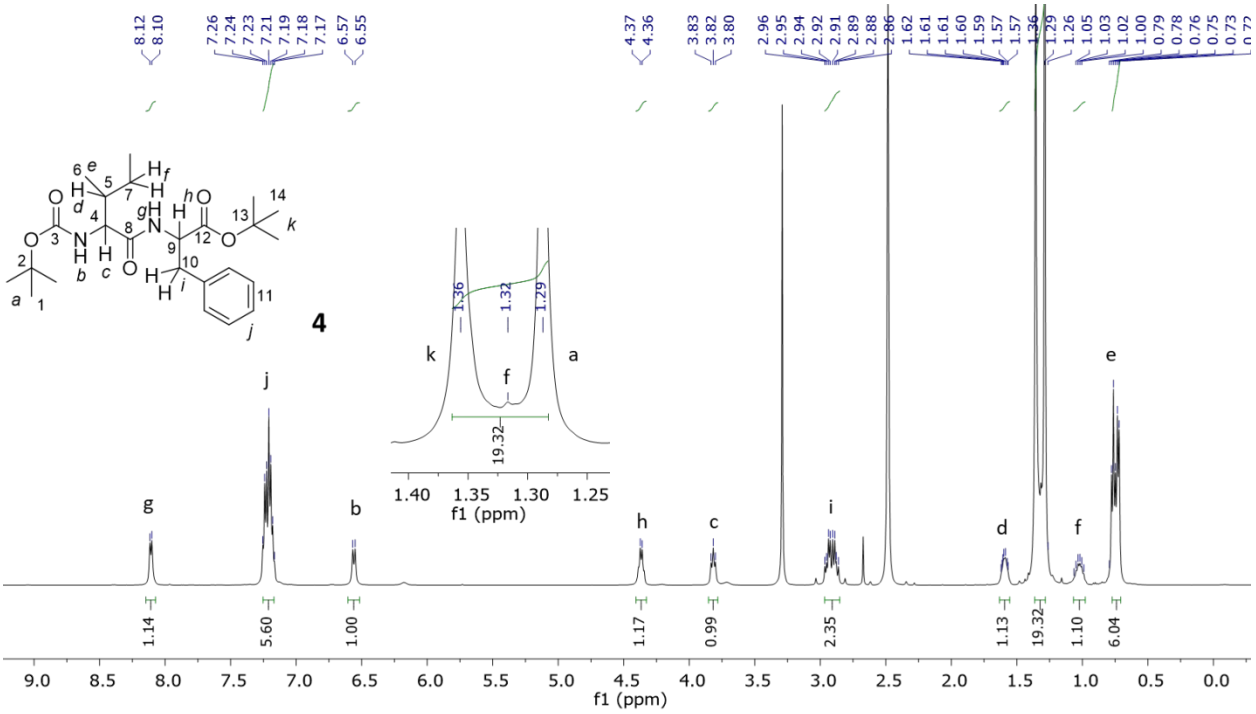


**Figure S10.** $^{1}$H NMR (500 MHz, $d_6$-DMSO) spectrum of Boc-Ile-Phe-O*t*Bu **4**.

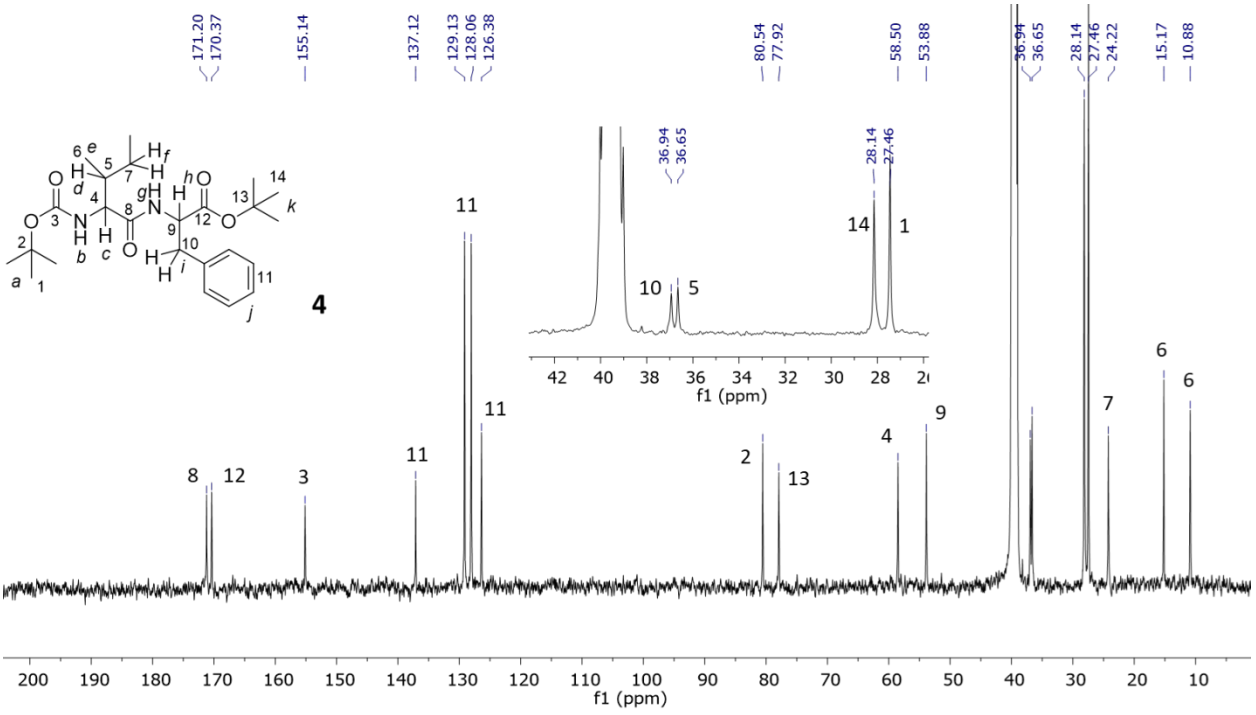


**Figure S11.** $^{13}$C NMR (126 MHz, $d_6$-DMSO) spectrum of Boc-Ile-Phe-O*t*Bu **4**.

### 1.1.5. Boc-Val-Phe-O*t*Bu 5

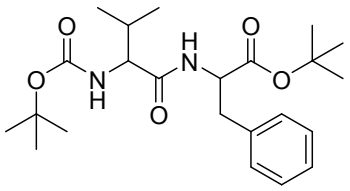

Yellow powder (60 % yield). **Melting point**: 110-113 ˚C.

**$^1$H NMR** (500 MHz, $d_6$-DMSO) δ 8.13 (d, $J$ = 7.7 Hz, 1H), 7.23 (dp, $J$ = 21.7, 7.4 Hz, 5H), 6.54 (d, $J$ = 9.2 Hz, 1H), 4.38 (q, $J$ = 7.5 Hz, 1H), 3.84 – 3.78 (m, 1H), 2.93 (qd, $J$ = 13.8, 7.4 Hz, 2H), 1.87 (h, $J$ = 6.9 Hz, 1H), 1.30 (s, 9H), 1.37 (s, 9H), 0.78 (dd, $J$ = 6.8, 3.2 Hz, 6H).

**$^{13}$C NMR** (126 MHz, $d_6$-DMSO) δ 171.2, 170.4, 155.3, 137.1, 129.1, 128.1, 126.4, 80.6, 77.9, 59.4, 53.9, 36.9, 30.5, 28.1, 27.4, 19.1, 18.0.

**HR-MS**: *m/z* for $C_{23}H_{36}N_2O_5$ $[M + Na]^+$ calculated 443.2400, found 443.2528.

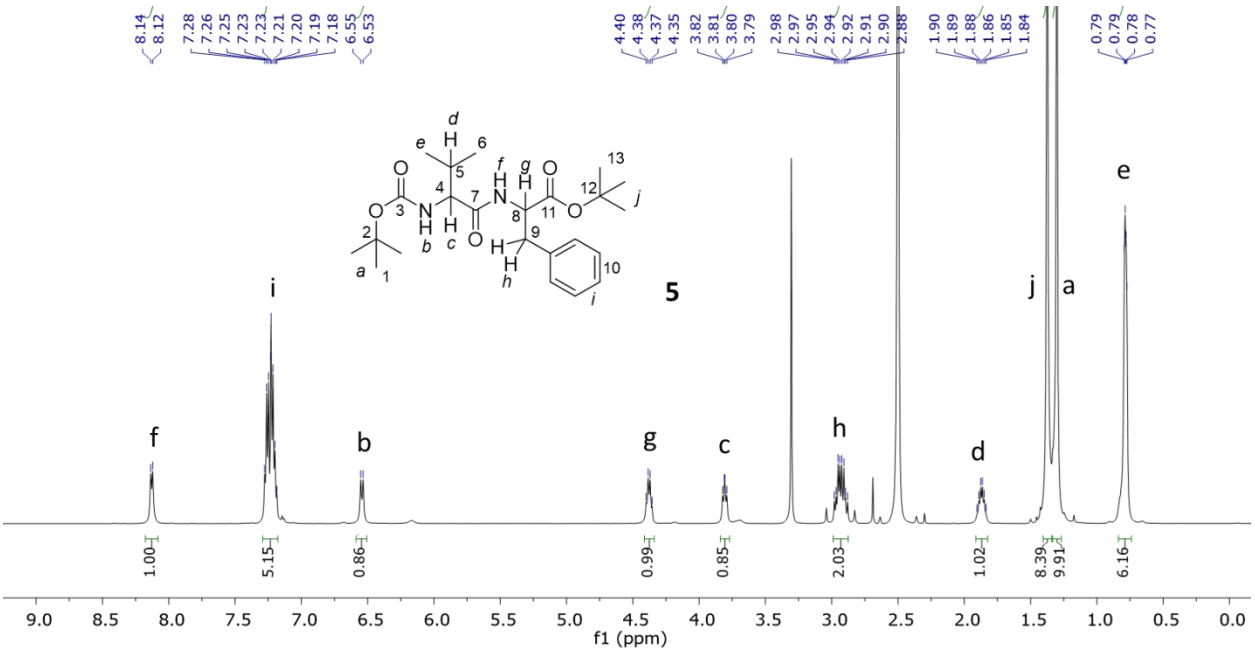

**Figure S12.** $^{1}$H NMR (500 MHz, $d_6$-DMSO) spectrum of Boc-Val-Phe-O*t*Bu **5**.

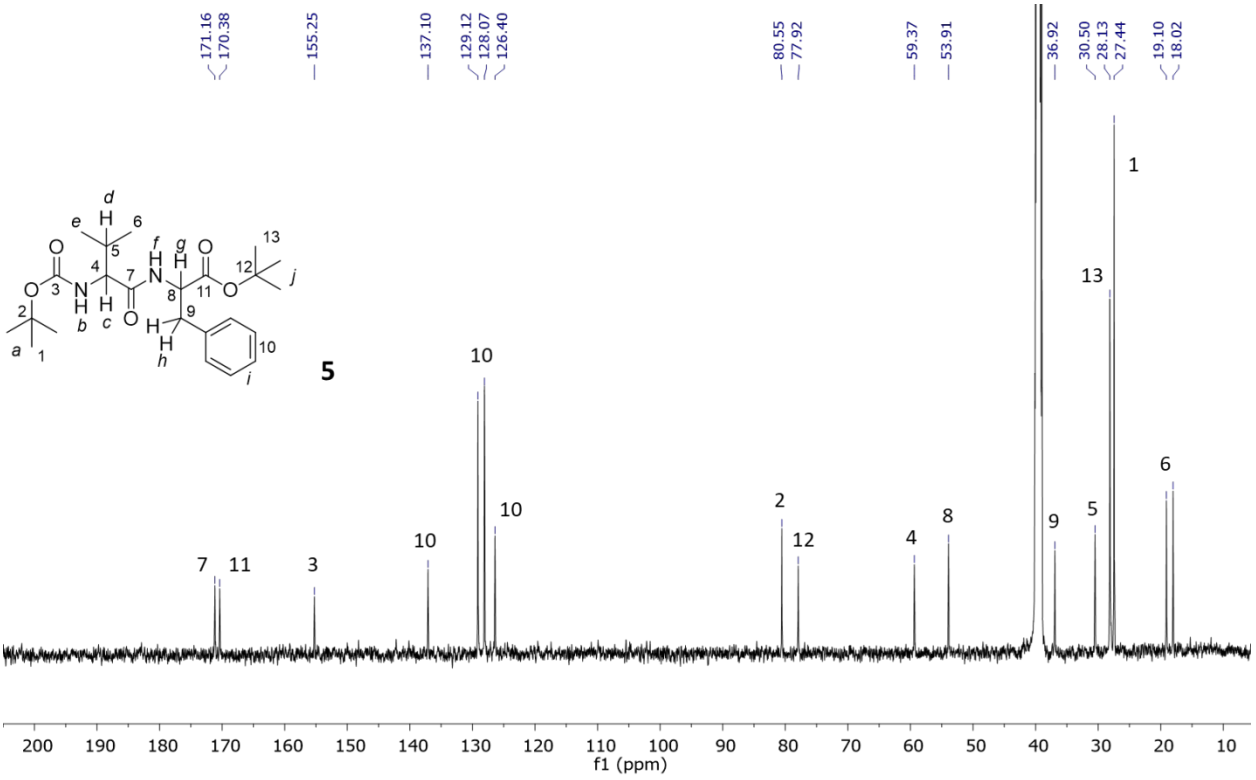


**Figure S13.** $^{13}$C NMR (126 MHz, $d_6$-DMSO) spectrum of Boc-Val-Phe-O*t*Bu **5**.

### 1.1.6. Boc-Ala-Phe-O*t*Bu 6

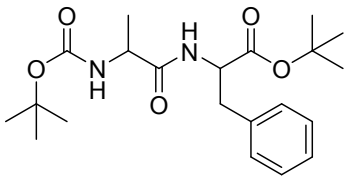

Yellow powder (54 % yield). **Melting point**: 44-47 ˚C.

**$^1$H NMR** (500 MHz, $d_6$-DMSO) δ 7.96 (d, $J$ = 7.6 Hz, 1H), 7.22 (dd, $J$ = 24.0, 7.3 Hz, 5H), 6.83 (d, $J$ = 7.9 Hz, 1H), 4.31 (q, $J$ = 7.3 Hz, 1H), 3.96 (p, $J$ = 7.3 Hz, 1H), 2.92 (h, $J$ = 7.6 Hz, 2H), 1.35 (s, 9H), 1.29 (s, 9H), 1.12 (d, $J$ = 7.2 Hz, 3H).

**$^{13}$C NMR** (126 MHz, $d_6$-DMSO) δ 172.6, 170.3, 154.9, 137.1, 129.2, 128.1, 126.4, 80.6, 78.0, 53.9, 49.4, 36.8, 28.2, 27.5, 18.2.

**HR-MS**: *m/z* for $C_{21}H_{32}N_2O_5$ $[M + Na]^+$ calculated 415.2100, found 415.2215.

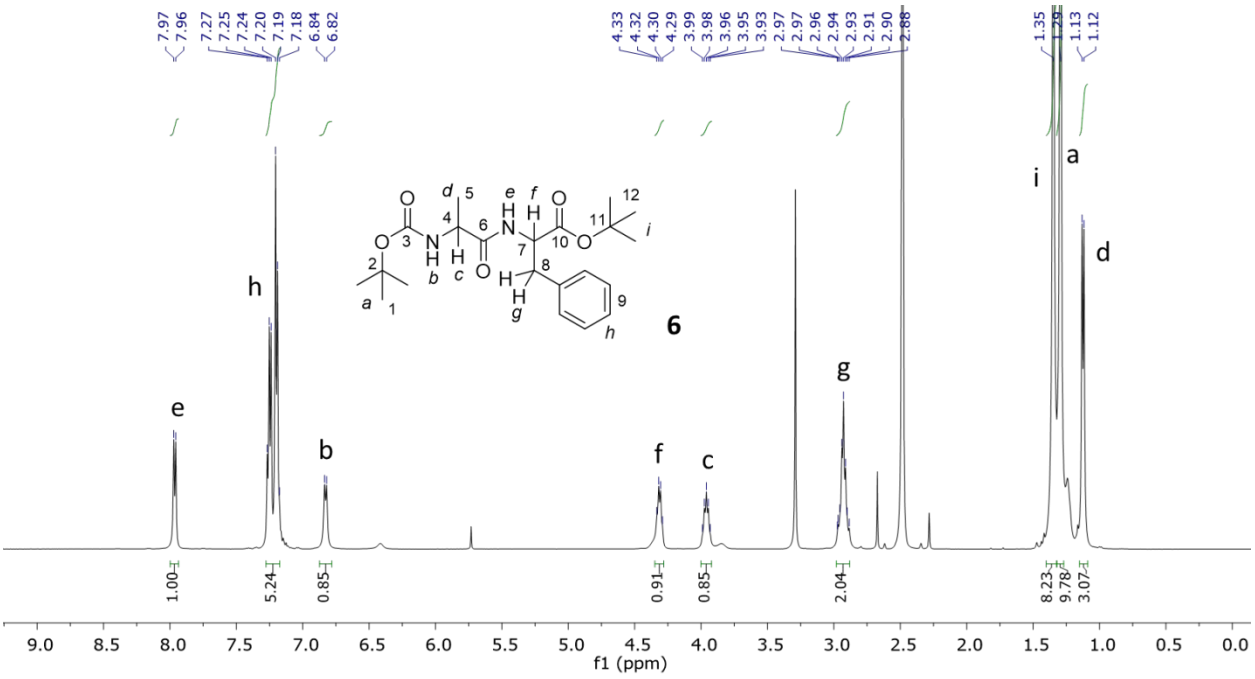


**Figure S14.** $^1$H NMR (500 MHz, $d_6$-DMSO) spectrum of Boc-Ala-Phe-O*t*Bu **6**.

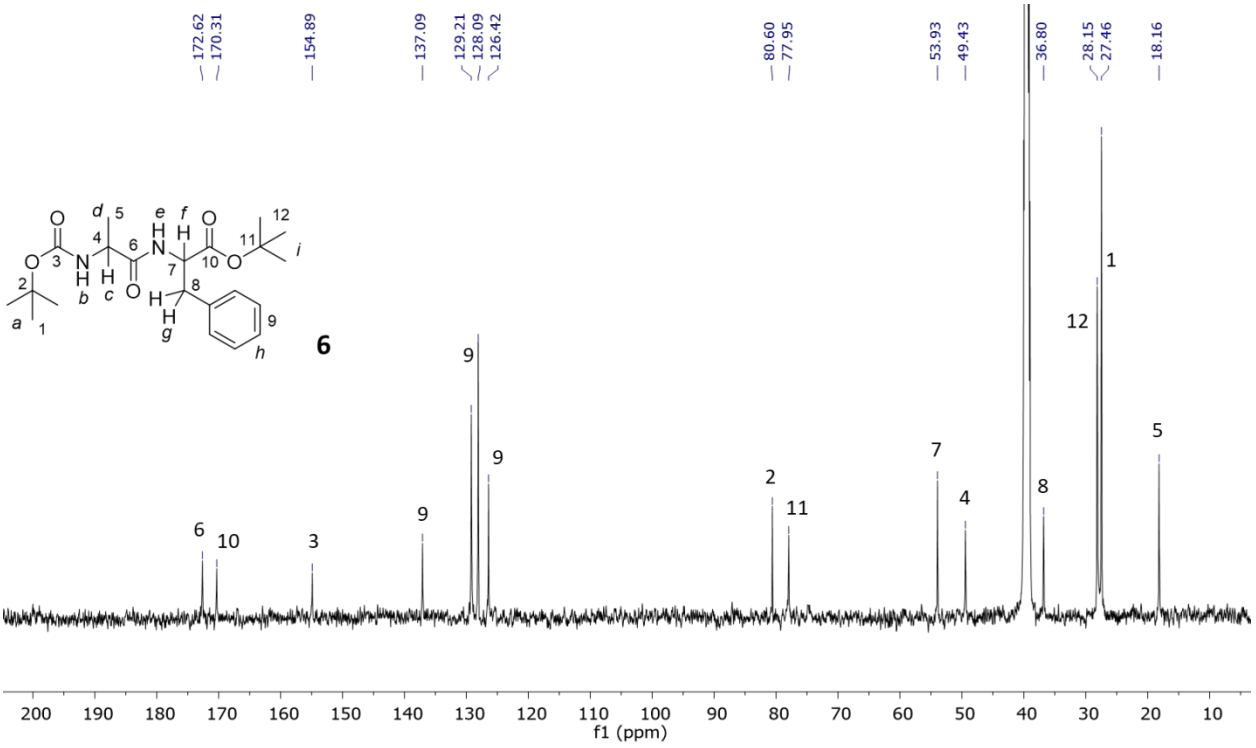


**Figure S15.** $^{13}$C NMR (126 MHz, $d_6$-DMSO) spectrum of Boc-Ala-Phe-O*t*Bu **6**.

### 1.1.7. Boc-Gly-Phe-O*t*Bu 7

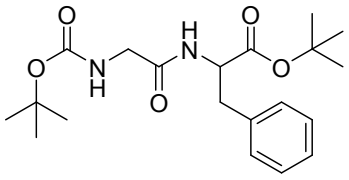

Yellow oil (66 % yield).

**$^1$H NMR** (500 MHz, $d_6$-DMSO) δ 8.03 (d, $J$ = 7.8 Hz, 1H), 7.24 (dt, $J$ = 31.3, 7.4 Hz, 5H), 6.91 (t, $J$ = 6.2 Hz, 1H), 4.37 (q, $J$ = 7.4 Hz, 1H), 3.57 – 3.51 (m, 1H), 2.98 – 2.88 (m, 2H), 1.37 (s, 9H), 1.31 (s, 9H).

**$^{13}$C NMR** (126 MHz, $d_6$-DMSO) δ 170.4, 169.3, 155.7, 137.0, 129.2, 128.1, 126.5, 80.7, 78.0, 53.9, 42.9, 37.0, 28.1, 27.5.

**HR-MS**: *m/z* for $C_{20}H_{30}N_2O_5$ [M + Na]$^+$ calculated 401.2000, found 401.2068.

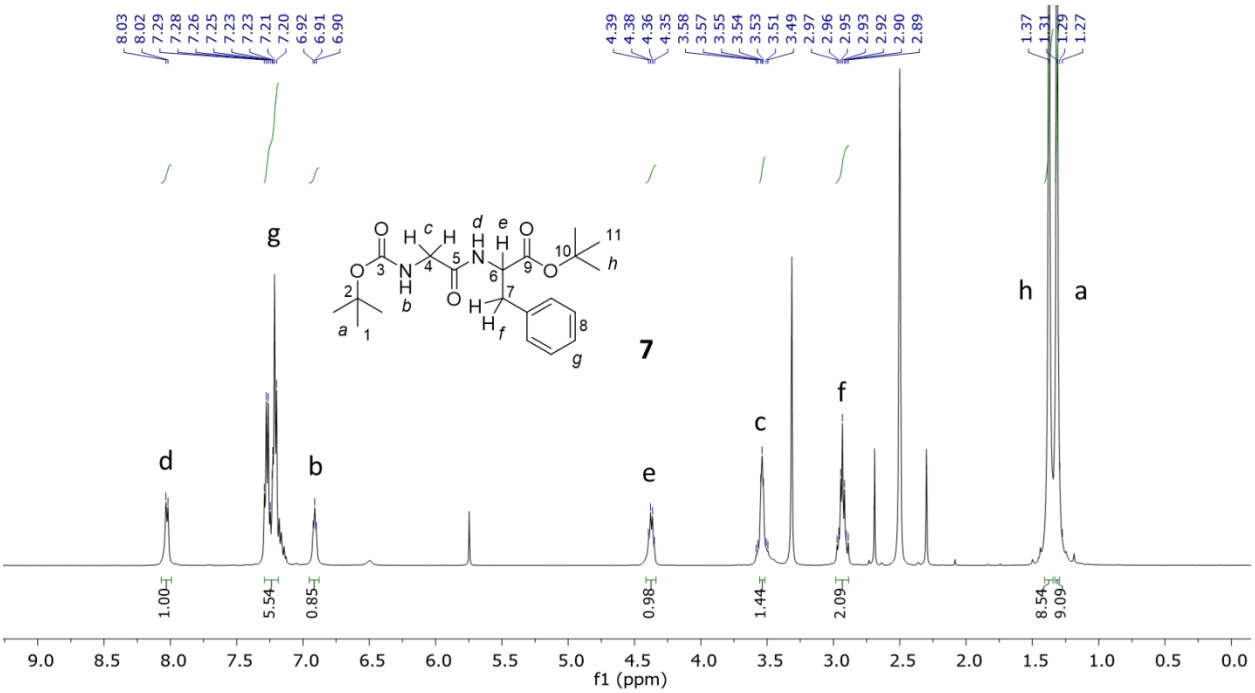


**Figure S16.** $^1$H NMR (500 MHz, $d_6$-DMSO) spectrum of Boc-Gly-Phe-O*t*Bu **7**.

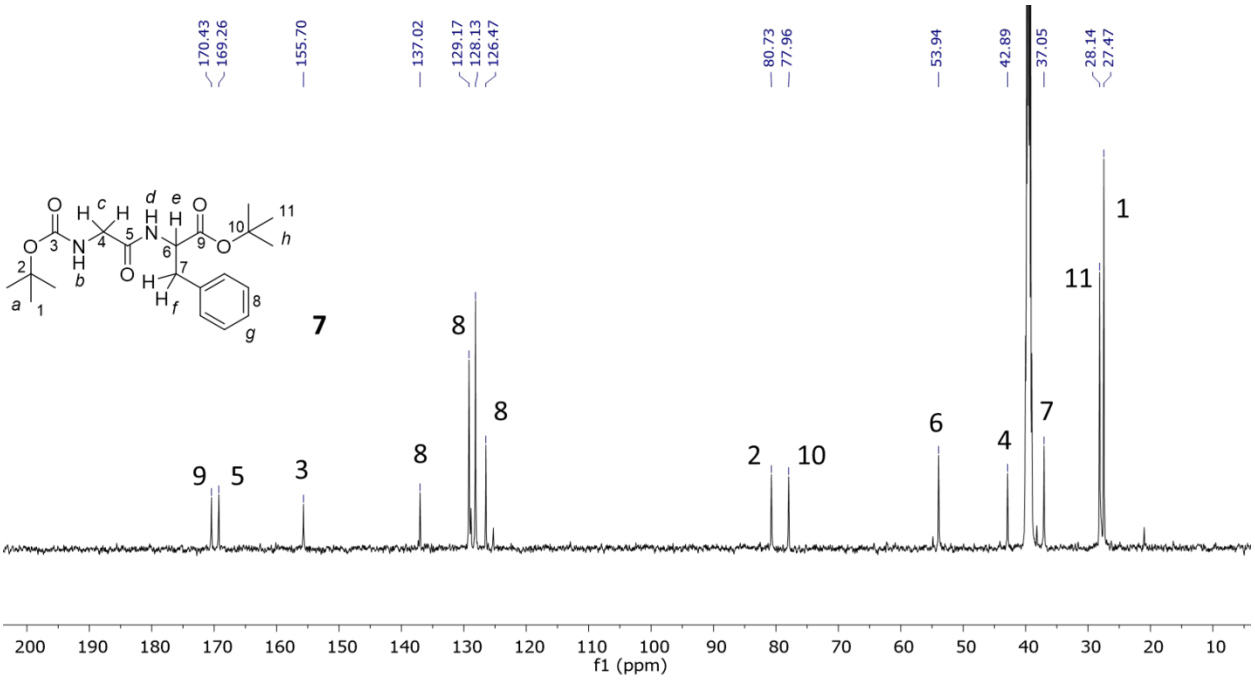

**Figure S17.** $^{13}$C NMR (126 MHz, $d_6$-DMSO) spectrum of Boc-Gly-Phe-O*t*Bu **7**.

### 1.1.8. Boc-Tyr-Phe-O*t*Bu 8

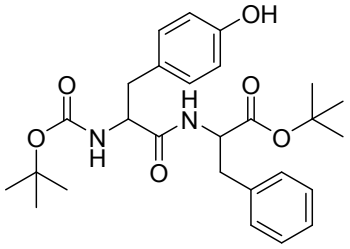


Yellow powder (63 % yield). **Melting point**: 77-84 ˚C.

**$^1$H NMR** (500 MHz, $d_6$-DMSO) δ 9.12 (s, 1H), 8.15 (d, $J$ = 7.5 Hz, 1H), 7.29 – 7.21 (m, 6H), 7.01 (d, $J$ = 8.1 Hz, 2H), 6.73 (d, $J$ = 8.7 Hz, 1H), 6.63 (d, $J$ = 8.0 Hz, 2H), 4.36 (q, $J$ = 7.3 Hz, 1H), 4.09 (td, $J$ = 9.5, 4.0 Hz, 1H), 3.01 – 2.92 (m, 2H), 2.80 (dd, $J$ = 14.0, 4.1 Hz, 1H), 2.58 (dd, $J$ = 13.9, 10.3 Hz, 1H), 1.31 (s, 9H), 1.30 (s, 9H).

**$^{13}$C NMR** (126 MHz, $d_6$-DMSO) δ 172.3, 170.9, 156.2, 155.6, 137.6, 130.5, 129.7, 129.4, 128.6, 127.0, 125.8, 115.3, 81.2, 78.4, 56.3, 54.5, 37.4, 37.1, 28.6, 28.0.

**HR-MS**: *m/z* for $C_{27}H_{36}N_2O_6$ $[M + Na]^+$ calculated 507.2400, found 507.2461.

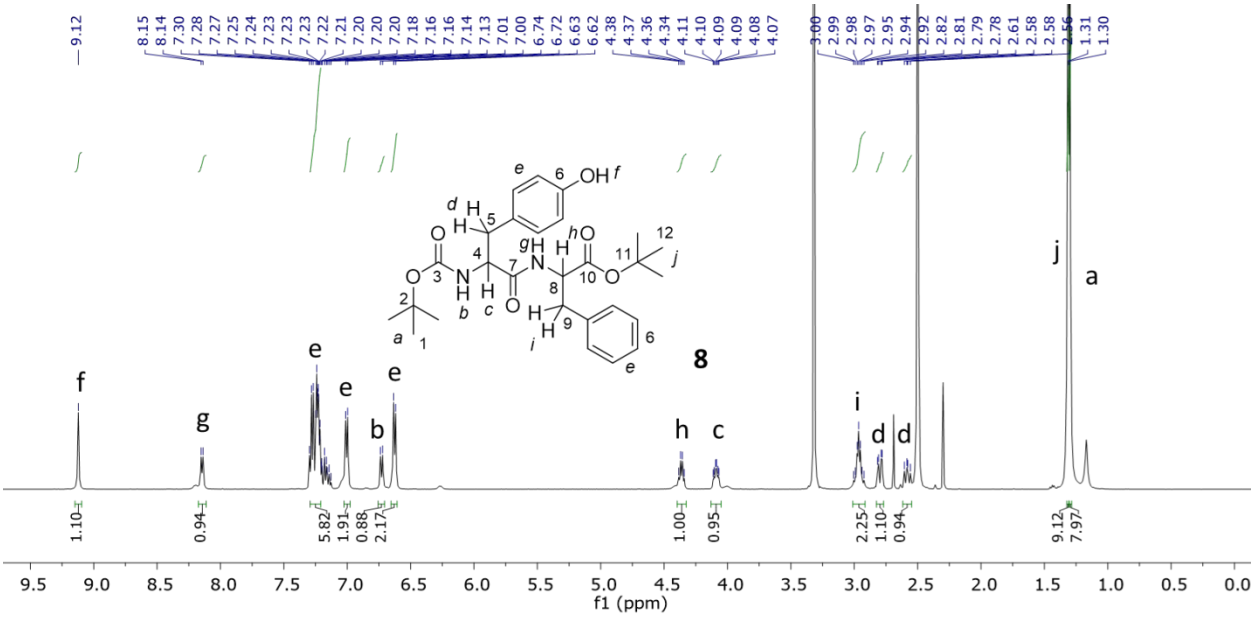


**Figure S18.** $^{1}$H NMR (500 MHz, $d_6$-DMSO) spectrum of Boc-Tyr-Phe-O*t*Bu **8**.

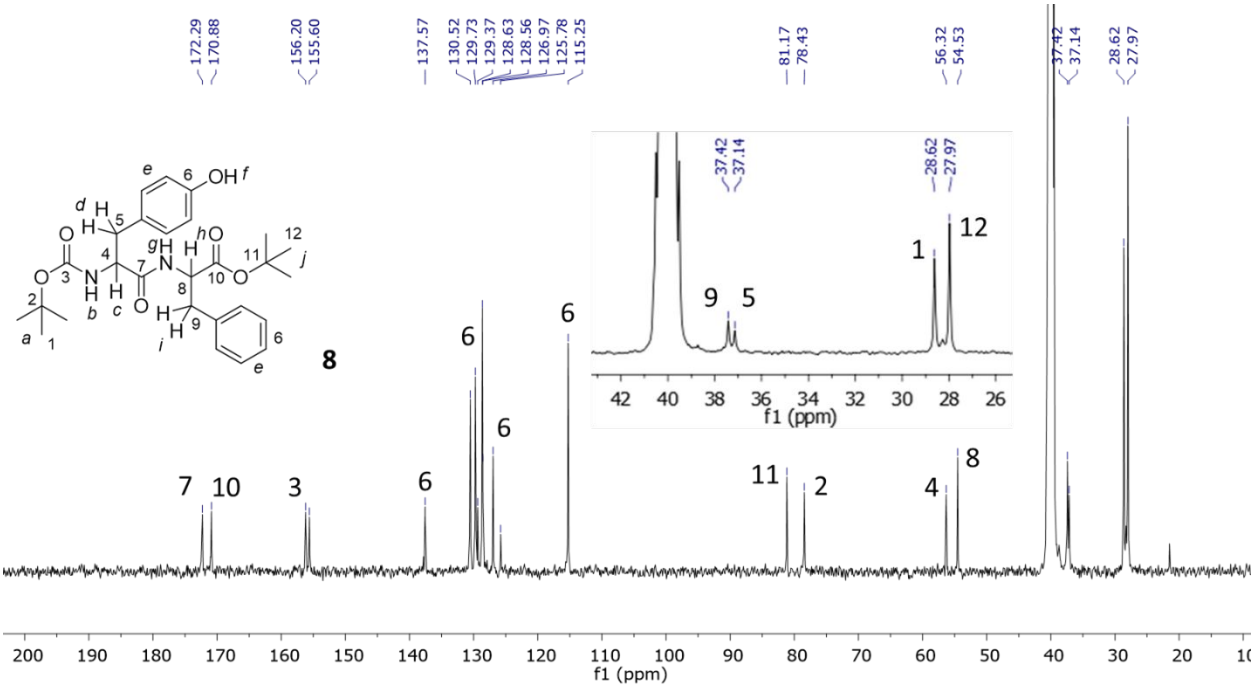


**Figure S19.** $^{13}$C NMR (126 MHz, $d_6$-DMSO) spectrum of Boc-Tyr-Phe-O*t*Bu **8**.

### 1.2. Synthesis of monoprotected compounds 1a-3a

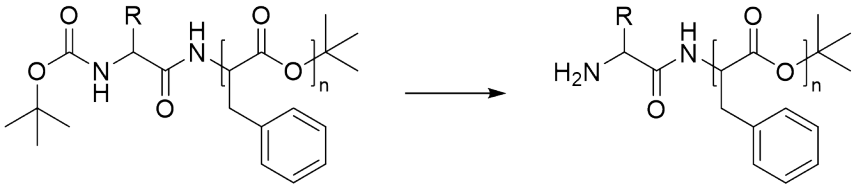

General protocol: Boc-protected precursor (1.0 equivalent) was suspended in *t*BuOAc at a concentration of 0.2 M. Concentrated $H_2SO_4$ (5.0 equivalent) was then added dropwise at R.T. After 1 hour, the reaction mixture was neutralised with a saturated solution of $NaHCO_3$ and extracted with ethyl acetate. The organic phase was then dried with $MgSO_4$ and evaporated under vacuum, yielding the desired compounds.

#### 1.2.1. Phe-Phe-O*t*Bu 1a

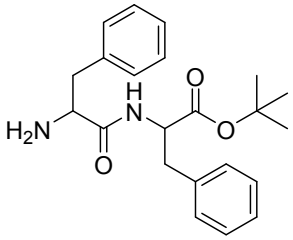

Yellow powder (95 % yield). **Melting point**: 63-67 °C.

**$^1$H NMR** (500 MHz, $d_6$-DMSO) δ 8.16 (d, $J$ = 8.0 Hz, 1H), 7.30 – 7.12 (m, 10H), 4.43 (q, $J$ = 7.2 Hz, 1H), 3.40 (dd, $J$ = 8.4, 4.6 Hz, 1H), 2.92 (dd, $J$ = 22.4, 5.8 Hz, 3H), 2.59 – 2.55 (m, 1H), 1.65 (s, 2H), 1.33 (s, 9H).

**$^{13}$C NMR** (126 MHz, $d_6$-DMSO) δ 174.2, 170.6, 138.7, 137.1, 129.5, 129.4, 128.3, 128.2, 126.7, 126.3, 81.0, 55.9, 53.6, 40.9, 37.4, 27.7.

**HR-MS**: *m/z* for $C_{22}H_{28}N_2O_3$ $[M + H]^+$ calculated 369.2100, found 369.2161.

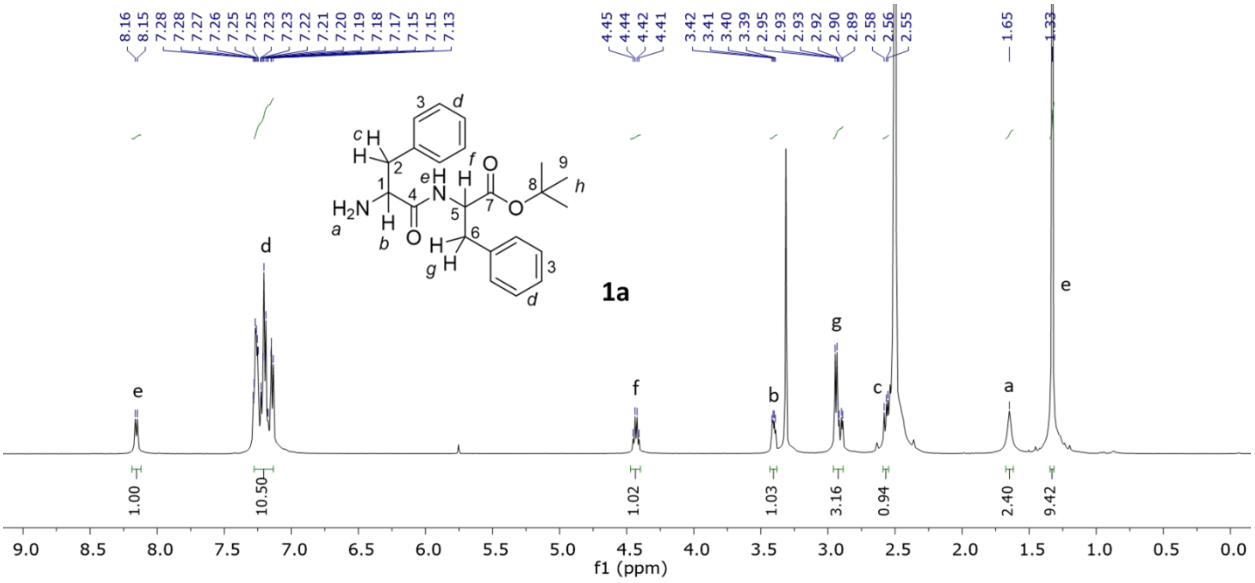


**Figure S20.** $^{1}$H NMR (500 MHz, $d_6$-DMSO) spectrum of Phe-Phe-O*t*Bu **1a**.

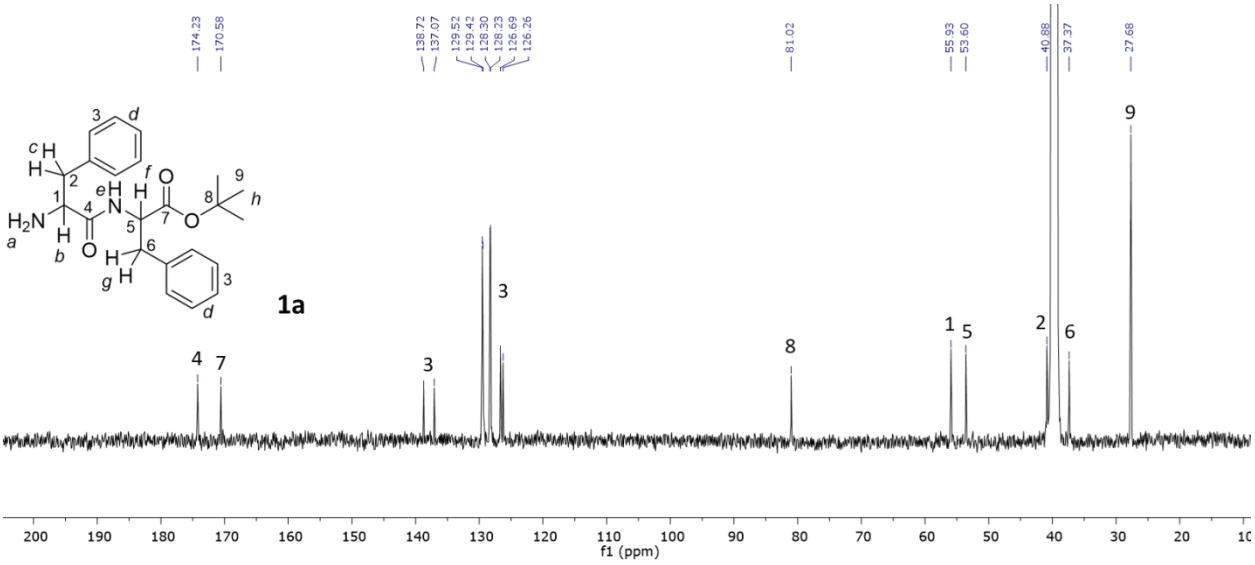


**Figure S21.** $^{13}$C NMR (126 MHz, $d_6$-DMSO) spectrum of Phe-Phe-O*t*Bu **1a**.

### 1.2.2. Phe-Phe-Phe-O*t*Bu 2a

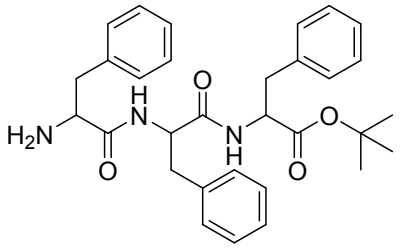

Colourless powder (95 % yield). **Melting point**: 184-187 ˚C.

**$^1$H NMR** (500 MHz, $d_6$-DMSO) δ 8.55 (d, $J$ = 7.5 Hz, 1H), 8.40 (s, 1H), 7.31 – 7.16 (m, 15H), 4.64 (td, $J$ = 8.6, 4.5 Hz, 1H), 4.40 (q, $J$ = 7.5 Hz, 1H), 3.66 (s, 1H), 3.05 – 2.90 (m, 4H), 2.81 (dd, $J$ = 13.9, 8.9 Hz, 1H), 2.70 – 2.62 (m, 1H), 1.32 (s, 9H).

**$^{13}$C NMR** (126 MHz, $d_6$-DMSO) δ 171.2, 170.9, 137.8, 137.5, 129.9, 129.8, 129.7, 128.8, 128.7, 128.5, 127.1, 127.0, 126.8, 81.2, 55.0, 54.7, 53.7, 38.4, 37.4, 28.0.

**HR-MS**: *m/z* for $C_{31}H_{37}N_3O_4$ $[M + H]^+$ calculated 516.2800, found 516.2876.

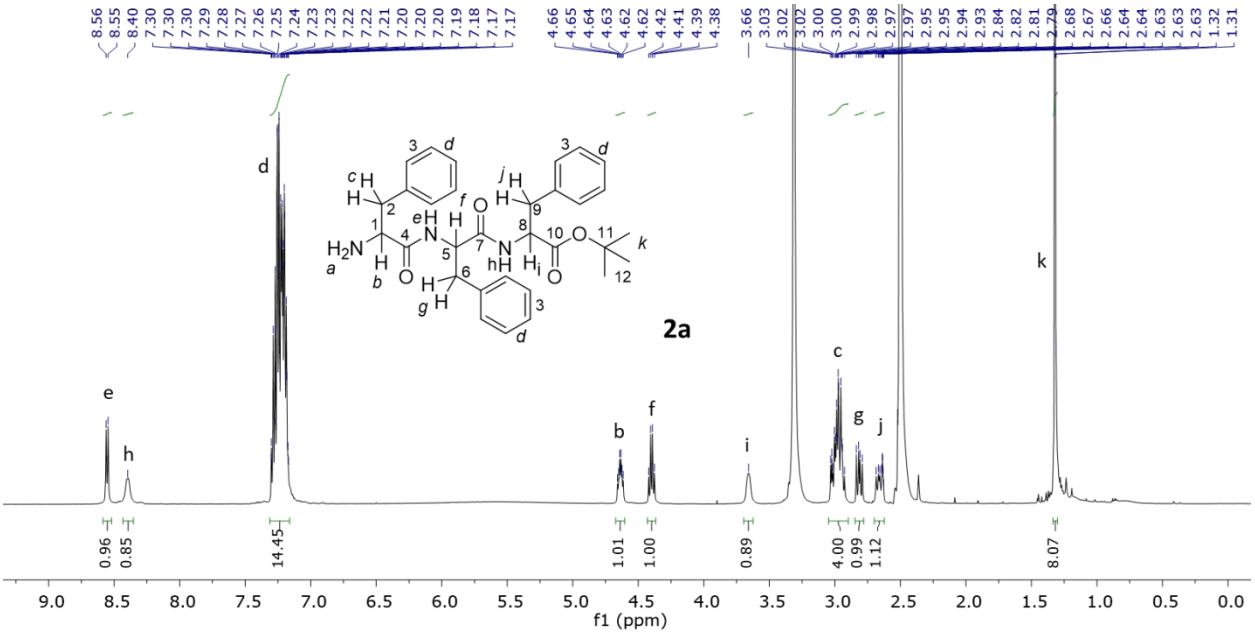


**Figure S22.** $^1$H NMR (500 MHz, $d_6$-DMSO) spectrum of Phe-Phe-Phe-O*t*Bu **2a**.

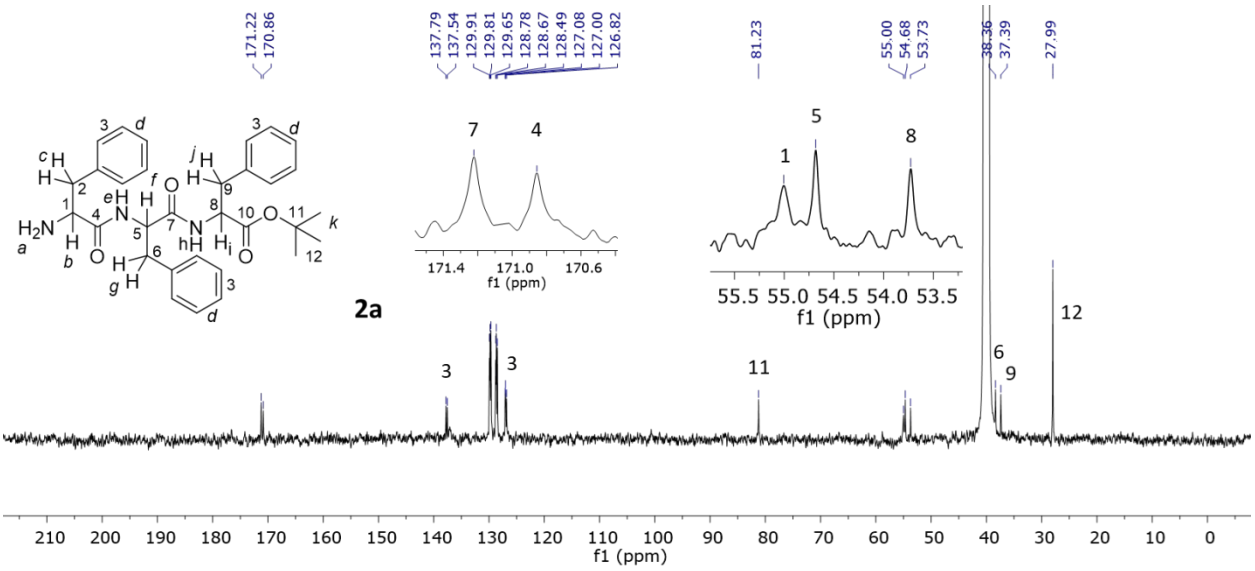


**Figure S23.** $^{13}$C NMR (126 MHz, $d_6$-DMSO) spectrum of Phe-Phe-Phe-O*t*Bu **2a**.

### 1.2.3. Leu-Phe-O*t*Bu 3a

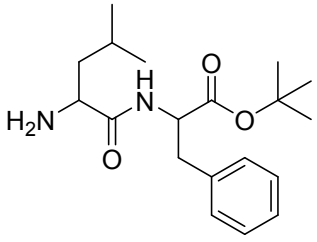

Yellow powder (78 % yield). **Melting point**: 88-93 ˚C.

**$^1$H NMR** (500 MHz, $d_6$-DMSO) δ 8.13 (d, $J$ = 8.0 Hz, 1H), 7.30 – 7.17 (m, 5H), 4.41 (q, $J$ = 7.3 Hz, 1H), 3.15 (dd, $J$ = 9.0, 5.3 Hz, 1H), 2.96 (qd, $J$ = 13.7, 7.1 Hz, 2H), 1.82 (d, $J$ = 25.1 Hz, 2H), 1.66 (dq, $J$ = 13.3, 6.8 Hz, 1H), 1.33 (s, 9H), 1.14 (ddd, $J$ = 14.0, 8.9, 5.9 Hz, 1H), 0.84 (dd, $J$ = 19.2, 6.6 Hz, 6H).

**$^{13}$C NMR** (126 MHz, $d_6$-DMSO) δ 175.3, 170.5, 137.0, 129.2, 128.1, 126.5, 80.7, 53.4, 52.8, 44.1, 37.1, 27.5, 24.0, 23.2, 21.8.

**HR-MS**: *m/z* for $C_{19}H_{30}N_2O_3$ $[M + H]^+$ calculated 335.2300, found 335.2327.

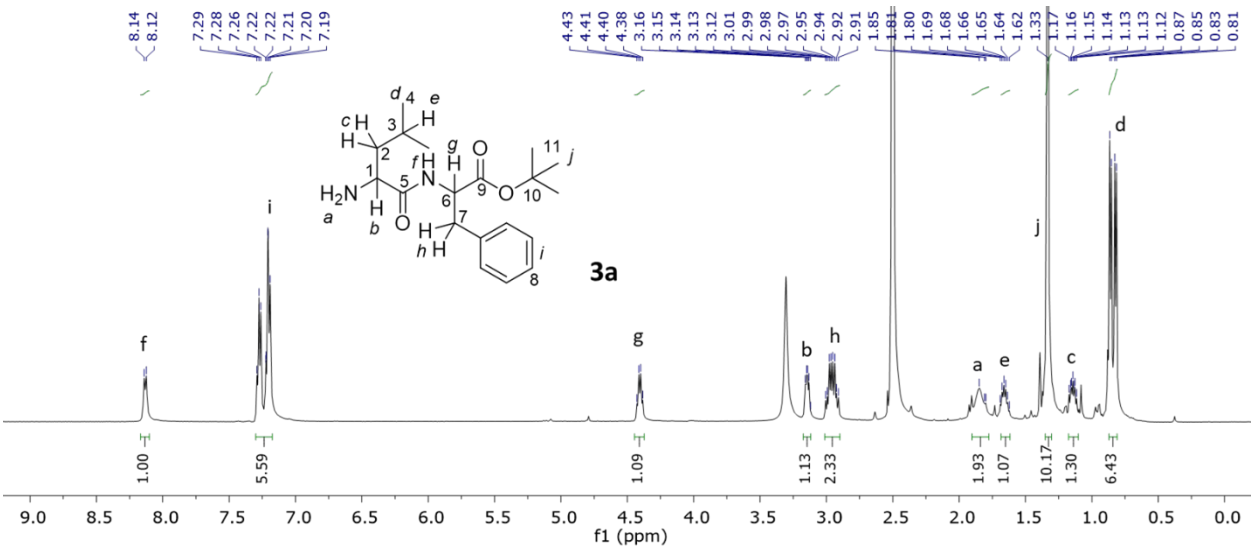


**Figure S24.** $^1$H NMR (500 MHz, $d_6$-DMSO) spectrum of Leu-Phe-O*t*Bu **3a**.

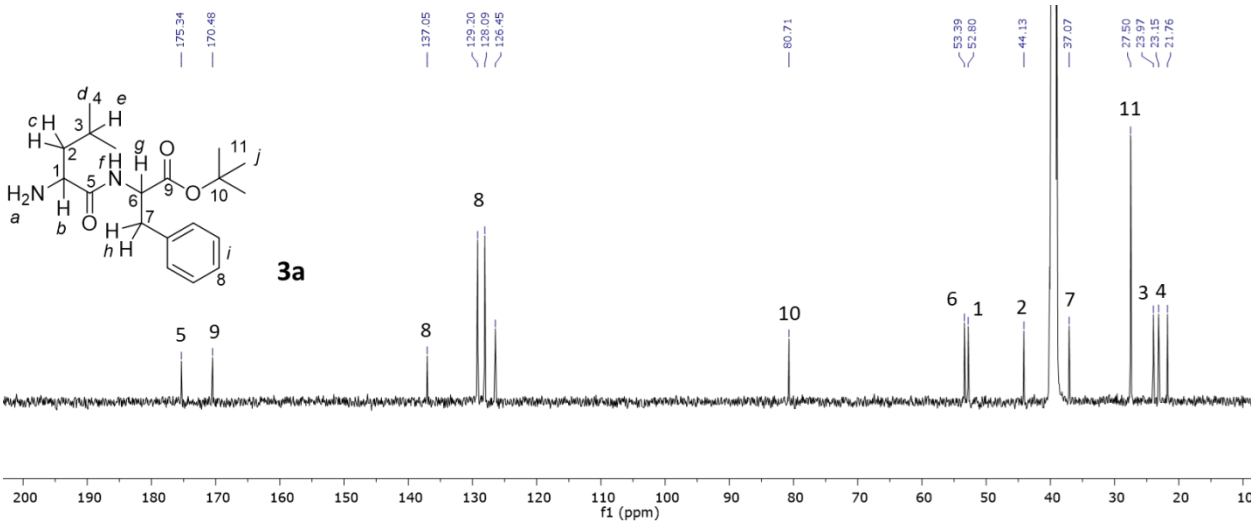


**Figure S25.** $^{13}$C NMR (126 MHz, $d_6$-DMSO) spectrum of Leu-Phe-O*t*Bu **3a**.

## 2 Gelation and gel characterization

### 2.1 Gelation protocol

Gel systems **I**, **II** and **III**: The precursor gelator (**1**, **2**, and **3**, respectively) was suspended in *t*BuOAc solvent (0.05M) and sonicated until a fine suspension formed, followed by the addition of concentrated $H_2SO_4$ (1.0 equivalent). The mixture was gently swirled and left to rest at R.T. for at least 12 h. Gelation was verified by the vial inversion method.

Gel system **IV**: The precursor gelators **1** and **2** were suspended in *t*BuOAc (1:1 ratio, final concentration 0.05 M) and sonicated until a fine suspension formed, followed by the addition of concentrated $H_2SO_4$ (1.0 equivalent). The mixture was gently swirled and left to rest at R.T. for at least 12 h. Gelation was verified by the vial inversion method.

## 2.2 Gel characterization by NMR

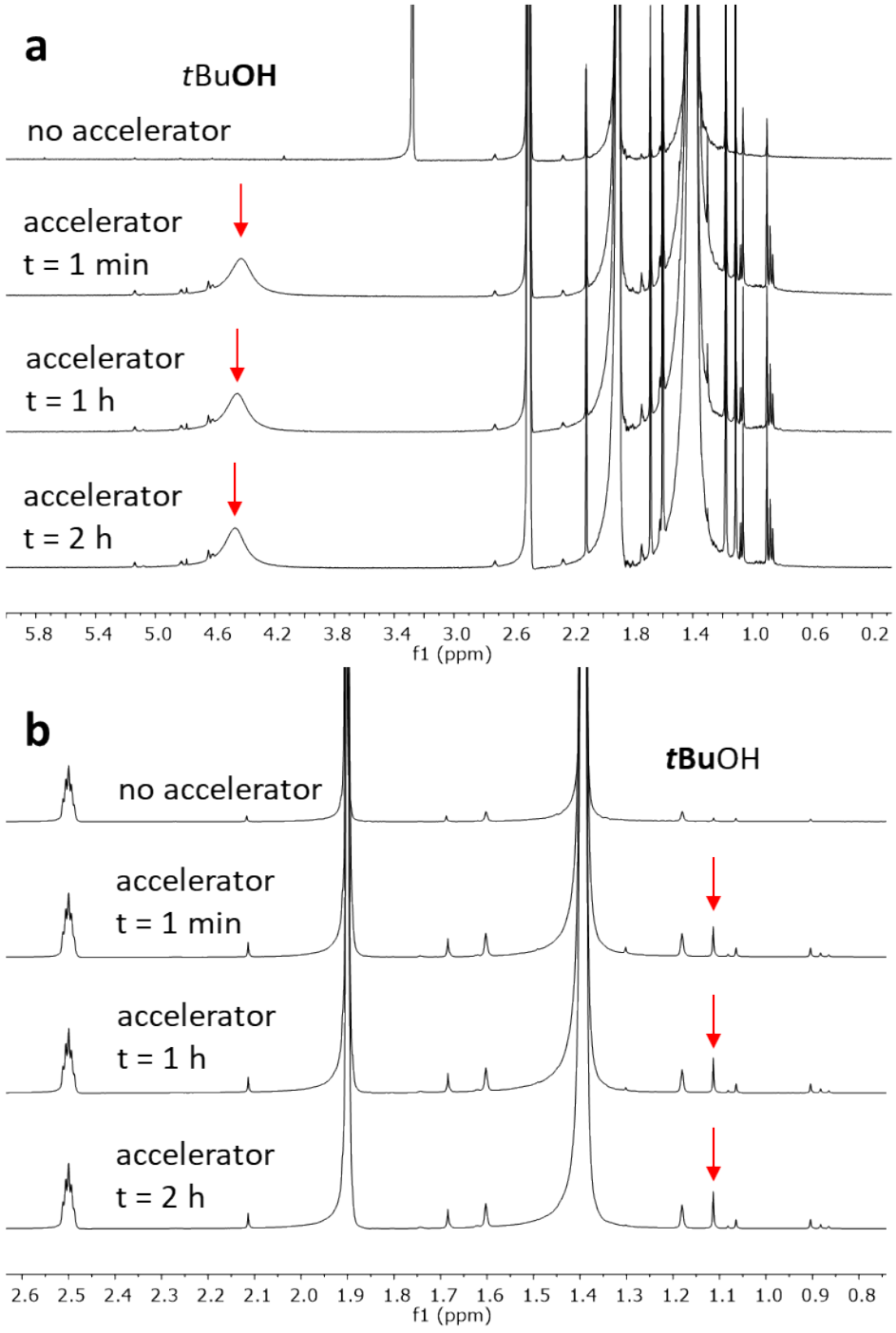


**Figure S26.** $^{1}$H NMR (300 MHz, $d_6$-DMSO) spectrum of *t*BuOAc solvent in **a)** hydroxyl region and **b)** methyl region. Before addition of accelerator (top rows) and hourwise monitoring.

### 2.2.1 Gel system I: Precursor Boc-Phe-Phe-O*t*Bu 1

*0.05 M, 1.0 eq $H_2SO_4$, day 1*

**$^1$H NMR** (300 MHz, $d_6$-DMSO) δ 8.89 (d, $J$ = 7.5 Hz, 1H), 8.83 (d, $J$ = 7.8 Hz, 1H), 8.05 (d, $J$ = 7.3 Hz, 6H), 7.37 – 7.21 (m, 20H), 4.58 – 4.46 (m, 1H), 4.04 (s, 2H), 3.13 (ddd, $J$ = 13.8, 10.7, 5.4 Hz, 3H), 3.02 – 2.89 (m, 3H), 1.32 (s, 9H).

**$^{13}$C NMR** (75 MHz, $d_6$-DMSO) δ 172.7, 170.4, 168.6, 168.6, 137.6, 137.2, 135.1, 135.1, 130.1, 129.7, 129.6, 129.0, 128.8, 128.8, 127.7, 127.7, 127.2, 127.2, 81.7, 54.9, 54.3, 53.6, 37.5, 37.4, 37.2, 28.0.

**HR-MS**: *m/z* for $C_{22}H_{28}N_2O_3$ $[M + H]^+$ calculated 369.2100, found 369.2164. *m/z* for $C_{18}H_{20}N_2O_3$ $[M + H]^+$ calculated 313.1500, found 313.1536.

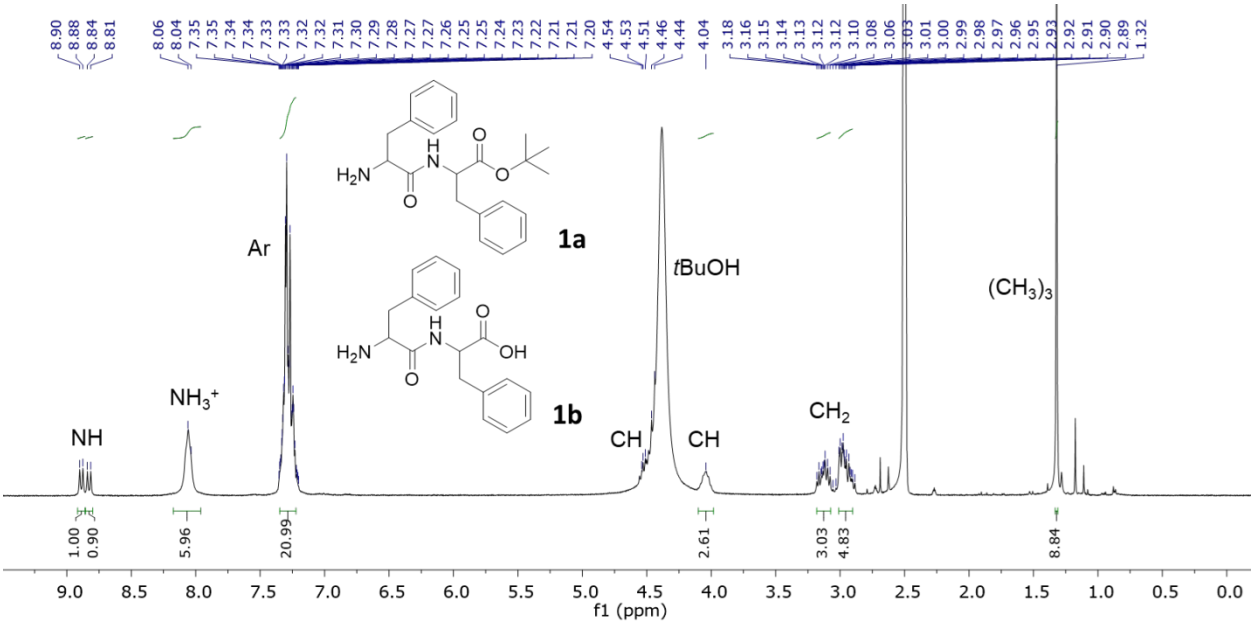


**Figure S27.** $^1$H NMR (300 MHz, $d_6$-DMSO) spectrum of xerogel **I**, 0.05M, 1.0 equivalent of $H_2SO_4$, day 1.

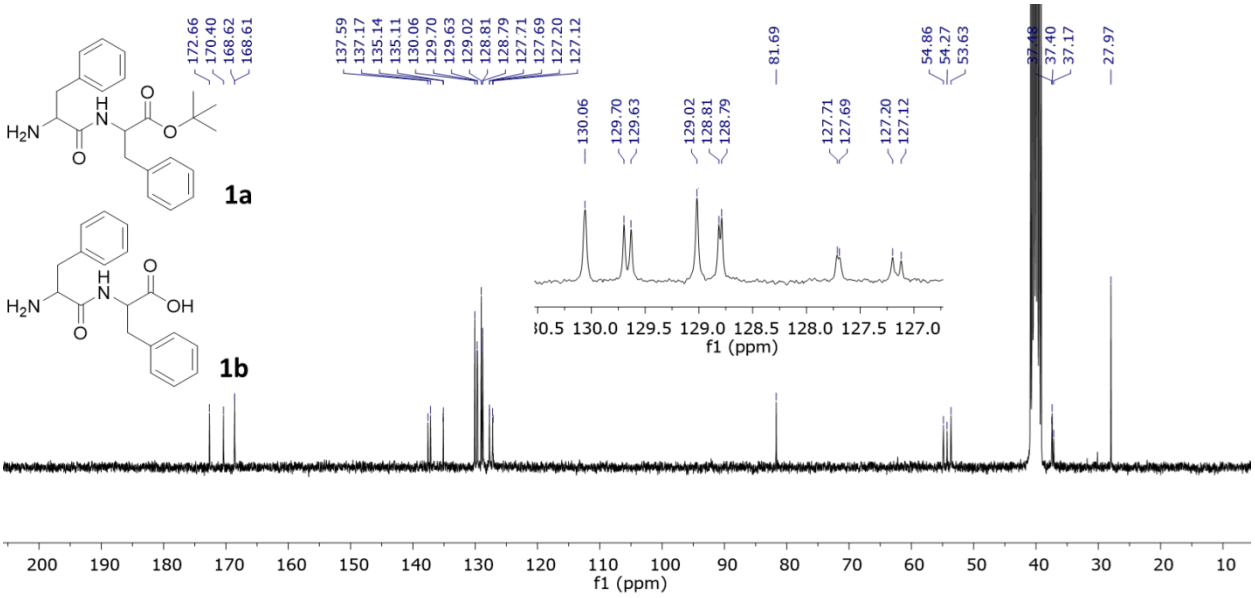


**Figure S28.** $^{13}$C NMR (75 MHz, $d_6$-DMSO) spectrum of xerogel **I**, 0.05M, 1.0 equivalent of $H_2SO_4$, day 1.

*0.05 M, 0.5 eq $H_2SO_4$, day 1*

**$^1$H NMR** (300 MHz, $d_6$-DMSO) δ 8.89 (d, $J$ = 7.5 Hz, 1H), 8.19 (d, $J$ = 7.5 Hz, 0.6H), 8.07 (s, 3H), 7.36 – 7.17 (m, 18H), 6.82 (d, $J$ = 8.6 Hz, 0.6H), 4.47 (t, $J$ = 7.3 Hz, 1H), 4.19 (s, 1H), 4.05 (s, 1H), 3.02 – 2.87 (m, 6H), 2.75 – 2.63 (m, 1H), 1.32 (d, $J$ = 2.1 Hz, 15H), 1.28 (s, 5H). Note: Presence of precursor marked by a star.

**$^{13}$C NMR** (126 MHz, $d_6$-DMSO) δ 169.9, 168.1, 136.7, 134.6, 129.6, 129.2, 128.5, 128.3, 127.2, 126.7, 81.2, 54.4, 53.1, 37.0, 36.9, 27.5.

**HR-MS**: *m/z* for $C_{22}H_{28}N_2O_3$ $[M + H]^+$ calculated 369.2100, found 369.2172. *m/z* for $C_{18}H_{20}N_2O_3$ $[M + H]^+$ calculated 313.1500, found 313.1564. *m/z* for $C_{27}H_{36}N_2O_5$ $[M + K]^+$ calculated 507.3500, found 507.2262.

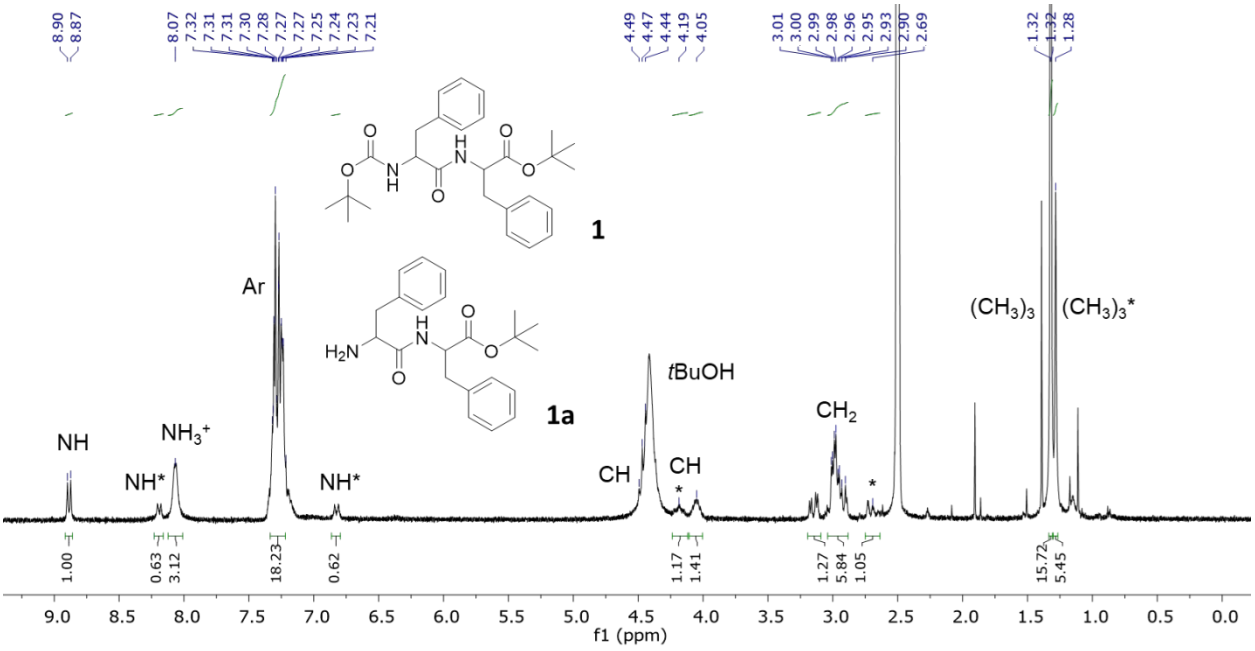


**Figure S29.** $^{1}$H NMR (300 MHz, $d_6$-DMSO) spectrum of xerogel **I**, 0.05M, 0.5 equivalent of $H_2SO_4$, day 1.

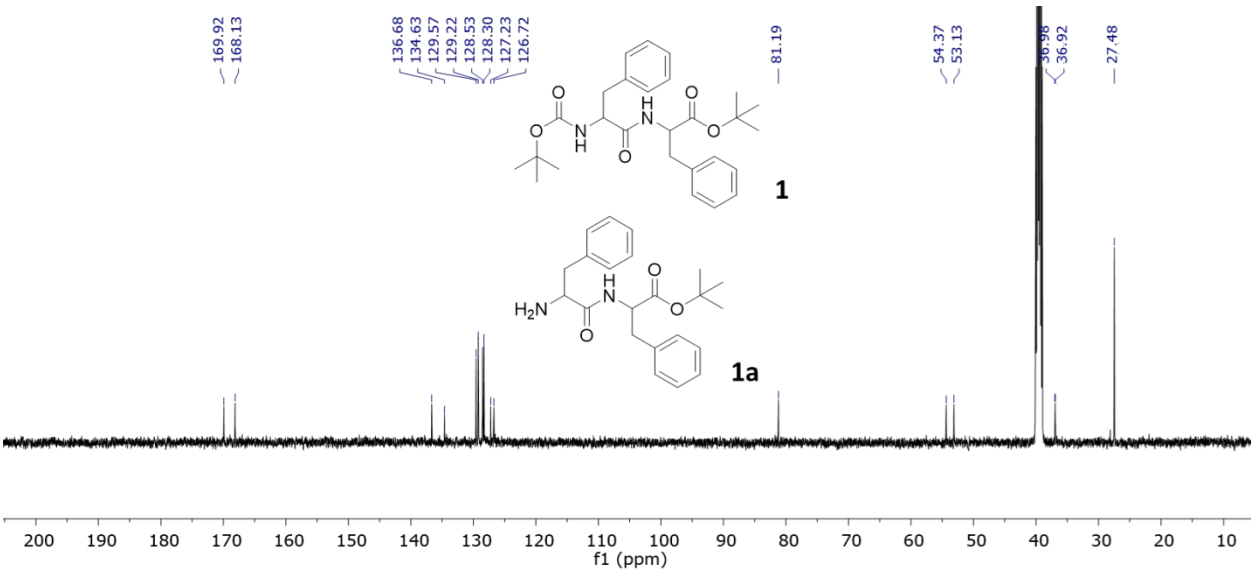


**Figure S30.** $^{13}$C NMR (126 MHz, $d_6$-DMSO) spectrum of xerogel **I**, 0.05M, 0.5 equivalent of $H_2SO_4$, day 1.

### 2.2.2 Gel system II: Precursor Boc-Phe-Phe-Phe-O*t*Bu 2

*0.05 M, 1.0 eq $H_2SO_4$, day 1*

**$^1$H NMR** (500 MHz, $d_6$-DMSO) δ 8.73 (d, *J* = 8.3 Hz, 1H), 8.70 (d, *J* = 8.4 Hz, 0.2H), 8.61 (d, *J* = 7.5 Hz, 1H), 8.53 (d, *J* = 7.9 Hz, 0.2H), 8.33 (d, *J* = 7.7 Hz, 0.1H), 8.22 (d, *J* = 7.9 Hz, 0.1H), 7.98 (d, *J* = 5.5 Hz, 3.5H), 7.32 – 7.20 (m, 20H), 4.65 (tt, *J* = 9.7, 4.7 Hz, 1H), 4.50 (dt, *J* = 8.2, 3.9 Hz, 0.4H), 4.42 (q, *J* = 7.5 Hz, 1H), 4.35 (d, *J* = 7.4 Hz, 0.2H), 3.13 – 2.78 (m, 8H), 1.32 (s, 9H). Note: Presence of a rotamer (peaks at 8.33 ppm and 8.22 ppm), as described in section **2.1.2**.

**$^{13}$C NMR** (126 MHz, $d_6$-DMSO) δ 172.0, 170.6, 170.3, 167.9, 137.3, 137.0, 134.6, 129.6, 129.3, 129.2, 128.5, 128.2, 128.1, 127.1, 126.5, 126.4, 80.8, 66.9, 54.2, 53.8, 53.1, 37.8, 37.0, 36.9, 31.3, 27.8, 27.5, 21.1.

**HR-MS**: *m/z* for $C_{31}H_{37}N_3O_4$ $[M + H]^+$ calculated 516.2800, found 516.2865. *m/z* for $C_{27}H_{29}N_3O_4$ $[M + H]^+$ calculated 460.2200, found 460.2240.

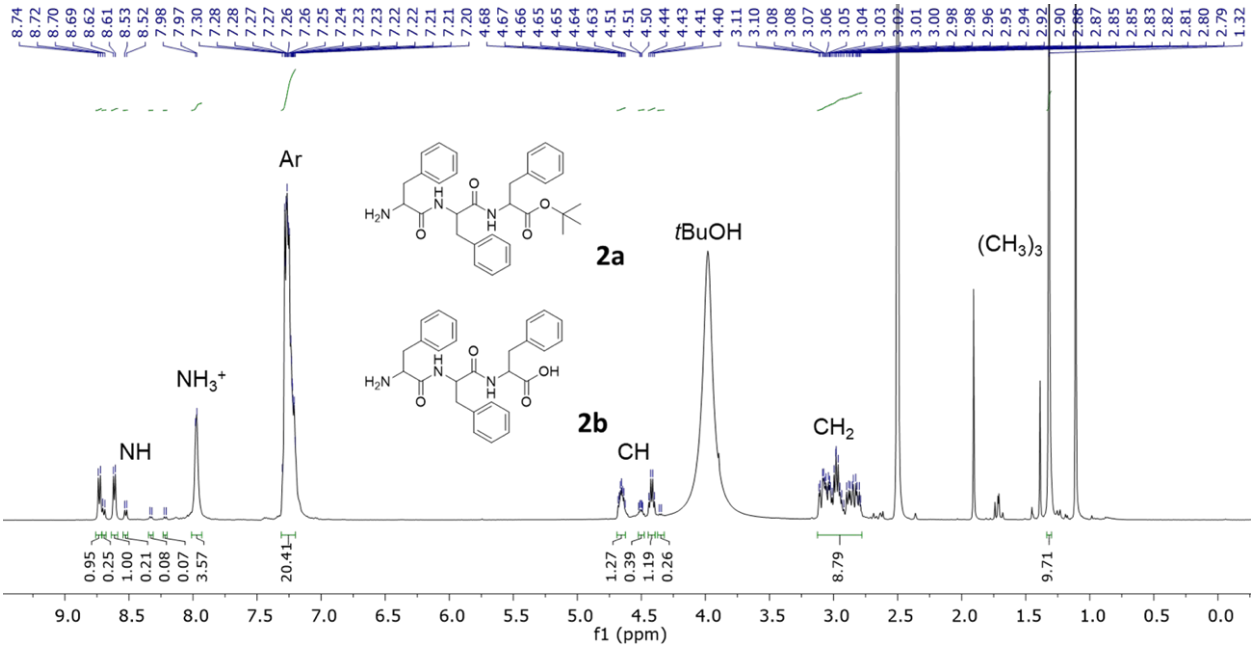


**Figure S31.** $^{1}$H NMR (500 MHz, $d_6$-DMSO) spectrum of xerogel **II**, 0.05M, 1.0 equivalent of $H_2SO_4$, day 1. Presence of a rotamer.

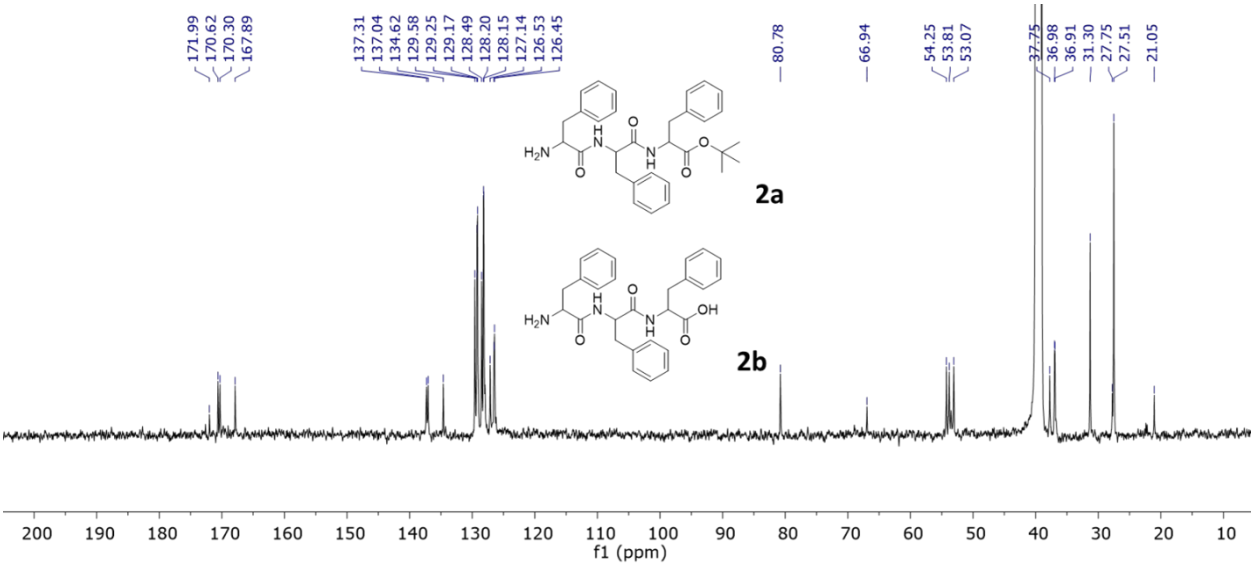


**Figure S32.** $^{1}$H NMR (126 MHz, $d_6$-DMSO) spectrum of xerogel **II**, 0.05M, 1.0 equivalent of $H_2SO_4$, day 1.

*0.05 M, 0.5 eq $H_2SO_4$, day 1*

**$^1$H NMR** (500 MHz, $d_6$-DMSO) δ 8.7 (d, $J$ = 8.3 Hz, 1H), 8.7 – 8.7 (m, 0.1H), 8.6 (d, $J$ = 7.4 Hz, 1H), 8.6 – 8.5 (m, 0.1H), 8.5 (d, $J$ = 7.4 Hz, 0.2H), 8.3 (d, $J$ = 7.7 Hz, 0.1H), 8.1 – 8.0 (m, 0.2H), 8.0 (d, $J$ = 5.3 Hz, 3H), 7.9 (d, $J$ = 8.4 Hz, 0.3H), 7.3 – 7.2 (m, 21H), 6.8 (d, $J$ = 8.8 Hz, 0.2H), 4.7 (td, $J$ = 8.8, 4.4 Hz, 1H), 4.6 – 4.6 (m, 0.3H), 4.4 (q, $J$ = 7.4 Hz, 1H), 4.4 (dd, $J$ = 12.5, 5.1 Hz, 0.4H), 4.1 (d, $J$ = 11.5 Hz, 0.6H), 4.0 (dt, $J$ = 9.6, 4.7 Hz, 2H), 3.1 – 2.8 (m, 7H), 1.3 (s, 8H), 1.3 (s, 3.3H), 1.3 (s, 1.5H). Note: Presence of precursor marked by a star.

**$^{13}$C NMR** (126 MHz, $d_6$-DMSO) δ 170.6, 170.3, 167.9, 137.3, 137.0, 134.6, 129.6, 129.3, 129.2, 128.5, 128.2, 128.1, 127.9, 127.1, 126.5, 126.4, 80.8, 54.2, 53.8, 53.1, 37.7, 37.0, 36.9, 31.3, 28.1, 27.7, 27.5.

**HR-MS**: *m/z* for $C_{36}H_{45}N_3O_6$ $[M + H]^+$ calculated 616.3300, found 616.3286. *m/z* for $C_{31}H_{37}N_3O_4$ $[M + H]^+$ calculated 516.2800, found 516.2785. *m/z* for $C_{27}H_{29}N_3O_4$ $[M + H]^+$ calculated 460.2200, found 460.2153.

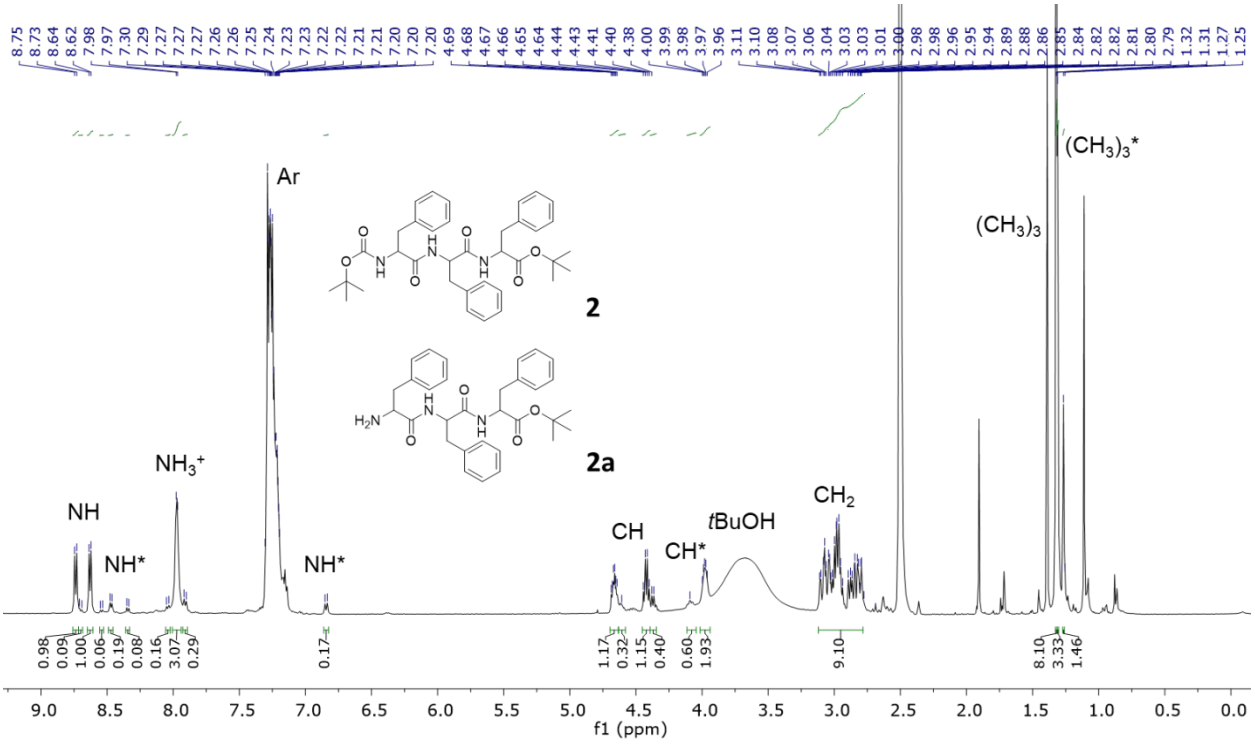


**Figure S33.** $^1$H NMR (500 MHz, $d_6$-DMSO) spectrum of xerogel **II**, 0.05M, 0.5 equivalent of $H_2SO_4$, day 1.

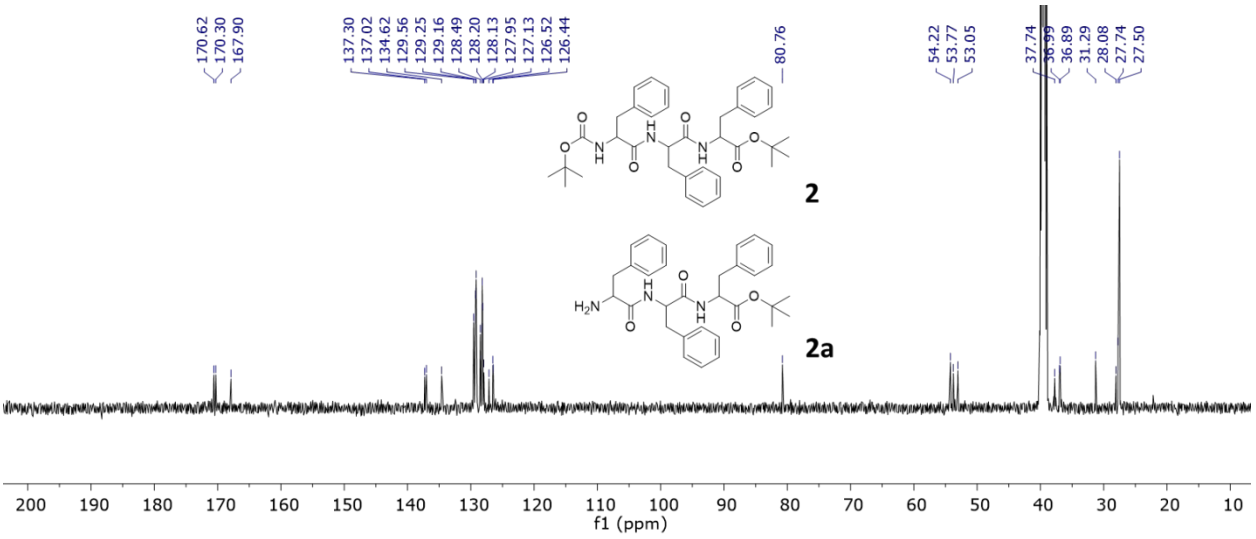


**Figure S34.** $^{1}$H NMR (126 MHz, $d_6$-DMSO) spectrum of xerogel **II**, 0.05M, 0.5 equivalent of $H_2SO_4$, day 1.

*0.05 M, 1.0 eq of $H_2SO_4$, day 5*

**$^{1}$H NMR** (300 MHz, $d_6$-DMSO) δ 8.72 (d, $J$ = 8.5 Hz, 1H), 8.67 (s, 0.2H), 8.60 (d, $J$ = 7.5 Hz, 1H), 8.51 (d, $J$ = 7.9 Hz, 0.2H), 8.31 (d, $J$ = 7.4 Hz, 0.1H), 8.20 (d, $J$ = 7.9 Hz, 0.1H), 8.02 – 7.93 (m, 4H), 7.25 (qd, $J$ = 8.4, 7.0, 3.9 Hz, 22H), 4.66 (td, $J$ = 8.7, 4.4 Hz, 1H), 3.98 (s, 1H), 3.15 – 2.76 (m, 5H), 1.32 (s, 9H).

**$^{13}$C NMR** (75 MHz, $d_6$-DMSO) δ 173.1, 171.9, 171.1, 170.8, 169.5, 168.4, 137.8, 137.5, 135.1, 130.1, 129.7, 129.6, 129.0, 128.7, 128.6, 128.4, 127.6, 127.0, 126.9, 81.3, 67.4, 54.7, 54.3, 53.6, 37.4, 31.8, 28.0.

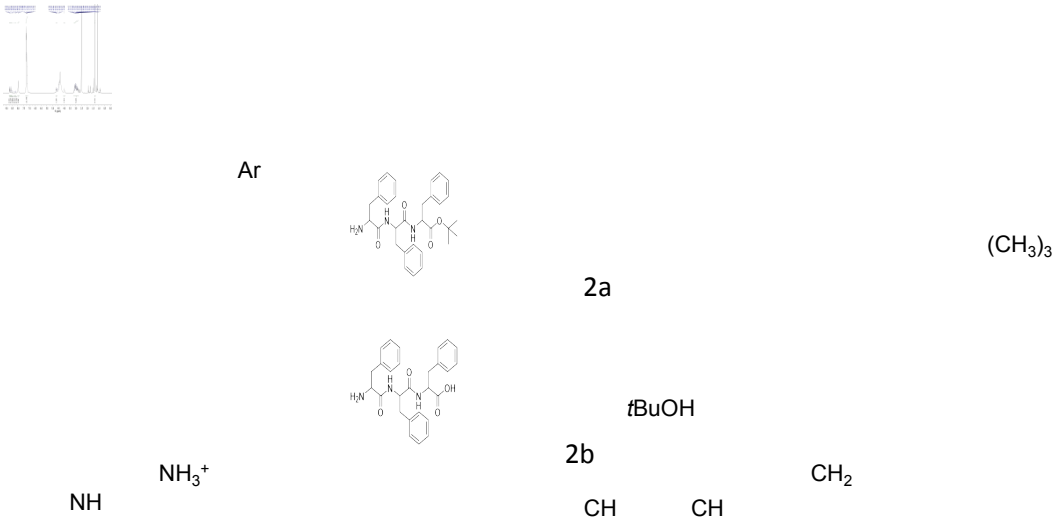


**Figure S35.** $^{1}$H NMR (300 MHz, $d_6$-DMSO) spectrum of xerogel **II**, 0.05M, 1.0 equivalent of $H_2SO_4$, day 5.

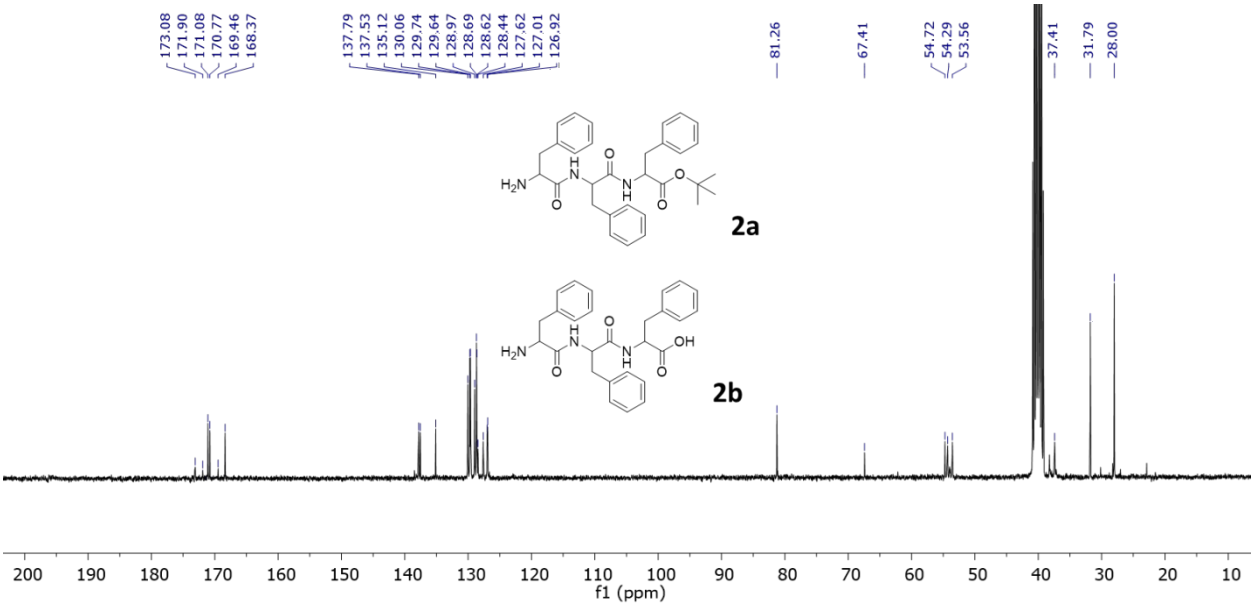

**Figure S36.** $^{1}$H NMR (126 MHz, $d_6$-DMSO) spectrum of xerogel **II**, 0.05M, 1.0 equivalent of $H_2SO_4$, day 5.

### 2.2.3. Gel system III: Precursor Boc-Leu-Phe-O*t*Bu 3

*0.05 M, 1.0 eq $H_2SO_4$, day 1*

**$^{1}$H NMR** (300 MHz, $d_6$-DMSO) δ 8.83 (d, $J$ = 7.4 Hz, 1H), 8.76 (d, $J$ = 7.6 Hz, 0.7H), 8.06 (s, 5.2H), 7.35 – 7.21 (m, 8.8H), 4.54 – 4.39 (m, 1.9H), 3.76 (s, 1.7H), 3.14 – 2.92 (m, 3.8H), 1.67 (d, $J$ = 6.9 Hz, 2.4H), 1.55 (d, $J$ = 7.5 Hz, 3.8H), 1.31 (s, 9H), 0.95 – 0.86 (m, 10.9H).

**$^{13}$C NMR** (75 MHz, $d_6$-DMSO) δ 172.2, 169.2, 137.2, 129.1, 128.3, 126.6, 53.8, 50.7, 36.5, 27.5, 23.4, 22.9, 21.7.

**HR-MS**: *m/z* for $C_{19}H_{30}N_2O_3$ $[M + H]^+$ calculated 335.2300, found 335.2335. *m/z* for $C_{15}H_{22}N_2O_3$ $[M + H]^+$ calculated 279.1600, found 279.1716.

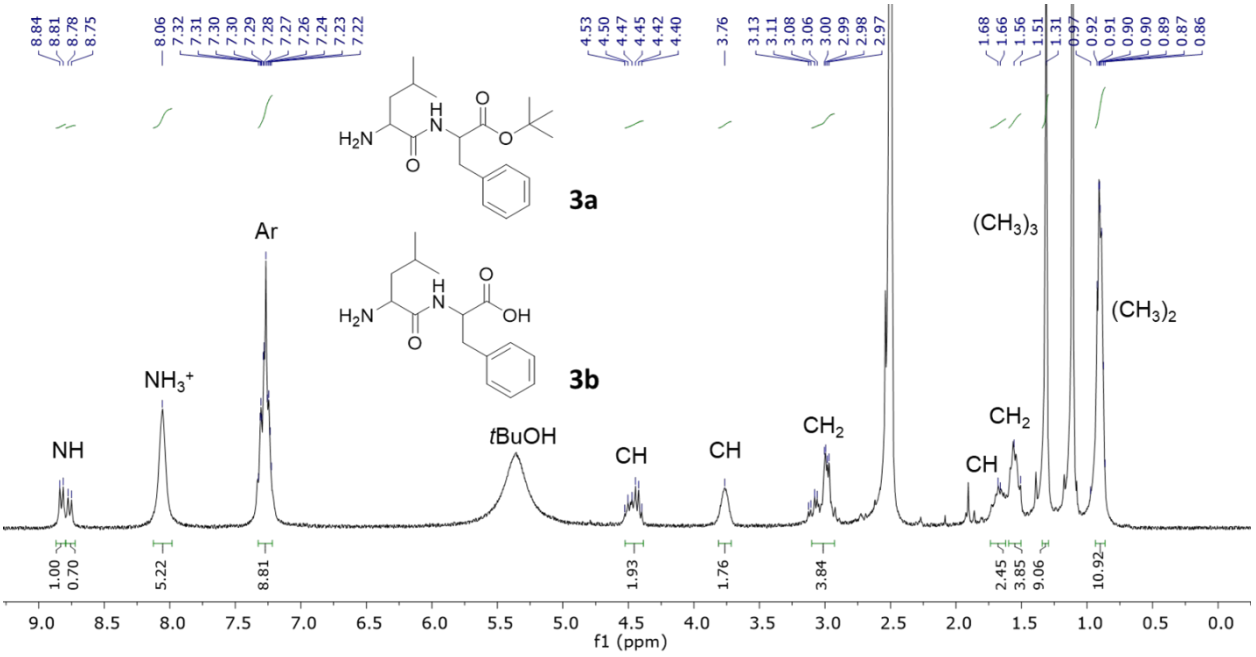


**Figure S37.** $^{1}$H NMR (300 MHz, $d_6$-DMSO) spectrum of xerogel **III**, 0.05M, 1.0 equivalent of $H_2SO_4$, day 1.

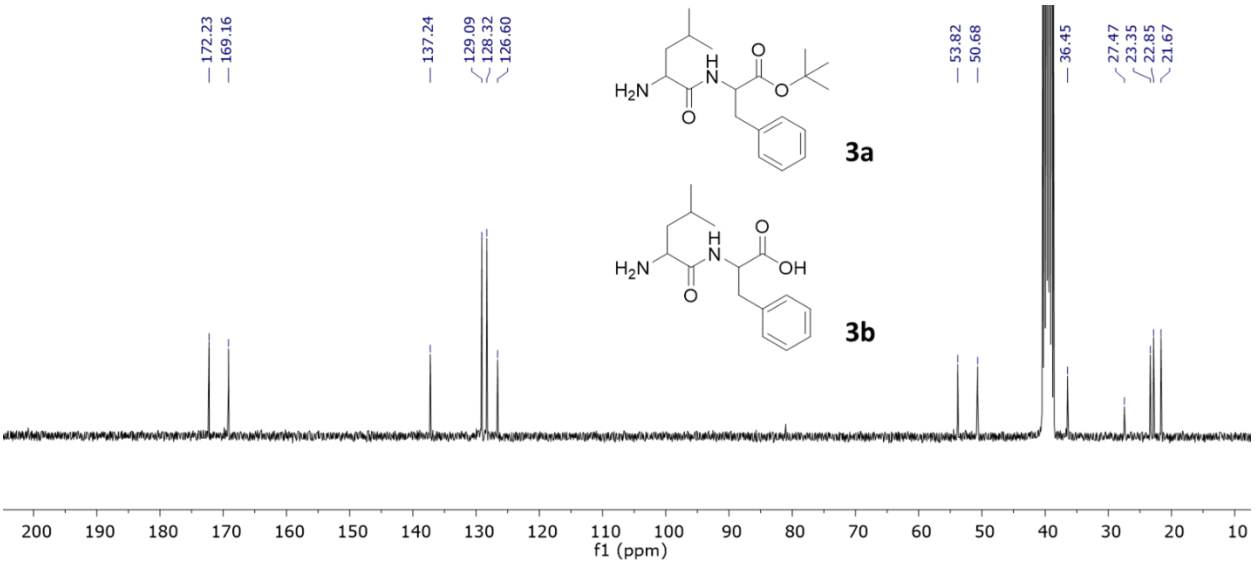


**Figure S38.** $^{13}$C NMR (75 MHz, $d_6$-DMSO) spectrum of xerogel **III**, 0.05M, 1.0 equivalent of $H_2SO_4$, day 1.

*0.05 M, 0.5 eq $H_2SO_4$, day 1*

**$^1$H NMR** (300 MHz, $d_6$-DMSO) δ 8.83 (d, *J* = 7.4 Hz, 1H), 8.06 (s, 3H), 7.98 (d, *J* = 7.7 Hz, 1H), 7.35 – 7.18 (m, 10H), 6.79 (d, *J* = 8.6 Hz, 1H), 4.44 (q, *J* = 7.4 Hz, 1H), 4.35 (q, *J* = 7.4 Hz, 1H), 4.02 – 3.92 (m, 1H), 3.76 (d, *J* = 6.0 Hz, 1H), 3.05 – 2.89 (m, 4H), 1.67 (dq, *J* = 12.7, 6.5, 6.1 Hz, 1H), 1.61 – 1.52 (m, 2H), 1.37 (s, 8H), 1.31 (s, 18H), 0.91 (dd, *J* = 6.3, 3.7 Hz, 6H), 0.84 (dd, *J* = 8.4, 6.5 Hz, 6H). Note: Presence of precursor marked by a star. **$^{13}$C NMR** (126 MHz, $d_6$-DMSO) δ 172.3, 169.2, 137.3, 129.1, 128.3, 128.1, 126.6, 126.5, 81.1, 80.7, 78.0, 53.8, 50.7, 36.5, 28.2, 27.5, 23.4, 22.9, 21.7.

**HR-MS**: *m/z* for $C_{15}H_{22}N_2O_3$ $[M + H]^+$ calculated 279.1600, found 279.1629. *m/z* for $C_{19}H_{30}N_2O_3$ $[M + H]^+$ calculated 335.2300, found 335.2242. *m/z* for $C_{24}H_{38}N_2O_5$ $[M + H]^+$ calculated 435.2800, found 435.2864.

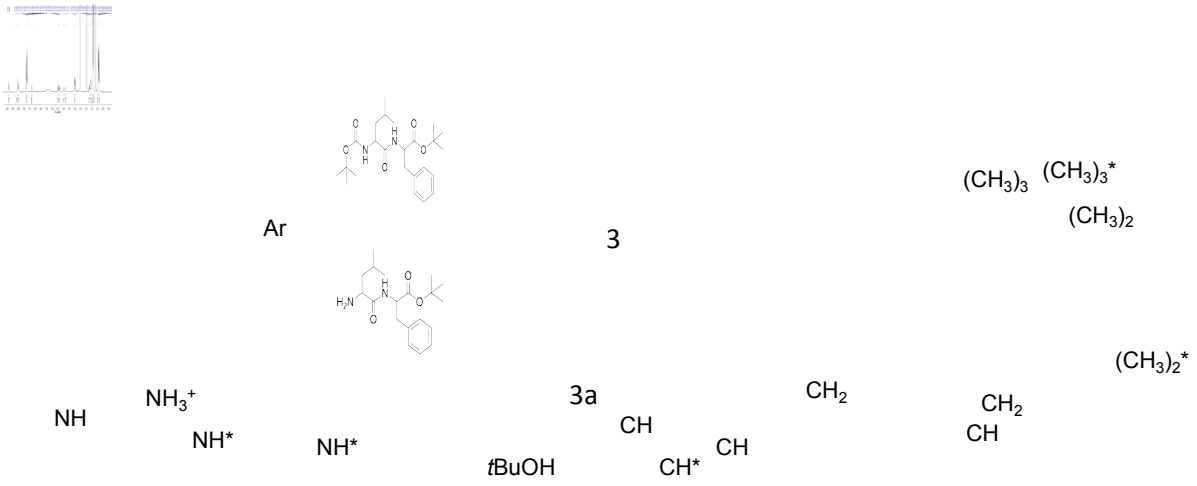


**Figure S39.** $^1$H NMR (300 MHz, $d_6$-DMSO) spectrum of xerogel **III**, 0.05M, 0.5 equivalent of $H_2SO_4$, day 1.

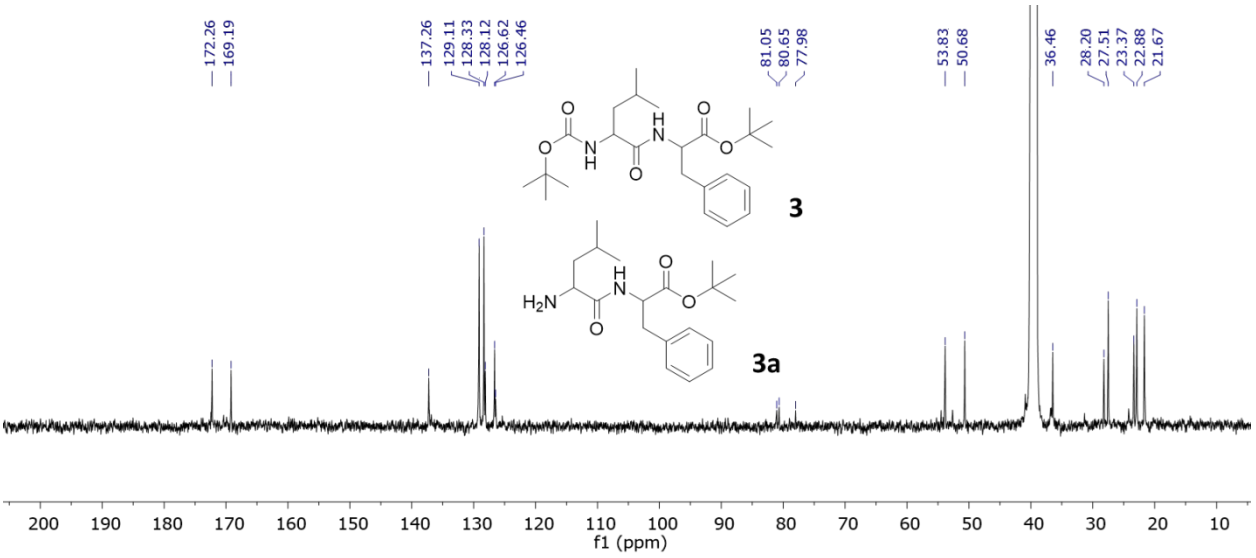


**Figure S40.** $^{13}$C NMR (126 MHz, $d_6$-DMSO) spectrum of xerogel **III**, 0.05M, 0.5 equivalent of $H_2SO_4$, day 1.

*0.05 M, 1.0 eq of $H_2SO_4$, day 10*

**$^1$H NMR** (300 MHz, $d_6$-DMSO) δ 8.82 (d, $J$ = 7.4 Hz, 1H), 8.76 (d, $J$ = 7.8 Hz, 0.15H), 8.06 (s, 3.5H), 7.35 – 7.20 (m, 6H), 4.44 (q, $J$ = 7.4 Hz, 1.3H), 3.76 (s, 1.3H), 3.07 – 2.93 (m, 2.3H), 1.66 (dt, $J$ = 12.5, 6.3 Hz, 1.6H), 1.61 – 1.52 (m, 2.6H), 1.31 (s, 9H), 0.91 (dd, $J$ = 6.3, 3.8 Hz, 7.7H).

**$^{13}$C NMR** (126 MHz, $d_6$-DMSO) δ 172.2, 169.8, 169.2, 169.1, 137.2, 136.8, 129.1, 129.1, 128.3, 128.3, 126.7, 126.6, 81.0, 54.5, 53.8, 50.6, 50.6, 36.7, 36.4, 29.7, 27.5, 23.4, 23.3, 22.8, 22.8, 21.7, 21.6.

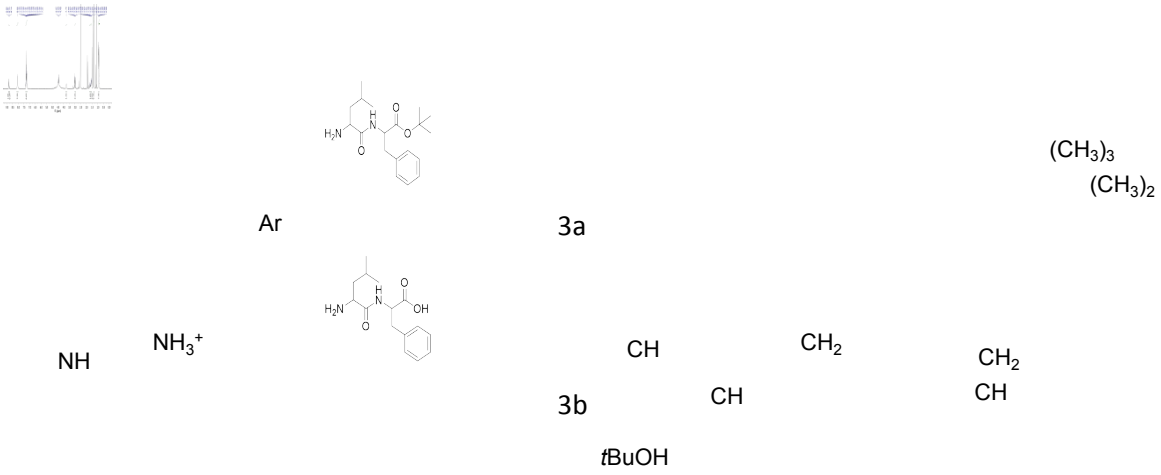


**Figure S41.** $^{1}$H NMR (300 MHz, $d_6$-DMSO) spectrum of xerogel **III**, 0.05M, 1.0 equivalent of $H_2SO_4$, day 10.

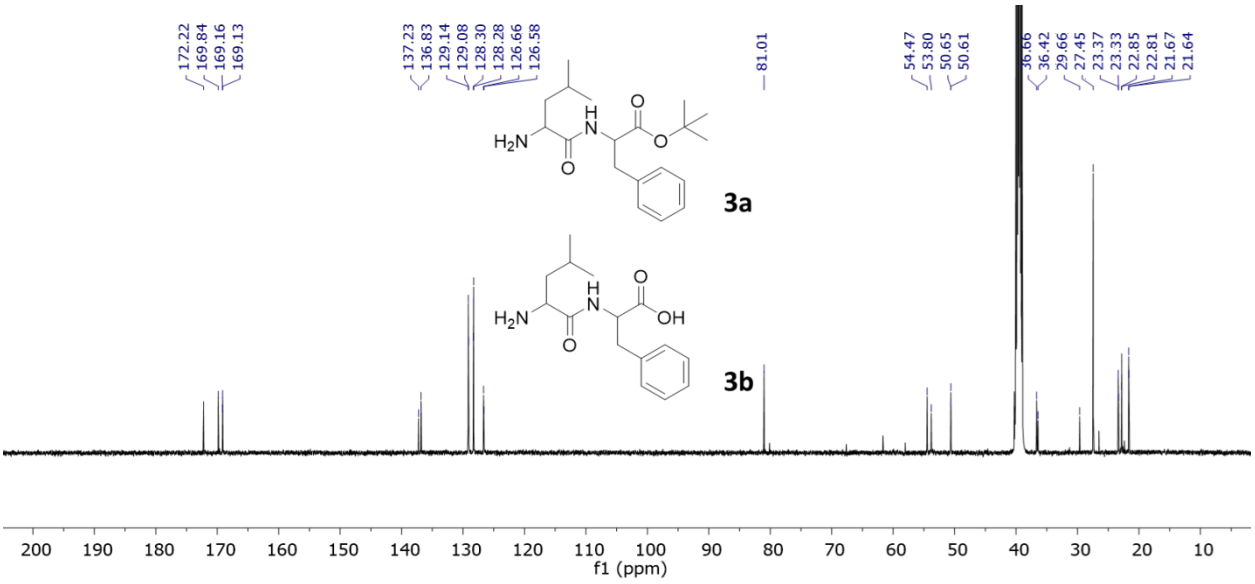


**Figure S42.** $^{13}$C NMR (126 MHz, $d_6$-DMSO) spectrum of xerogel **III**, 0.05M, 1.0 equivalent of $H_2SO_4$, day 10.

### 2.2.4. Gel system IV: Precursor Boc-Phe-Phe-O*t*Bu 1 + Boc-Leu-Phe-O*t*Bu 3, 1:1 ratio

*0.05 M, 1.0 eq $H_2SO_4$, day 1*

**$^1$H NMR** (300 MHz, $d_6$-DMSO) δ 8.88 (d, *J* = 7.5 Hz, 0.6H), 8.82 (d, *J* = 7.5 Hz, 1H), 8.76 (d, *J* = 7.8 Hz, 0.3H), 8.06 (s, 5.6H), 7.36 – 7.21 (m, 15H), 4.48 (ddd, *J* = 19.1, 7.7, 5.3 Hz, 2.5H), 4.04 (s, 1H), 3.76 (s, 1H), 3.19 – 2.87 (m, 6H), 1.67 (q, *J* = 6.4 Hz, 1.2H), 1.60 – 1.49 (m, 2H), 1.32 (s, 4.6H), 1.32 (s, 5.3H), 0.96 – 0.86 (m, 7.2H). Note: this spectrum (system **IV**) is the superimpose of the individual gel spectra (systems **I** and **III**).

**$^{13}$C NMR** (75 MHz, $d_6$-DMSO) δ 172.7, 172.7, 169.6, 168.6, 137.7, 137.6, 135.1, 130.1, 129.7, 129.6, 129.6, 129.0, 128.8, 128.8, 127.7, 127.1, 127.1, 54.3, 53.6, 51.2, 37.4, 37.2, 36.9, 28.0, 23.8, 23.3, 22.2.

**HR-MS**: *m/z* for $C_{15}H_{22}N_2O_3$ $[M + H]^+$ calculated 279.1600, found 279.1703. *m/z* for $C_{18}H_{20}N_2O_3$ $[M + H]^+$ calculated 313.1500, found 313.1552. *m/z* for $C_{19}H_{30}N_2O_3$ $[M + H]^+$ calculated 335.2300, found 335.2249. *m/z* for $C_{22}H_{28}N_2O_3$ $[M + H]^+$ calculated 369.2100, found 369.2095.

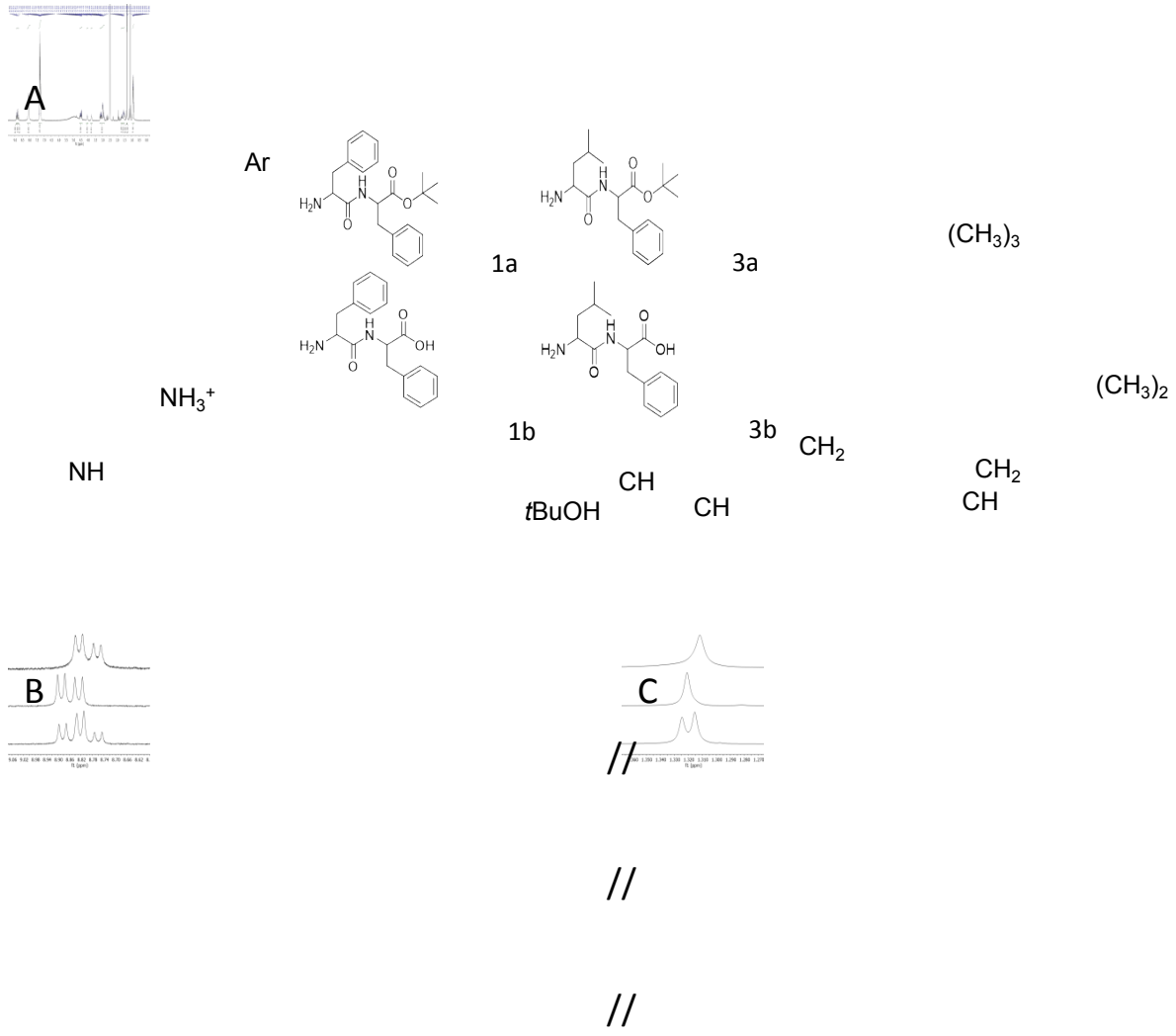


**Figure S43.** $^{1}$H NMR (300 MHz, $d_6$-DMSO) spectrum of **(A)** xerogel **IV**, 0.05M, 1.0 equivalent of $H_2SO_4$, day 1, **(B)** N-H region expansion showing system **III** (top), system **I** (middle) and system **IV** (bottom) and **(C)** *t*Bu protective group region expansion showing system **III** (top), system **I** (middle) and system **IV** (bottom).

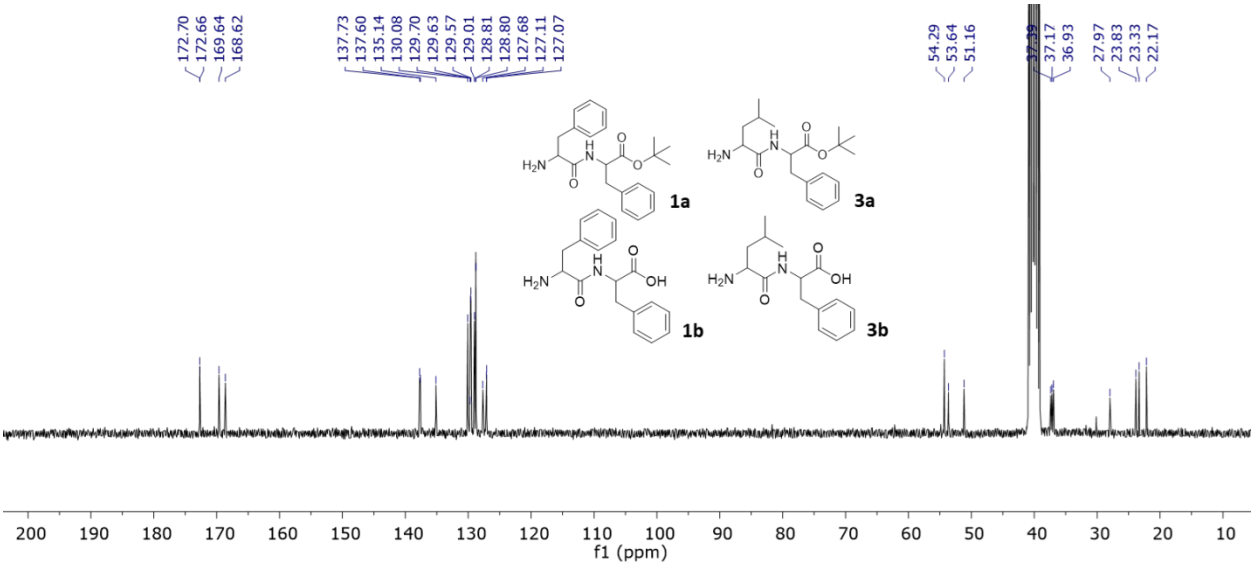


**Figure S44.** $^{13}$C NMR (75 MHz, $d_6$-DMSO) spectrum of xerogel **IV**, 0.05M, 1.0 equivalent of $H_2SO_4$, day 1.

*0.05 M, 0.5 eq $H_2SO_4$, day 1*

**$^1$H NMR** (300 MHz, $d_6$-DMSO) δ 8.89 (d, $J$ = 7.5 Hz, 1H), 8.83 (d, $J$ = 7.4 Hz, 0.9H), 8.19 (d, $J$ = 7.4 Hz, 1H), 8.07 (s, 6H), 7.98 (d, $J$ = 7.6 Hz, 1H), 7.27 (ddt, $J$ = 16.0, 13.3, 5.4 Hz, 30H), 6.81 (t, $J$ = 9.3 Hz, 2H), 4.41 (ddd, $J$ = 25.5, 11.2, 6.3 Hz, 3H), 4.19 (s, 1H), 4.06 (s, 1H), 4.01 – 3.92 (m, 1H), 3.77 (s, 1H), 3.21 – 2.87 (m, 10H), 1.69 (td, $J$ = 13.3, 12.4, 5.5 Hz, 1H), 1.61 – 1.50 (m, 3H), 1.37 (s, 6H), 1.32 (s, 10H), 1.31 (s, 18H), 1.28 (s,59H), 0.91 (dd, $J$ = 6.3, 3.7 Hz, 6H), 0.84 (dd, $J$ = 8.4, 6.5 Hz, 7H). Note: Presence of precursor marked by a star.

**$^{13}$C NMR** (75 MHz, $d_6$-DMSO) δ 172.7, 172.7, 170.4, 170.3, 169.7, 168.6, 137.7, 137.6, 137.3, 137.2, 135.2, 135.1, 130.1, 129.7, 129.7, 129.6, 129.0, 128.8, 127.7, 127.2, 127.1, 127.07, 81.7, 81.5, 55.0, 54.9, 54.3, 53.7, 51.2, 37.5, 37.4, 37.2, 37.0, 27.98, 27.95, 23.9, 23.8, 23.3, 22.2.

**HR-MS**: *m/z* for $C_{15}H_{22}N_2O_3$ calculated 279.1600, found 279.1621. *m/z* for $C_{18}H_{20}N_2O_3$ $[M + H]^+$ calculated 313.1500, found 313.1472. *m/z* for $C_{19}H_{30}N_2O_3$ $[M + H]^+$ calculated 335.2300, found 335.2245. *m/z* for $C_{22}H_{28}N_2O_3$ $[M + H]^+$ calculated 369.2100, found 369.2090. *m/z* for

$C_{24}H_{38}N_2O_5$ [M + H]$^+$ calculated 435.2800, found 435.2768. *m/z* for $C_{27}H_{36}N_2O_5$ [M + H]$^+$ calculated 469.2600, found 469.2603.

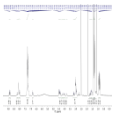

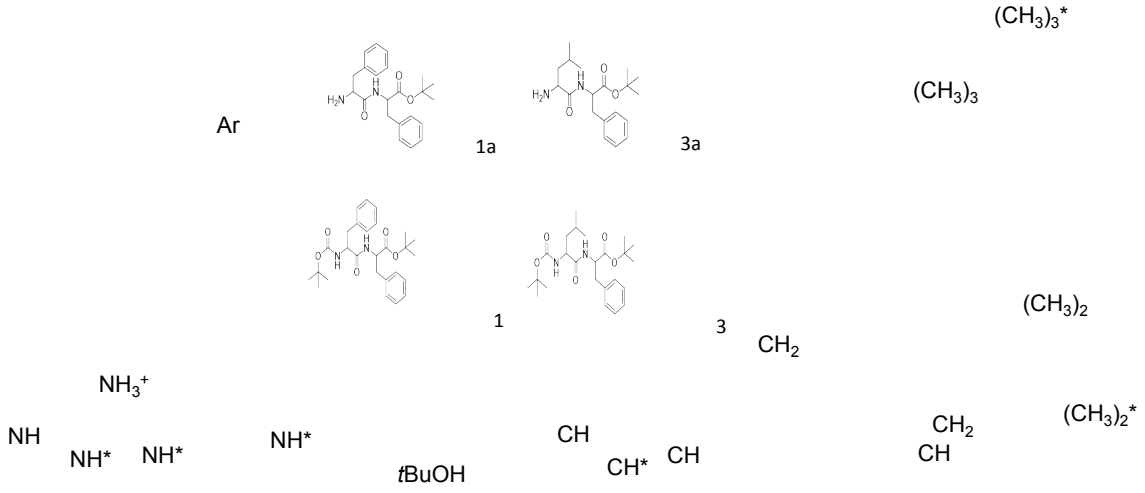


**Figure S45.** $^1$H NMR (300 MHz, $d_6$-DMSO) spectrum of xerogel **IV**, 0.05M, 0.5 equivalent of $H_2SO_4$, day 1.

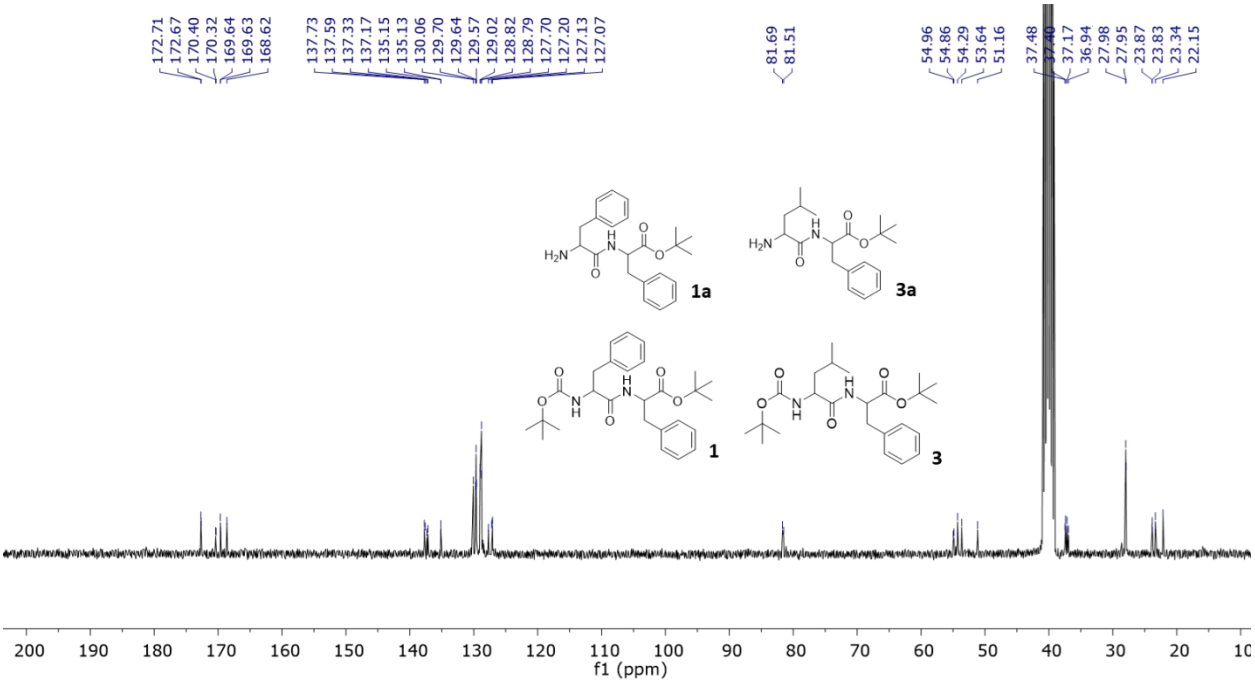


**Figure S46.** $^{13}$C NMR (75 MHz, $d_6$-DMSO) spectrum of xerogel **IV**, 0.05M, 0.5 equivalent of $H_2SO_4$, day 1.

*0.05 M, 1.0 eq $H_2SO_4$, day 5.*

**$^1$H NMR** (300 MHz, $d_6$-DMSO) δ 8.90 (d, $J$ = 7.5 Hz, 0.8H), 8.83 (d, $J$ = 7.4 Hz, 1H), 8.77 (d, $J$ = 7.8 Hz, 0.2H), 8.07 (d, $J$ = 5.5 Hz, 6H), 7.36 – 7.20 (m, 16H), 4.53 – 4.38 (m, 2H), 4.06 (s, 1H), 3.77 (d, $J$ = 7.7 Hz, 1H), 3.16 – 2.89 (m, 6H), 1.75 – 1.61 (m, 1H), 1.56 (td, $J$ = 6.8, 2.8 Hz, 2H), 1.32 (s, 5H), 1.31 (s, 6H), 0.89 (dq, $J$ = 8.4, 5.1, 4.5 Hz, 7H).

**$^{13}$C NMR** (126 MHz, $d_6$-DMSO) δ 172.3, 172.2, 169.2, 168.2, 137.3, 137.1, 134.7, 129.6, 129.2, 129.1, 128.6, 128.4, 128.3, 127.2, 126.7, 126.6, 61.7, 53.8, 53.8, 53.2, 50.7, 36.9, 36.7, 36.5, 29.7, 23.4, 22.9, 21.7.

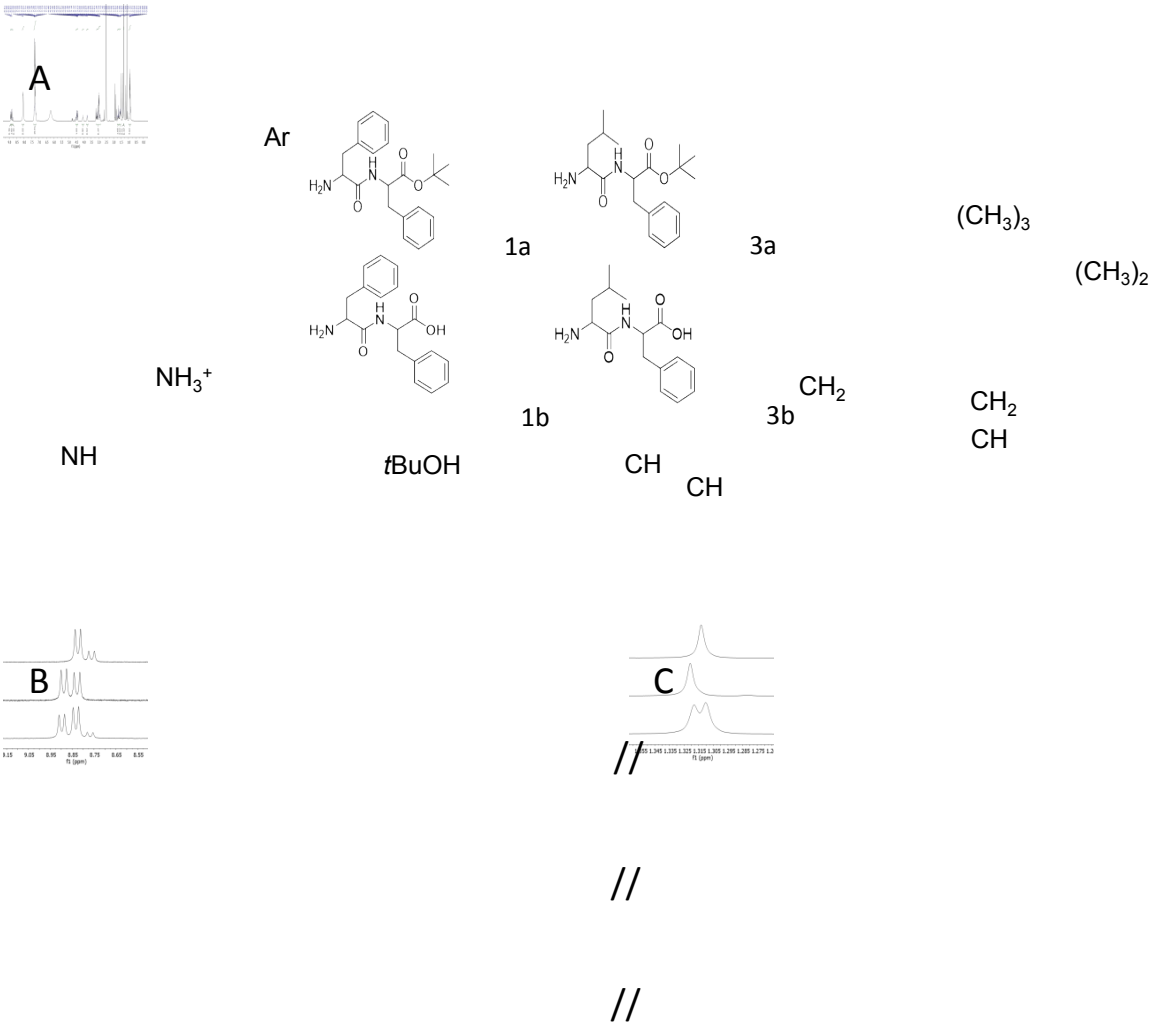


**Figure S47.** $^1$H NMR (300 MHz, $d_6$-DMSO) spectrum of **(A)** xerogel **IV**, 0.05M, 1.0 equivalent of $H_2SO_4$, day 5, **(B)** N-H region expansion showing system **III** (top), system **I** (middle) and system **IV** (bottom) and **(C)** *t*Bu protective group region expansion showing system **III** (top), system **I** (middle) and system **IV** (bottom).

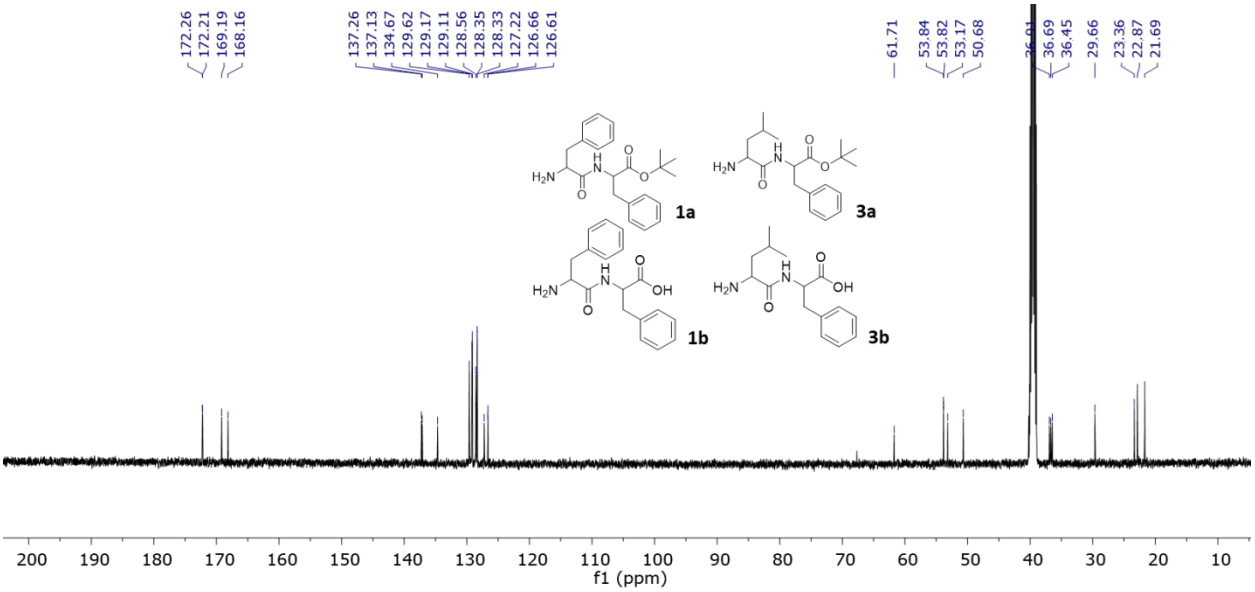


**Figure S48.** $^{13}C$ NMR (126 MHz, $d_6$-DMSO) spectrum of xerogel **IV**, 0.05M, 1.0 equivalent of $H_2SO_4$, day 5.

### 2.2.5. Gelation attempt in DCM

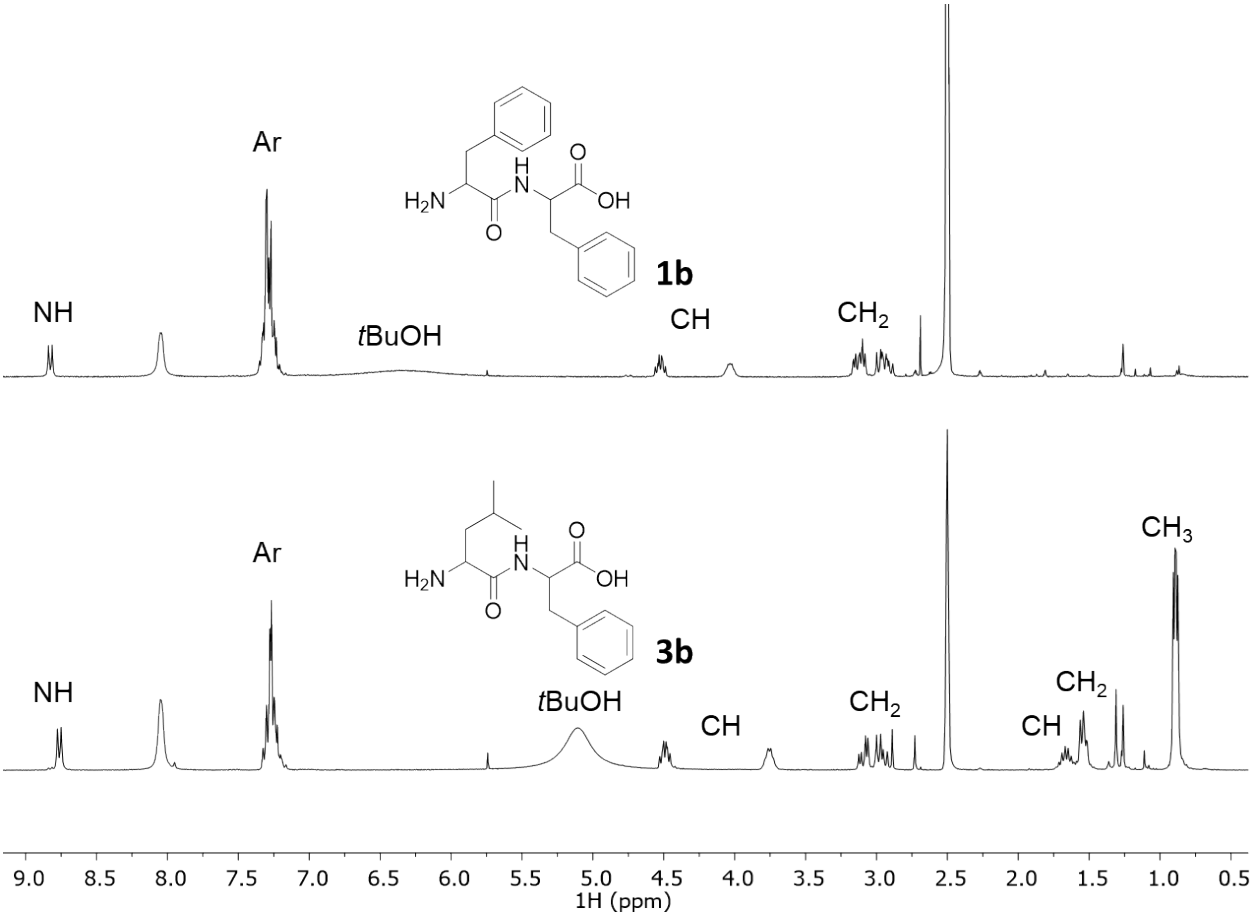


**Figure S49.** $^{1}$H NMR (300 MHz, $d_6$-DMSO) spectrum of precipitates in DCM.

## 2.3. Solvatochromism and concentration study by UV-vis

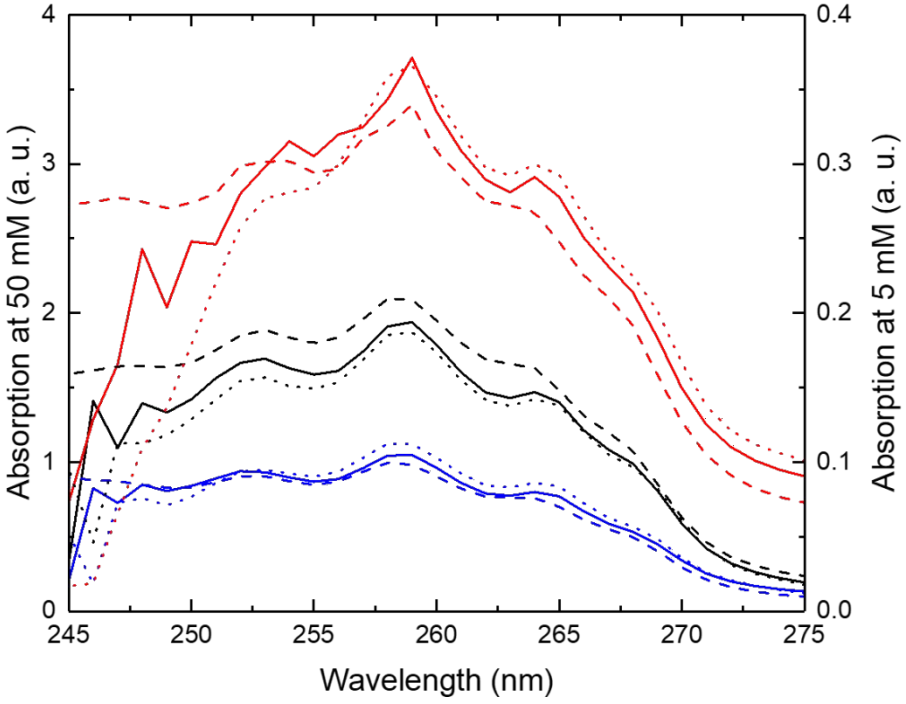


**Figure S50.** UV spectra of precursor gelators **1** (black), **2** (red) and **3** (blue) at 5 mM (plane) and 50 mM (dash) in *t*BuOAc and 50 mM in ACN (dots).

## 2.4. Phase-transition temperature

Phase-transition temperatures were measured by gradually heating the gel specimens starting from 25 ˚C, by 5 ˚C increments at 10 min intervals. The self-supporting character of the gels was assessed by the vial inversion method.

***Table S1****. Phase transition temperature (˚C) of gel systems* ***I, II, III*** *and* ***IV*** *depending on the gel concentration.*

| $T_{gel-sol}$ ( ℃) | Gel concentration |
|---|---|

| | 0.025 M | 0.05 M | 0.1 M |
|---|---|---|---|
| Gel system I | 45 | 50 | 55 |
| Gel system II | 55 | 65 | 65 |
| Gel system III | 40 | 45 | 50 |
| Gel system IV | 35 | 40 | 45 |

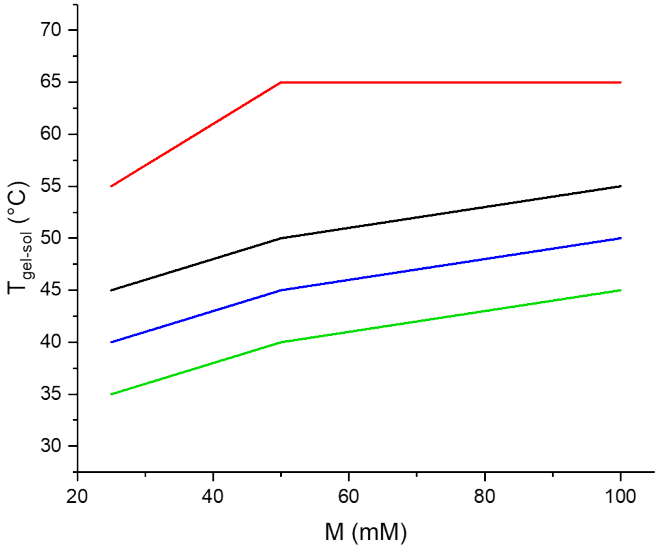


**Figure S51.** Phase transition temperature in function of gel concentration for gel system **I** (black), **II** (red), **III** (blue) and **IV** (green).

### 2.5. Gelation concentration screening

***Table S2****. Concentration screening trials of gel system* ***I*** *in tBuOAc solvent (1.0 mL) at R.T.*

| M | Boc-Phe-Phe-O*t*Bu **1** (mg) | $H_2SO_4$ | $H_2SO_4$ | Gelation outcome | Lifespan |
|---|---|---|---|---|---|

| (mol/L) | | (eq) | (μL) | | (day) |
|---|---|---|---|---|---|
| 0.1 | 47 | 1.5 | 7.8 | SSG[a], opaque | 3 |
| 0.1 | 47 | 1.0 | 5.3 | SSG, opaque | 15-17 |
| 0.1 | 47 | 0.5 | 2.7 | SSG, opaque | /[b] |
| 0.05 | 23.5 | 1.5 | 4 | SSG, opaque | 3-4 |
| 0.05 | 23.5 | 1.0 | 2.7 | SSG, opaque | 4-6 |
| 0.05 | 23.5 | 0.5 | 1.3 | SSG, opaque | / |
| 0.025 | 11.8 | 1.5 | 2 | SSG, opaque | n.m.[c] |
| 0.025 | 11.8 | 1.0 | 1.3 | SSG, opaque | n.m. |
| 0.025 | 11.8 | 0.5 | 0.6 | SSG, opaque | n.m. |

[a] self-supporting gel [b] no transitivity [c] not measured

***Table S3****. Concentration screening trials of gel system* ***II*** *in tBuOAc solvent (1.0 mL) at R.T.*

| M (mol/L) | Boc-Phe-Phe-Phe-O*t*Bu **2** (mg) | $H_2SO_4$ (eq) | $H_2SO_4$ (μL) | Gelation outcome | Lifespan (day) |
|---|---|---|---|---|---|
| 0.1 | 61.5 | 1.0 | 5.3 | SSG[a], opaque | 15 |
| 0.1 | 61.5 | 0.5 | 2.7 | SSG, opaque | /[b] |
| 0.05 | 30.8 | 1.5 | 4.0 | SSG, opaque | 5-7 |
| 0.05 | 30.8 | 1.0 | 2.7 | SSG, opaque | 7-11 |
| 0.05 | 30.8 | 0.5 | 1.3 | SSG, opaque | / |
| 0.025 | 15.4 | 1.0 | 1.3 | SSG, opaque | 11 |

| | | | | | |
|---|---|---|---|---|---|
| 0.025 | 15.4 | 0.5 | 0.6 | SSG, opaque | / |

[a] self-supporting gel [b] no transitivity

***Table S4****. Concentration screening trials of gel system* ***III*** *in tBuOAc solvent (1.0 mL) at R.T.*

| M (mol/L) | Boc-Leu-Phe-O*t*Bu **3** (mg) | $H_2SO_4$ (eq) | $H_2SO_4$ (μL) | Gelation outcome | Lifespan (day) |
|---|---|---|---|---|---|
| 0.1 | 43.4 | 1.5 | 7.8 | SSG[a], transparent | 4-5 |
| 0.1 | 43.4 | 1.0 | 5.3 | SSG, transparent | 25 |
| 0.1 | 43.4 | 0.5 | 2.7 | SSG, transparent | /[b] |
| 0.05 | 21.7 | 1.5 | 4.0 | SSG, transparent | 1-2 |
| 0.05 | 21.7 | 1.0 | 2.7 | SSG, transparent | 22 |
| 0.05 | 21.7 | 0.5 | 1.3 | SSG, transparent | / |
| 0.025 | 10.8 | 1.5 | 2.0 | SSG, transparent | 18-20 |
| 0.025 | 10.8 | 1.0 | 1.3 | SSG, transparent | 28-34 |
| 0.025 | 10.8 | 0.5 | 0.6 | SSG, transparent | / |

[a] self-supporting gel [b] no transitivity

***Table S5****. Concentration screening trials of gel system* ***IV*** *in tBuOAc solvent (1.0 mL) at R.T.*

| M (mol/L) | Boc-Phe-Phe-O*t*Bu **1** (mg) | Boc-Leu-Phe-O*t*Bu **3** (mg) | $H_2SO_4$ (eq) | $H_2SO_4$ (μL) | Gelation outcome | Lifespan (day) |
|---|---|---|---|---|---|---|
| 0.1 | 23.5 | 21.7 | 1.5 | 7.8 | SSG[a], transparent | 1-2 |

| | | | | | | |
|---|---|---|---|---|---|---|
| 0.1 | 23.5 | 21.7 | 1.0 | 5.3 | SSG, transparent | 10 |
| 0.1 | 23.5 | 21.7 | 0.5 | 2.7 | SSG, transparent | /[b] |
| 0.05 | 11.8 | 10.8 | 1.5 | 4.0 | SSG, transparent | 1-2 |
| 0.05 | 11.8 | 10.8 | 1.0 | 2.7 | SSG, transparent | 7-9 |
| 0.05 | 11.8 | 10.8 | 0.5 | 1.3 | SSG, transparent | / |
| 0.025 | 5.8 | 5.4 | 1.5 | 2.0 | solution | n.m.[c] |
| 0.025 | 5.8 | 5.4 | 1.0 | 1.3 | SSG, transparent | 5 |
| 0.025 | 5.8 | 5.4 | 0.5 | 0.6 | SSG, transparent | / |

[a] self-supporting gel [b] no transitivity [c] not measured

3. **FTIR spectra of compounds 1-8, 1a-3a and xerogels I-IV**

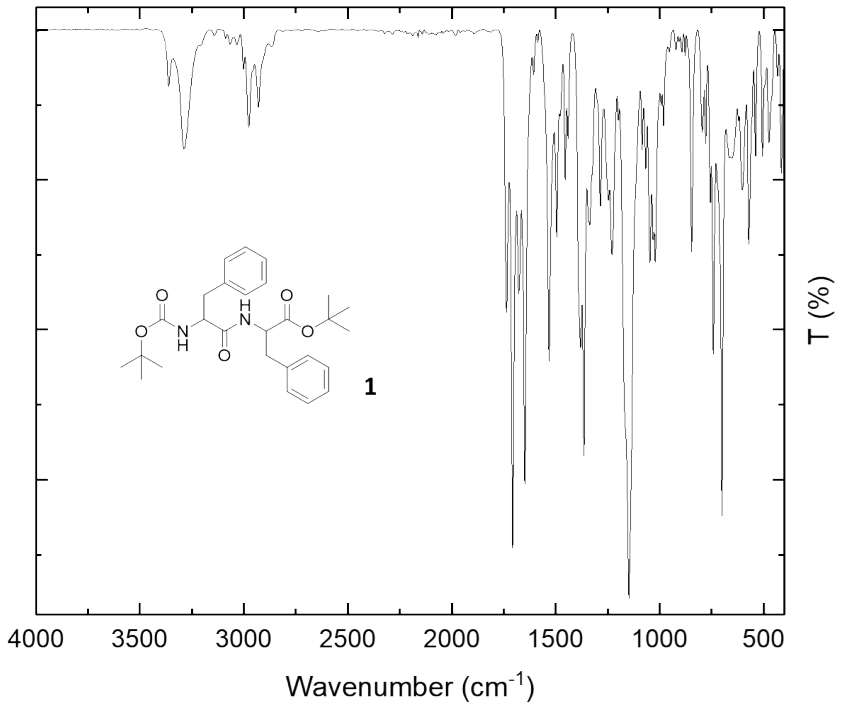


**Figure S52.** ATR-FTIR spectrum of Boc-Phe-Phe-O*t*Bu **1**.

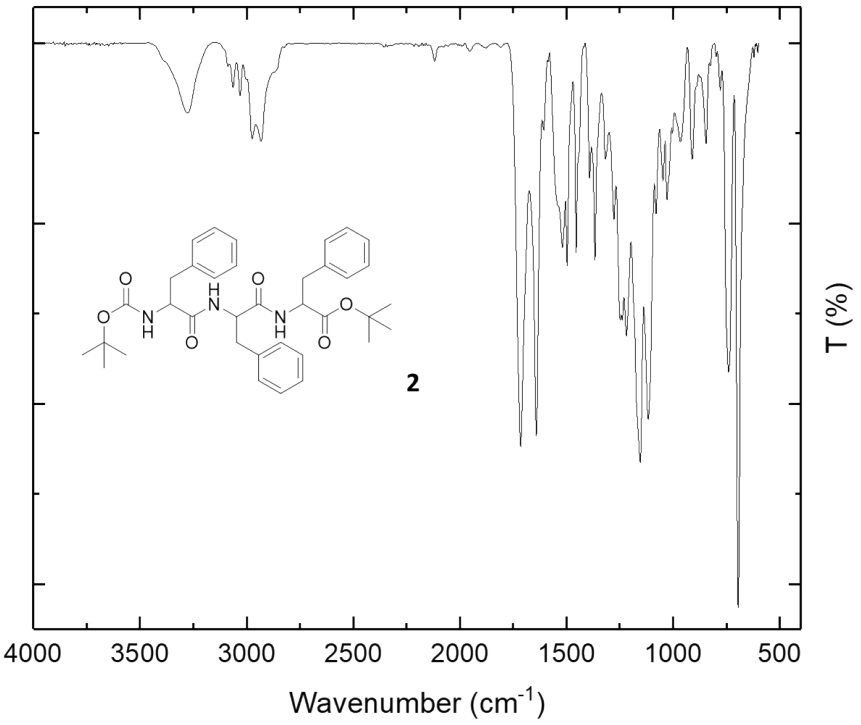

**Figure S53.** ATR-FTIR spectrum of Boc-Phe-Phe-Phe-O*t*Bu **2**.

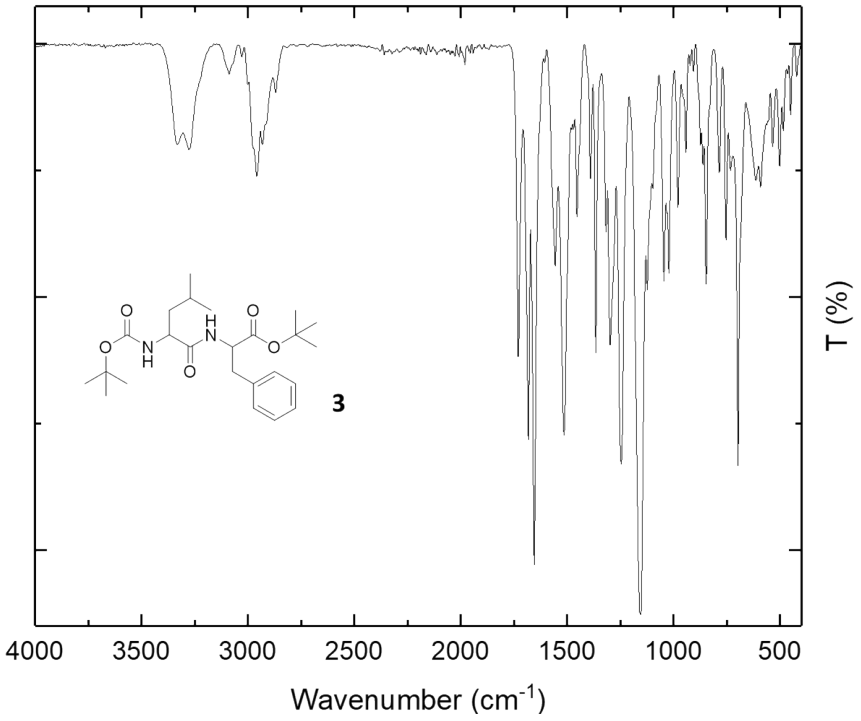


**Figure S54.** ATR-FTIR spectrum of Boc-Leu-Phe-O*t*Bu **3**.

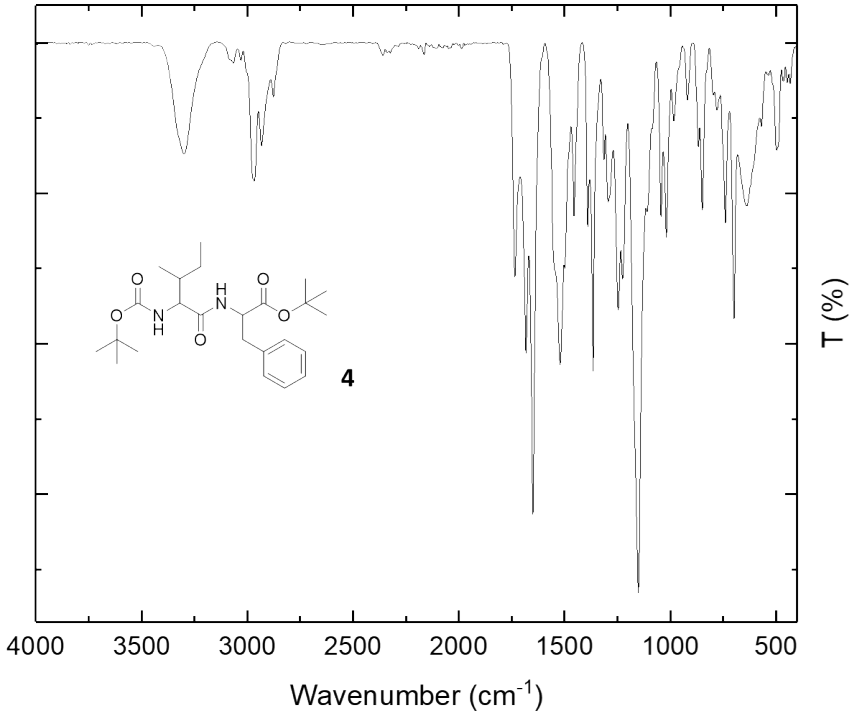

**Figure S55.** ATR-FTIR spectrum of Boc-Ile-Phe-O*t*Bu **4**.

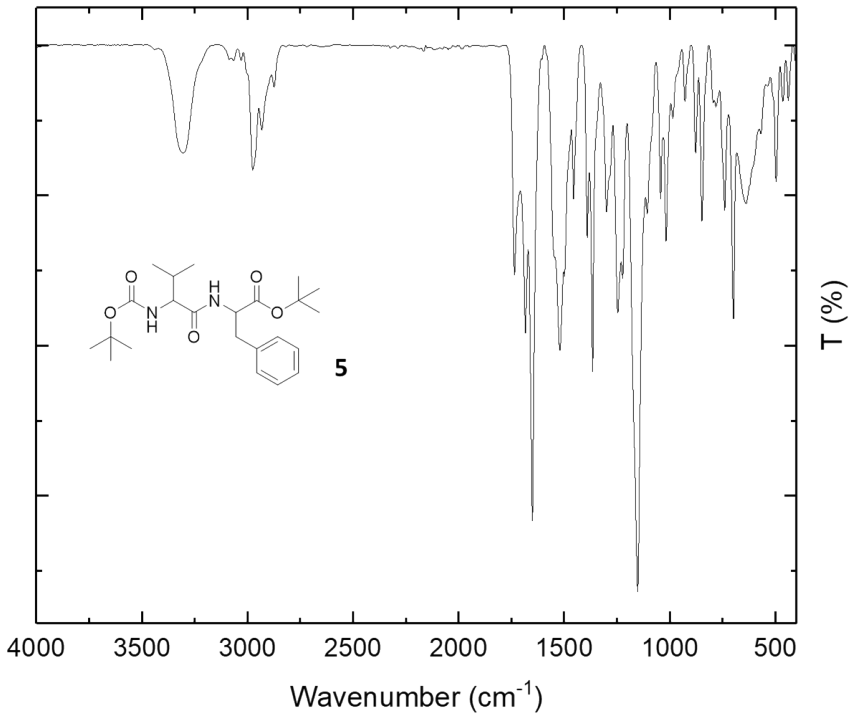


**Figure S56.** ATR-FTIR spectrum of Boc-Val-Phe-O*t*Bu **5**.

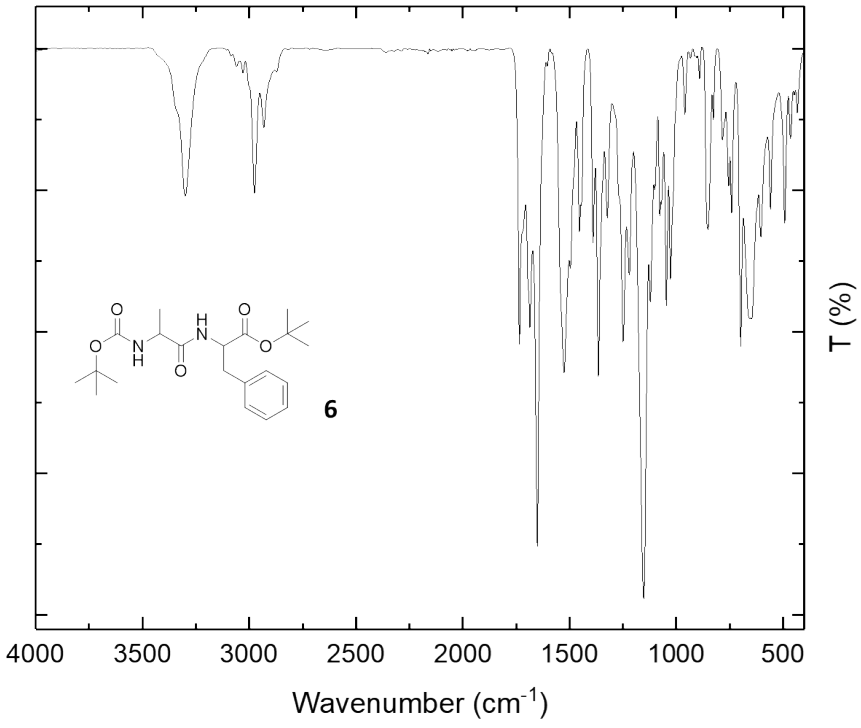

**Figure S57.** ATR-FTIR spectrum of Boc-Ala-Phe-O*t*Bu **6**.

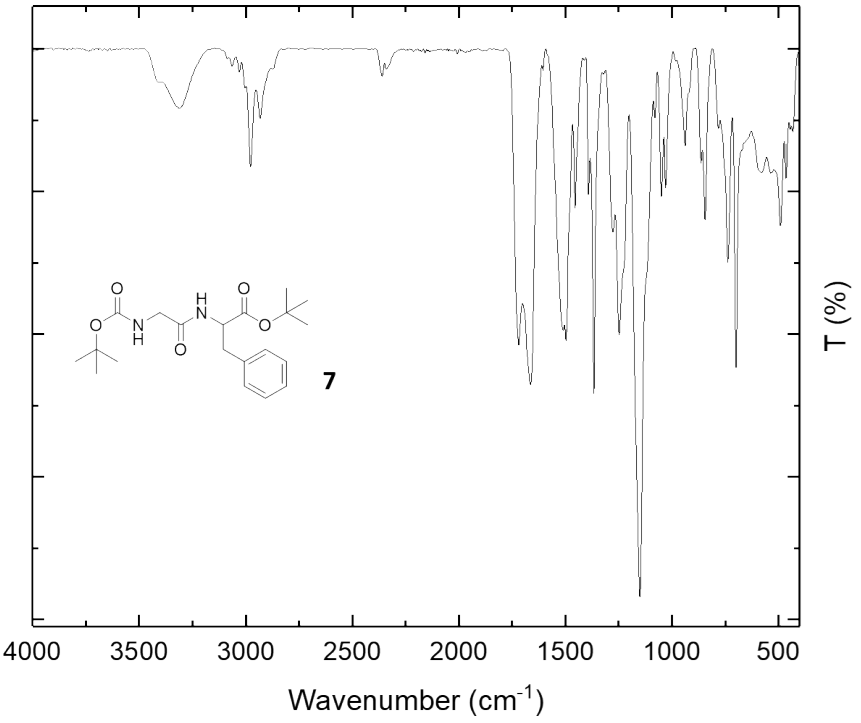


**Figure S58.** ATR-FTIR spectrum of Boc-Gly-Phe-O*t*Bu **7**.

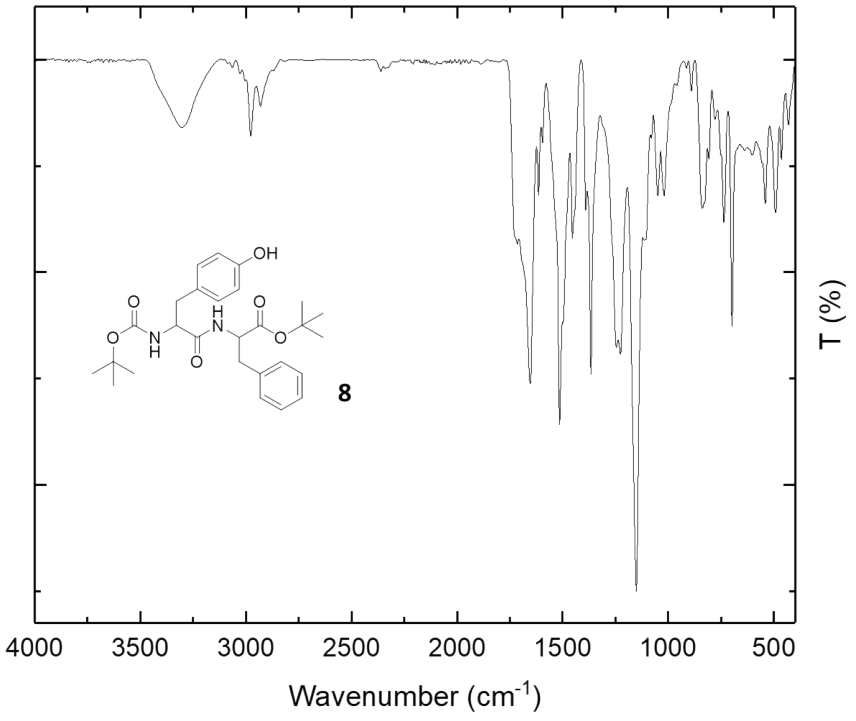

**Figure S59.** ATR-FTIR spectrum of Boc-Tyr-Phe-O*t*Bu **8**.

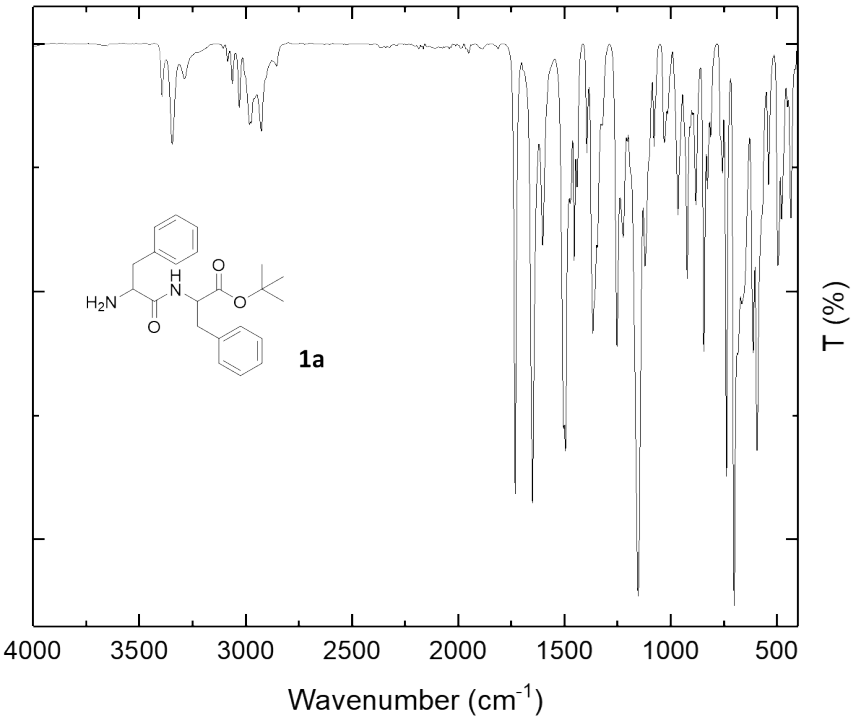


**Figure S60.** ATR-FTIR spectrum of Phe-Phe-O*t*Bu **1a**.

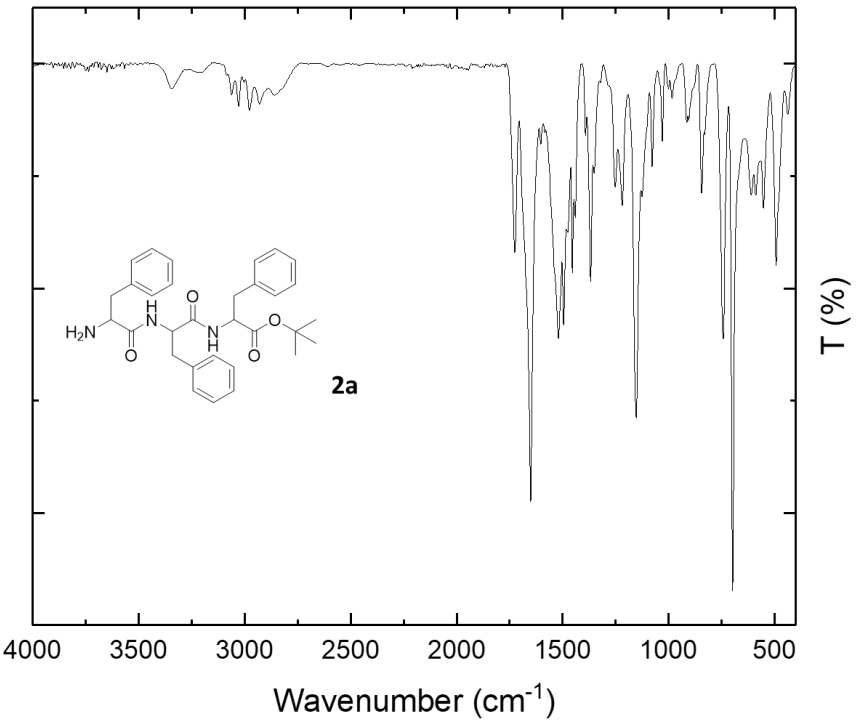


**Figure S61.** ATR-FTIR spectrum of Phe-Phe-Phe-O*t*Bu **2a**.

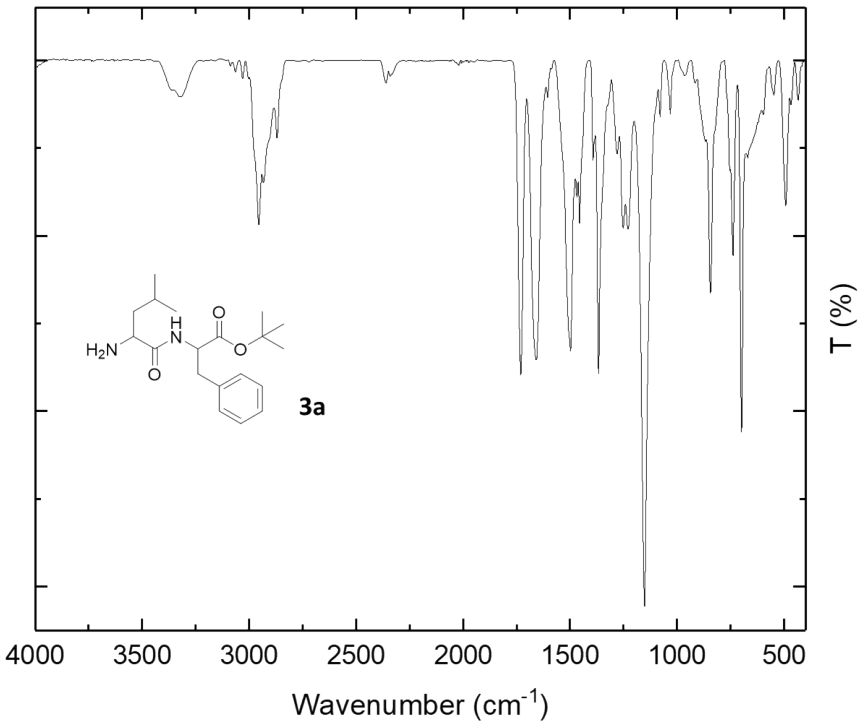


**Figure S62.** ATR-FTIR spectrum of Leu-Phe-O*t*Bu **3a**.

a)

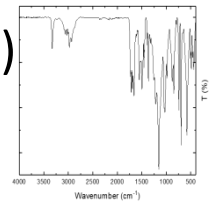


b)

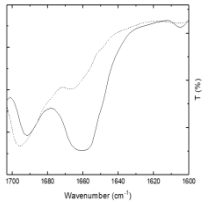


**Figure S63**. a) ATR-FTIR spectrum of xerogel **I** and b) ATR-FTIR spectrum magnified in the amide I region of xerogel **I** (solid line) and non-dried "wet" gel **I** (dashed line).

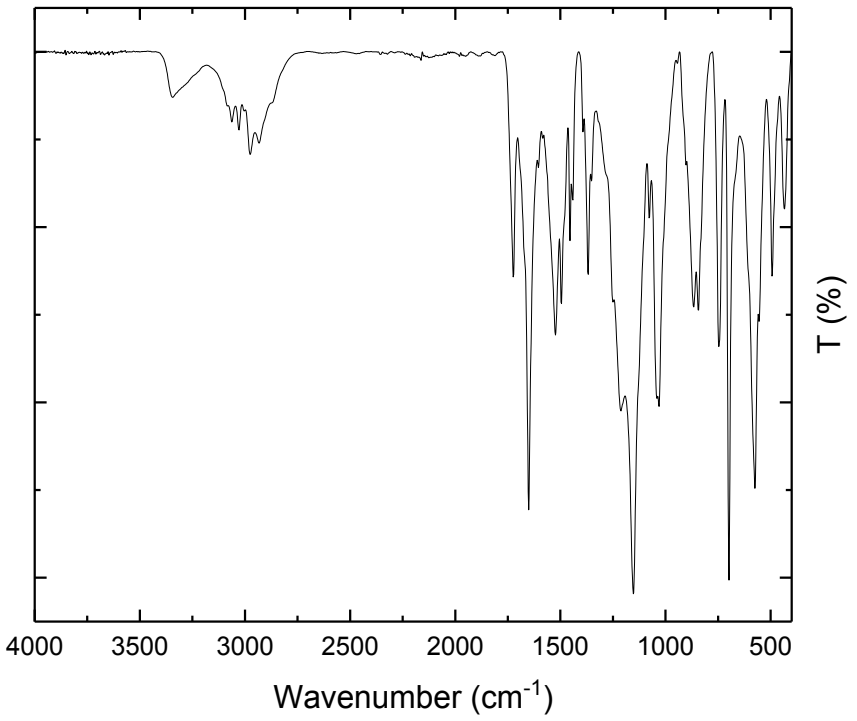


**Figure S64**. ATR-FTIR spectrum of xerogel **II**.


**Figure S65**. a) ATR-FTIR spectrum of xerogel **III** and b) ATR-FTIR spectrum magnified in the amide I region of xerogel **III** (solid line) and non-dried "wet" gel **III** (dashed line).

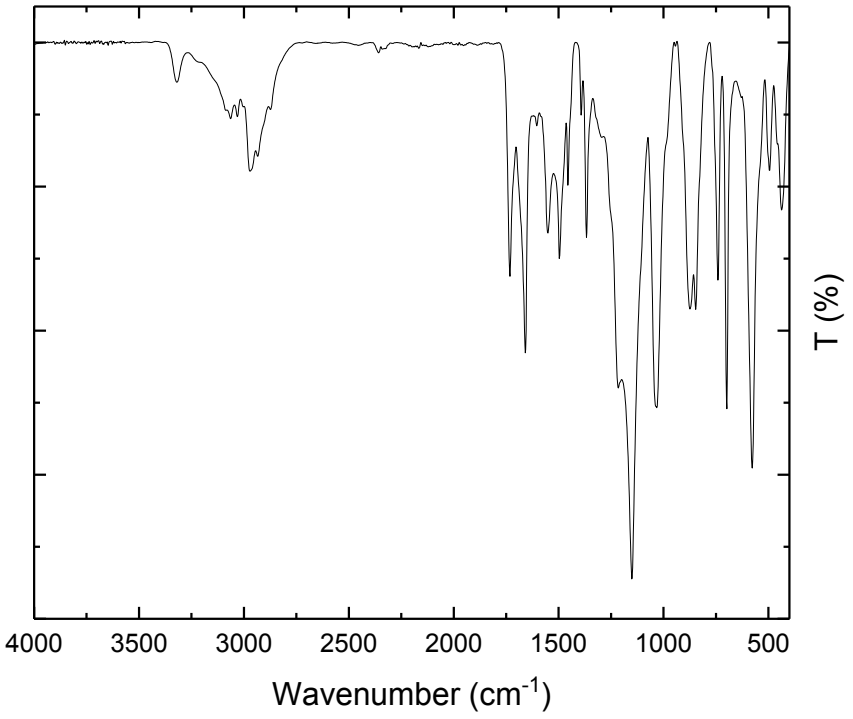


**Figure S66**. ATR-FTIR spectrum of xerogel **IV**.

4. **UV-vis spectra of compounds 1-1a, 2-2a and 3-3a**

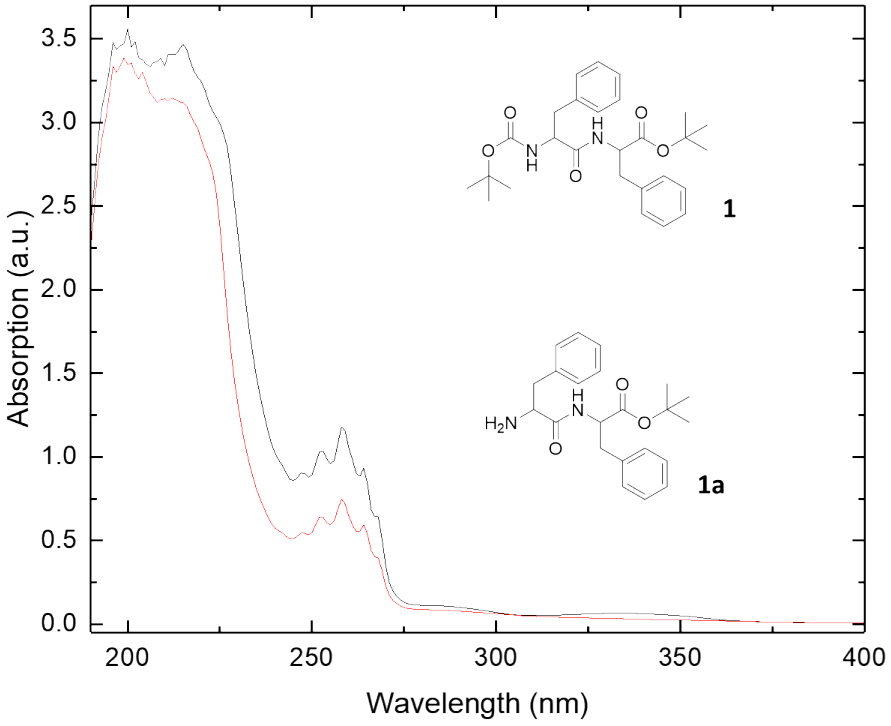


**Figure S67.** UV-vis spectra of Boc-Phe-Phe-O*t*Bu **1** (black) and Phe-Phe-O*t*Bu **1a** (red) at 25 mM in ACN.

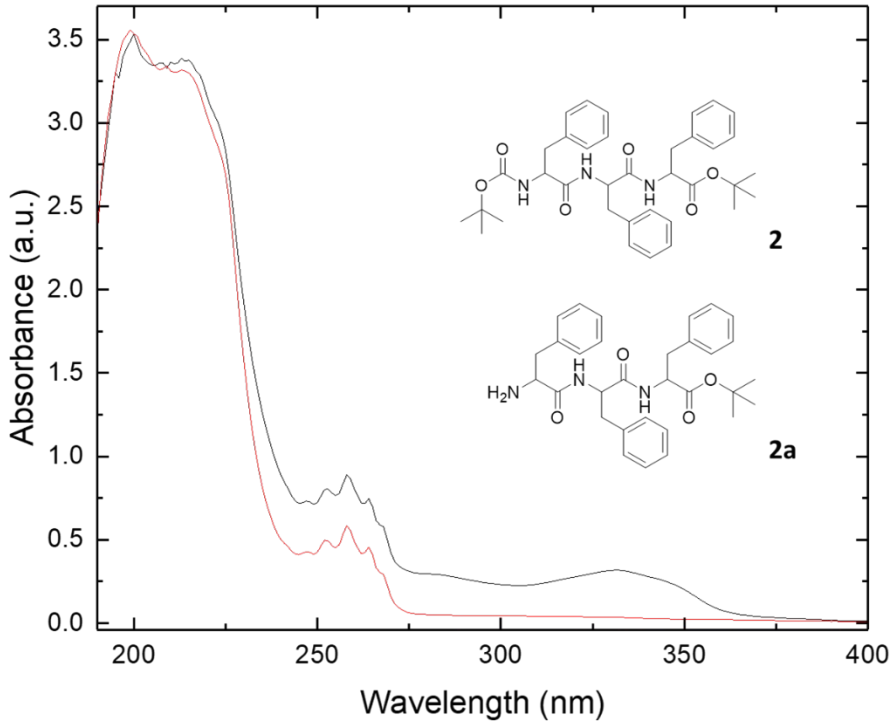


**Figure S68.** UV-vis spectra of Boc-Phe-Phe-Phe-O*t*Bu **2** (black) and Phe-Phe-Phe-O*t*Bu **2a** (red) at 1 mM in ACN.

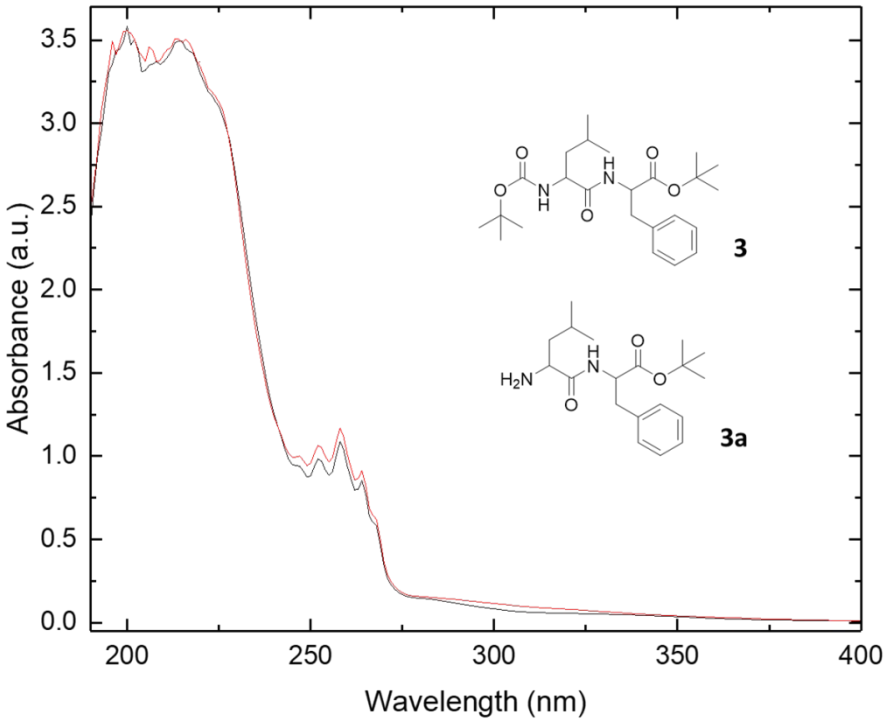

**Figure S69.** UV-vis spectra of Boc-Leu-Phe-O*t*Bu **3** (black) and Leu-Phe-O*t*Bu **3a** (red) at 5 mM in ACN.

## 5. Rheology measurement plots of gel systems I, II, III and IV

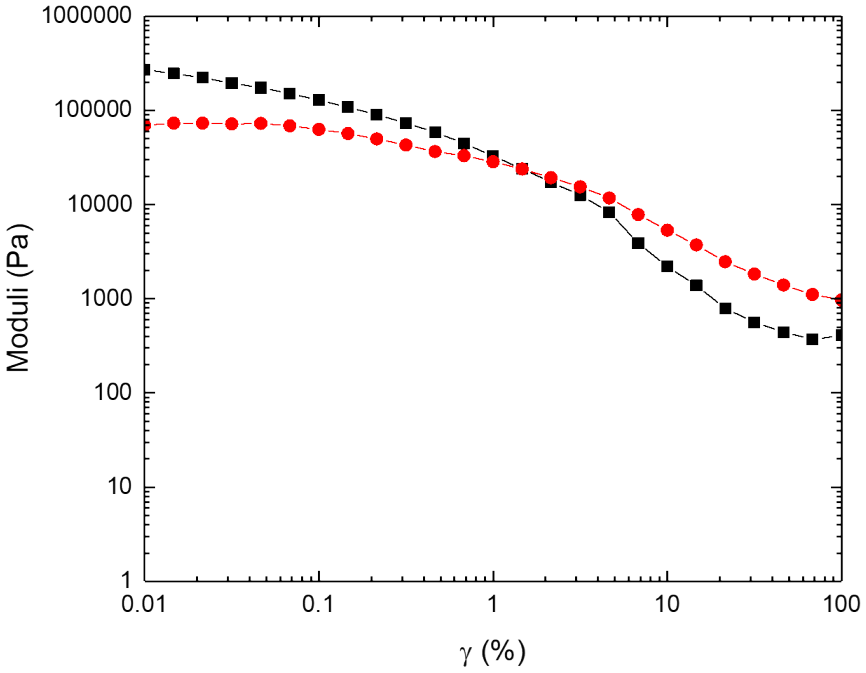


**Figure S70.** Amplitude sweep measurement of gel system **I** (0.05 M, 1.0 equivalent of $H_2SO_4$). Storage modulus G´ (black curve, square points) and loss modulus G´´ (red curve, circle points).

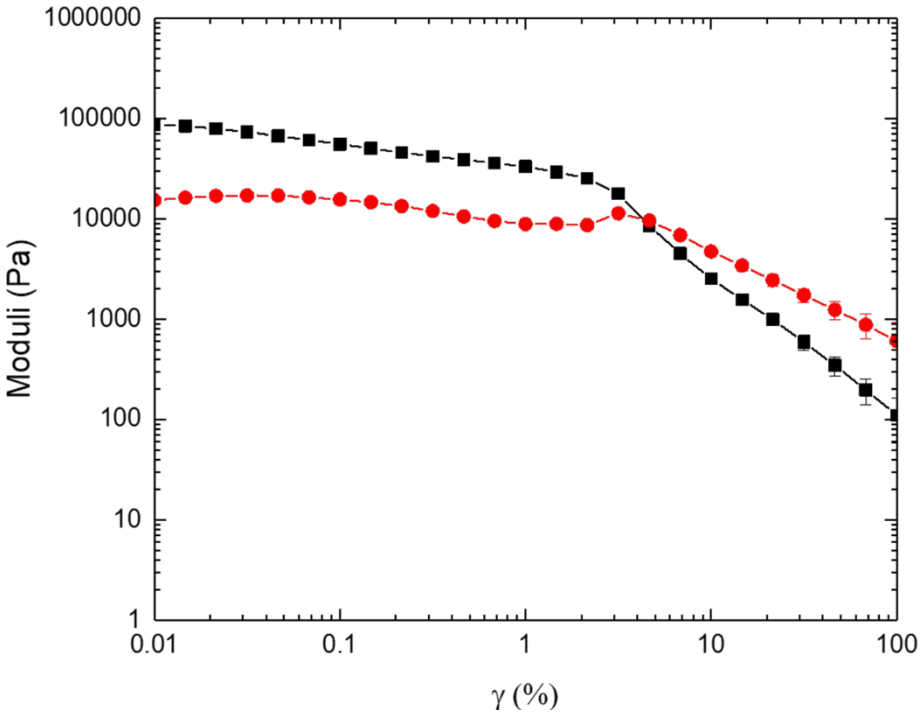

**Figure S71.** Amplitude sweep measurement of gel system **I** (0.05 M, 0.5 equivalent of $H_2SO_4$). Storage modulus G´ (black curve, square points) and loss modulus G´´ (red curve, circle points).

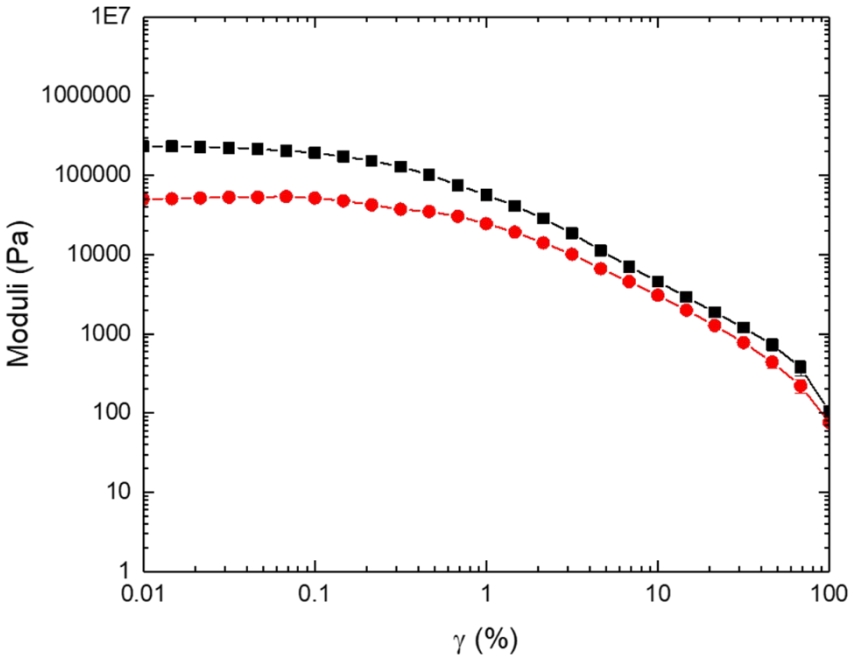


**Figure S72.** Amplitude sweep measurement of gel system **II** (0.05 M, 1.0 equivalent of $H_2SO_4$). Storage modulus G´ (black curve, square points) and loss modulus G´´ (red curve, circle points).

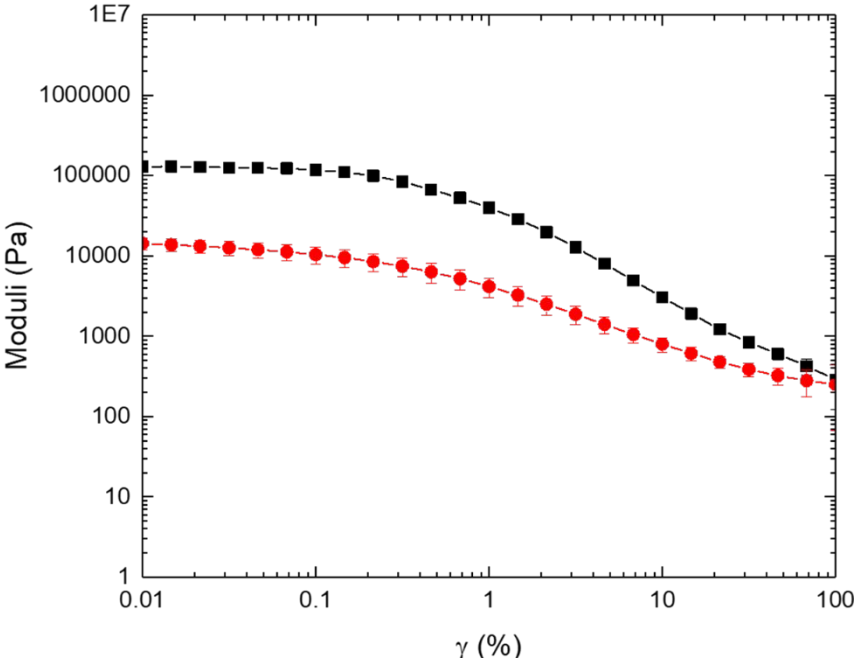

**Figure S73.** Amplitude sweep measurement of gel system **II** (0.05 M, 0.5 equivalent of $H_2SO_4$). Storage modulus G´ (black curve, square points) and loss modulus G´´ (red curve, circle points).

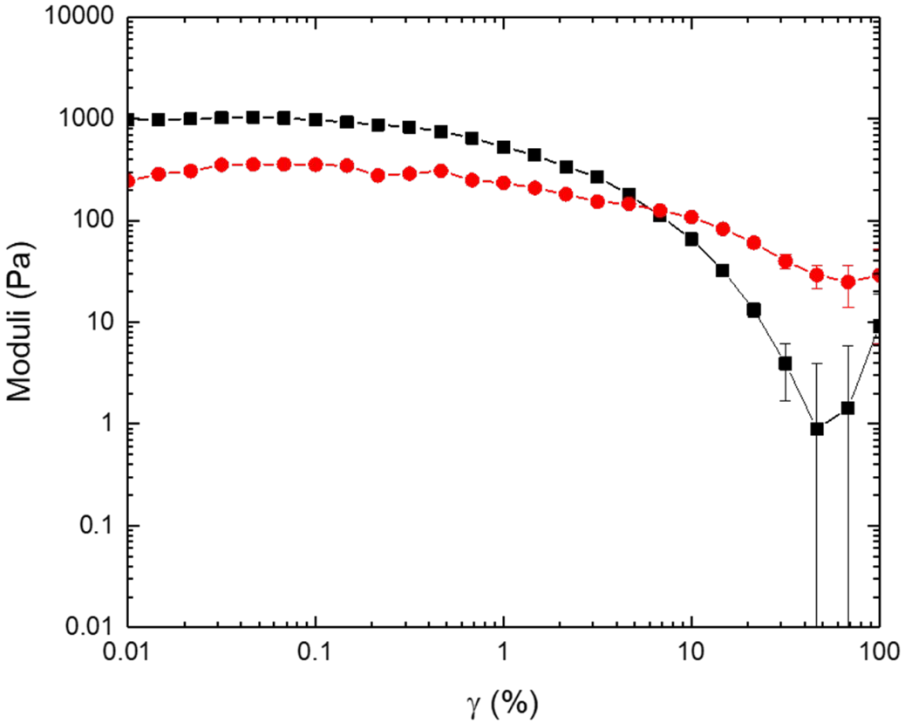


**Figure S74.** Amplitude sweep measurement of gel system **III** (0.025 M, 1.0 equivalent of $H_2SO_4$). Storage modulus G´ (black curve, square points) and loss modulus G´´ (red curve, circle points).

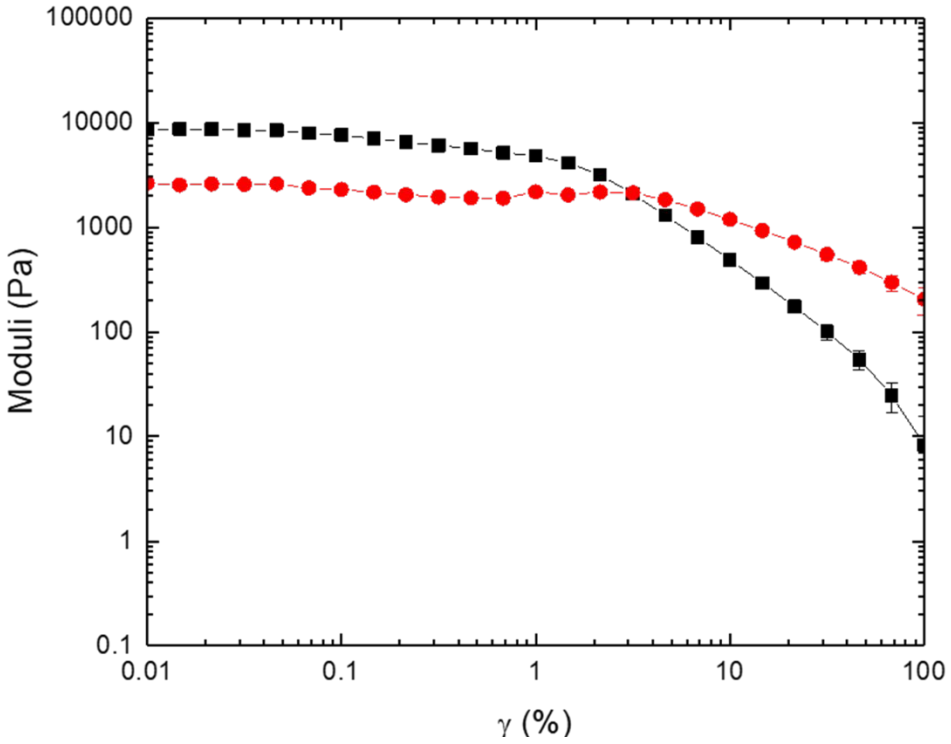


**Figure S75.** Amplitude sweep measurement of gel system **III** (0.05 M, 1.0 equivalent of $H_2SO_4$). Storage modulus G´ (black curve, square points) and loss modulus G´´ (red curve, circle points).

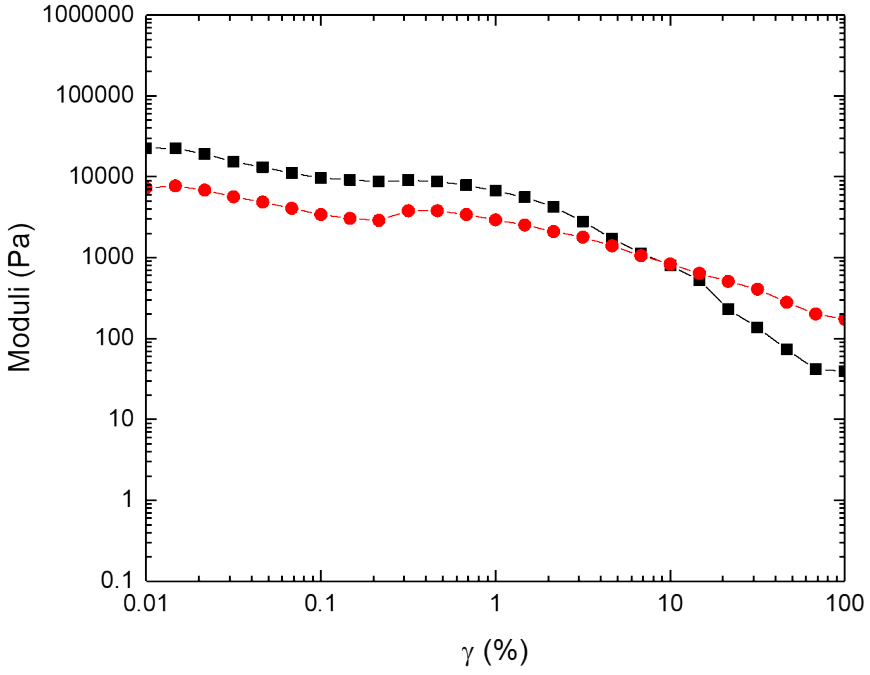


**Figure S76.** Amplitude sweep measurement of gel system **III** (0.05 M, 0.5 equivalent of $H_2SO_4$). Storage modulus G´ (black curve, square points) and loss modulus G´´ (red curve, circle points).

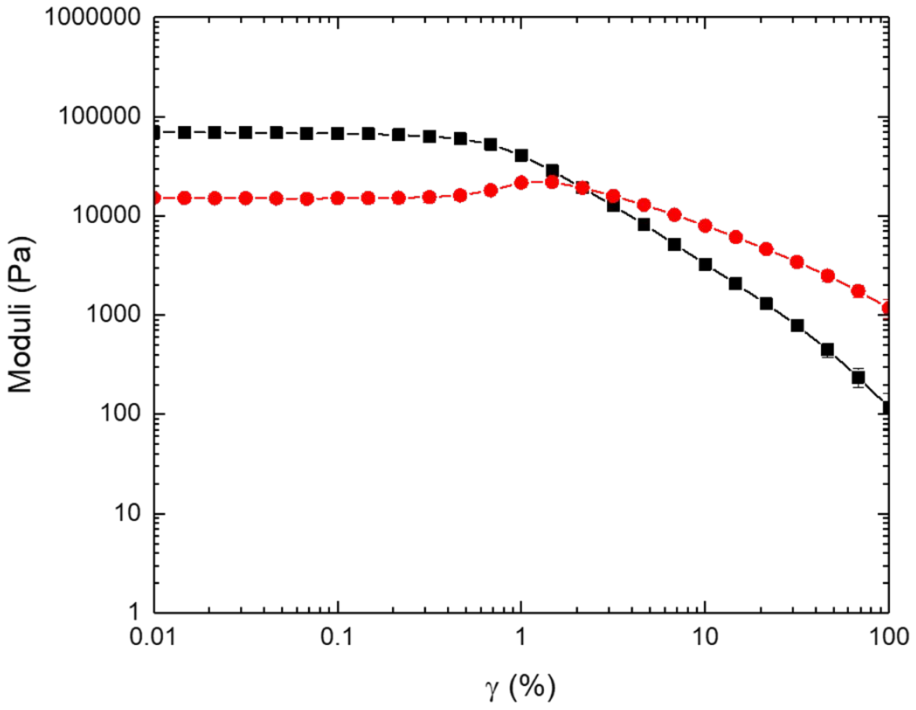


**Figure S77.** Amplitude sweep measurement of gel system **III** (0.1 M, 1.0 equivalent of $H_2SO_4$). Storage modulus G´ (black curve, square points) and loss modulus G´´ (red curve, circle points).

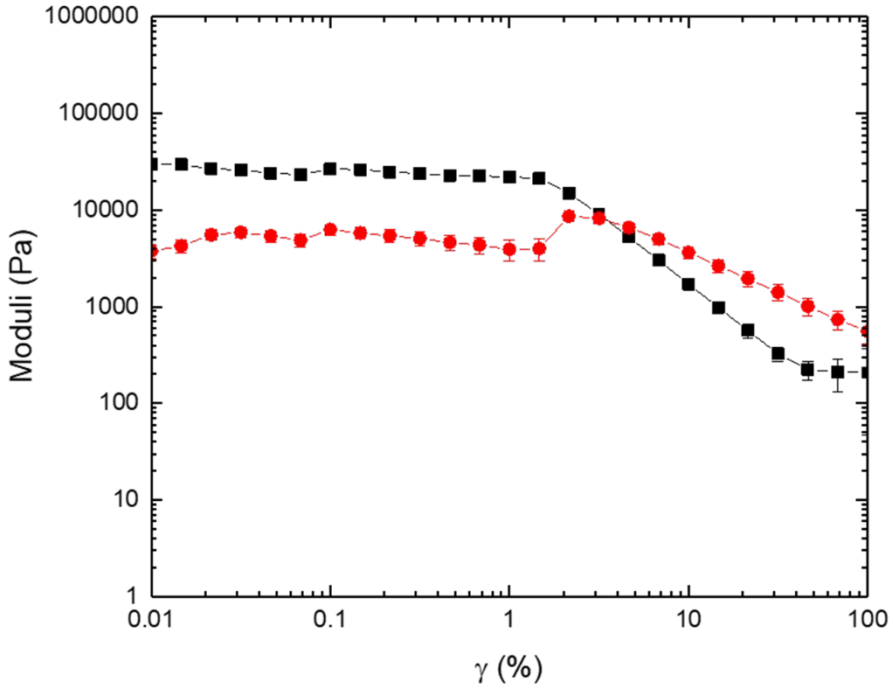


**Figure S78.** Amplitude sweep measurement of gel system **IV** (0.05 M, 1.0 equivalent of $H_2SO_4$). Storage modulus G´ (black curve, square points) and loss modulus G´´ (red curve, circle points).

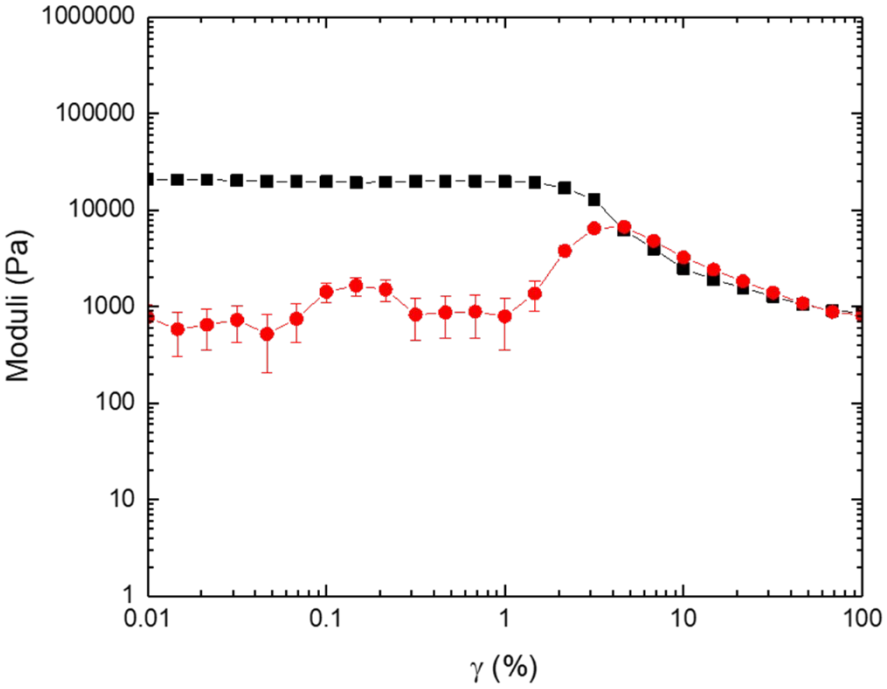


**Figure S79.** Amplitude sweep measurement of gel system **IV** (0.05 M, 0.5 equivalent of $H_2SO_4$). Storage modulus G´ (black curve, square points) and loss modulus G´´ (red curve, circle points).

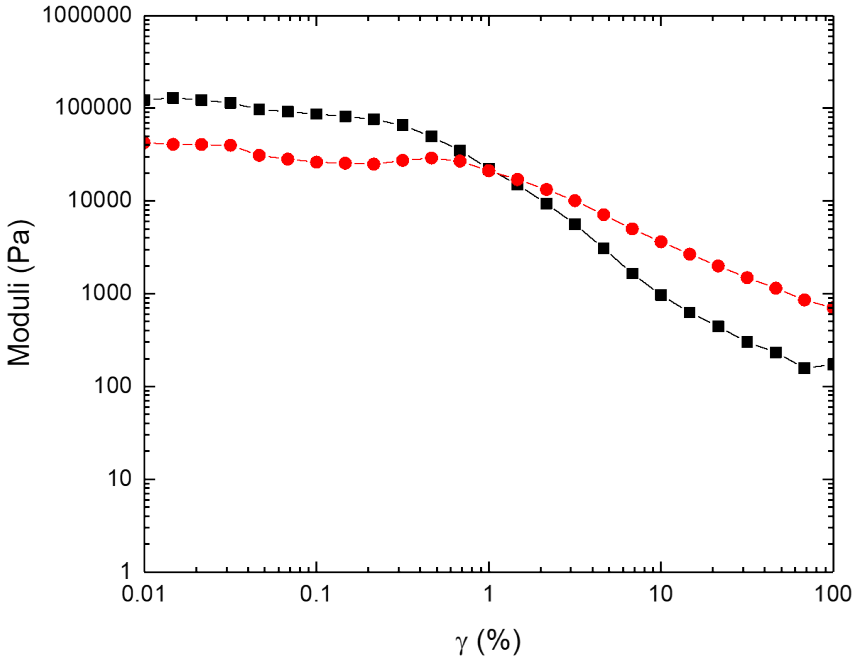


**Figure S80.** Amplitude sweep measurement of gel system **IV** (0.1 M, 1.0 equivalent of $H_2SO_4$). Storage modulus G´ (black curve, square points) and loss modulus G´´ (red curve, circle points).